

RESEARCH PROJECT, EASA.2022.C11

D-1.1 VRS KNOWLEDGE REPORT

Helicopter Vortex Ring State Experimental Research

Disclaimer



Funded by the European Union. Views and opinions expressed are however those of the author(s) only and do not necessarily reflect those of the European Union or the European Union Aviation Safety Agency (EASA). Neither the European Union nor EASA can be held responsible for them.

This deliverable has been carried out for EASA by an external organisation and expresses the opinion of the organisation undertaking this deliverable. It is provided for information purposes. Consequently it should not be relied upon as a statement, as any form of warranty, representation, undertaking, contractual, or other commitment binding in law upon the EASA.

Ownership of all copyright and other intellectual property rights in this material including any documentation, data and technical information, remains vested to the European Union Aviation Safety Agency. All logo, copyrights, trademarks, and registered trademarks that may be contained within are the property of their respective owners. For any use or reproduction of photos or other material that is not under the copyright of EASA, permission must be sought directly from the copyright holders.

Reproduction of this deliverable, in whole or in part, is permitted under the condition that the full body of this Disclaimer remains clearly and visibly affixed at all times with such reproduced part.

DELIVERABLE NUMBER AND TITLE:	VRS, D-1.1 VRS knowledge report
CONTRACT NUMBER:	EASA.2022.C11
CONTRACTOR / AUTHOR:	ONERA / Laurent Binet – Pierre-Marie Basset
IPR OWNER:	European Union Aviation Safety Agency
DISTRIBUTION:	Public

APPROVED BY:	AUTHORS	REVIEWER	MANAGING DEPARTMENT
	Laurent Binet Pierre-Marie Basset	Raffaele Di Caprio	Helder Mendes

DATE: 25 April 2024

CONTENTS

CONTENTS	3
ABBREVIATIONS	5
1. Introduction	7
1.1 Scope of the document	7
2. VRS Knowledge - Theory	8
2.1 What is the Vortex Ring State phenomenon	8
2.2 VRS symptoms, description and characterization	16
2.2.1 Summary of VRS symptoms, description and characterization	20
2.3 Review of the main parameters influencing VRS onsets	21
2.3.1 Rotor disk loading – downwash	21
2.3.2 Flight parameters	21
2.3.3 Rotor/blade design parameters	34
2.3.4 Aggravating factors	34
2.3.5 Summary of the main parameters influencing VRS onsets	38
2.4 Analysis of the current available analytical and simulation methods for prediction of the VRS	38
2.4.1 Example of VRS domain mapping	38
2.4.2 Criteria defining the envelop of the VRS domain	39
2.4.3 VRS phenomenon simulation	45
2.4.4 Summary of the current available analytical and simulation methods for prediction of the VRS	58
3. VRS Knowledge – Flight test campaigns	60
3.1 ONERA/DGA-EV flights test campaigns	60
3.1.1 Dauphin 6075	60
3.1.2 Fennec flight tests at EPNER in 2004	68
3.1.3 Dauphin/Fennec flight tests “VibRS”	72
3.2 Review of published results from flight tests	79
3.2.1 V-22 flight test campaigns	79
3.2.2 Royal Aircraft Establishment (RAE)	81
3.3 Summary of the knowledge gained through previous flight tests	82
4. Avoiding VRS – Recovery techniques	83
4.1 Avoiding VRS	83
4.2 Review of the recovery techniques and associated recommendations	83
4.3 Summary of the review of the recovery techniques and associated recommendations	87

5. Review and analysis of alerting system patents.....	88
5.1 Summary of the alerting system patents	89
6. Gap analysis of the current knowledge for the complete description and prediction of the phenomena.....	90
6.1 VRS domain knowledge	90
6.2 Dynamic VRS	90
6.3 Predicting methods/simulations	91
6.4 Recovery techniques	91
6.5 Rotor technologies	92
6.6 Pitch-roll cross-coupling considerations	92
6.7 New architectures (eVTOL / UAM)	93
7. Conclusions.....	94
Bibliography	95

ABBREVIATIONS

ACRONYM	DESCRIPTION
AFCS	Automatic Flight Control System
Ax	Longitudinal acceleration - Earth referenced
Az	Vertical acceleration – Earth referenced
CFD	Computational Fluid Dynamics
DDL	Lateral cyclic input (%)
DDM	Longitudinal cyclic input (%)
DDN	Pedal input (%)
DL	Disk Loading
DTO	Collective input (in % if pilot control, in deg for collective blade pitch angle)
FATO	Final Approach and TakeOff
ft	Feet
ft/min	Feet per minute
g	Gravitational constant
HOGE	Hover Out of Ground Effect
HOST	Helicopter Overall Simulation Tool – Airbus Helicopters flight mechanics code
IAS / KIAS	Indicated AirSpeed / IAS in kts
IFR	Instrument Flight Rules
i_{mr}	Rotor mast tilt angle
I_{xx}	Helicopter roll inertia
I_{yy}	Helicopter Pitch inertia
kt(s)	Knot(s)
m	Helicopter mass
n	Normal acceleration
P_{level}	Required power in level flight
R	Rotor Radius
RoD	Rate of Descent
RPM	Rotation speed (Rev. Per Minute)
T	Rotor thrust
TAS	True AirSpeed
TQ	Rotor Torque
URANS	Unsteady Reynolds Averaged Navier-Stokes
V_{air}	Helicopter airspeed
V_H	Helicopter horizontal speed (airspeed): $V_H = \sqrt{V_X^2 + V_Y^2}$
V_i	Induced velocity
V_{i0}	Induced velocity in hover
V_{Ground}	Helicopter ground speed: $V_{Ground} = V_{air} + V_{wind}$

Vx	Helicopter longitudinal speed (airspeed)
Vy	Helicopter lateral speed (airspeed)
V _{wind}	Wind velocity
Vz	Helicopter vertical speed
VPM	Vortex Panel Method
VRS	Vortex Ring State
VTM	Vorticity Transport Method
W	Helicopter Weight
α_D	Rotor disk angle of attack
γ_{Ground}	Glide path angle, in earth frame
γ_{air}	Air glide path angle
θ / TETA	Helicopter pitch angle
ϕ / PHI	Helicopter roll angle

1. Introduction

1.1 Scope of the document

This report represents deliverable 'D-1.1' of the Helicopter Vortex-Ring-State Experimental Research project (EASA.2022.C11).

The objective of this document is to present a state of the art of the basic knowledge regarding the Vortex-Ring-State (noted VRS hereafter), by reviewing and analysing available studies and researches, as well as documents from helicopter manufacturers.

Thus, an analysis of the available knowledge on the VRS is developed. In particular, the following topics are summarised in this report:

- Theory of the VRS;
- Analysis of the available analytical and simulation methods for prediction of the VRS.
- Analysis of the previous research studies on the VRS with particular regard to the experimental flight test programmes.
- Gap analysis of the current knowledge for the complete description and prediction of the phenomena

A critical analysis and synthesis of the relevant information has been done for the different topics.

This document is based on ONERA, DGA-EV and EASA knowledge and experience on Vortex-Ring-State and a relatively large bibliographical review.

Thus, this document relies on published and available data in all type of documents. Nevertheless, it has to be noted that some information (from ONERA) have never been publicly presented before.

The objective is to provide the most representative and exhaustive status of the current knowledge but it is sure that some lacks could be reported.

This document presents a review on many different topics linked to the VRS, but doesn't present the conclusions of the current Helicopter Vortex-Ring-State Experimental Research Project.

This document, and in particular the analyses performed, reflects only the author's view and can be discussed.

2. VRS Knowledge - Theory

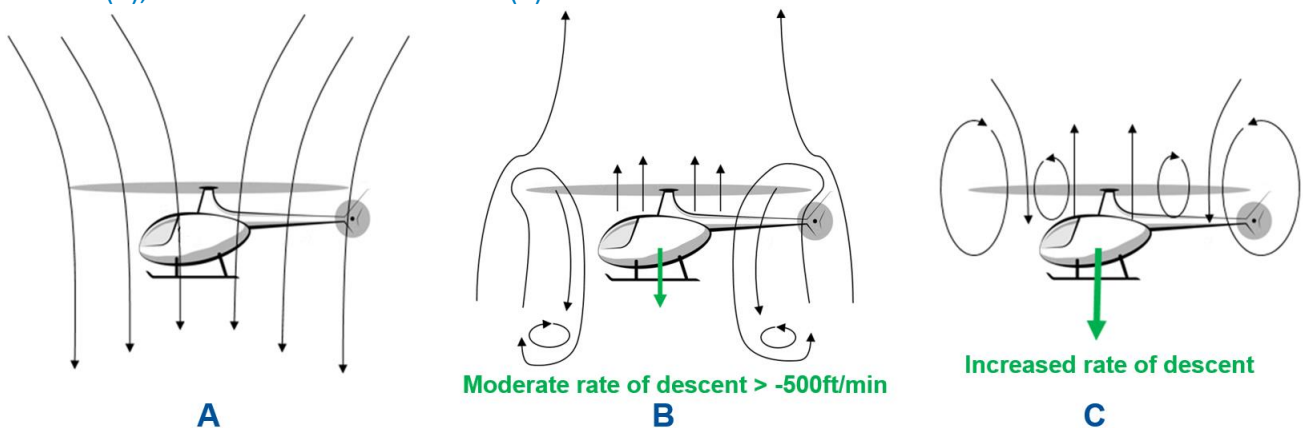
2.1 What is the Vortex Ring State phenomenon

The Vortex Ring State (VRS) phenomenon can be defined from several standpoints: the physics, the theory and the practical points of view.

From the physics, the VRS consists in the merging of the rotor wake vortices into a huge vortex torus surrounding the rotor periphery. The cause is the fact that the rotor is descending at a speed close to the convecting speed of the vortices composing its wake, that is why the airflow recirculates through the periphery of the rotor disk.

In HOGE (Hover Out of Ground Effect), level flight or climb, a downward flow of air is induced through the rotor blades creating a downwash that is added to the rotational relative wind. The airflow is through the rotor in the opposite direction of thrust. This downward flow is able to continuously move away from the rotor disk plane as shown in Figure 2-1 (A), e.g. cases of hover and climb. The trailing tip vortices are downstream of the path of each subsequent passing rotor blade.

► **Figure 2-1** Downward flow generated by the rotor in normal flight conditions (A), in moderate rate of descent (B), in increased rate of descent (C)



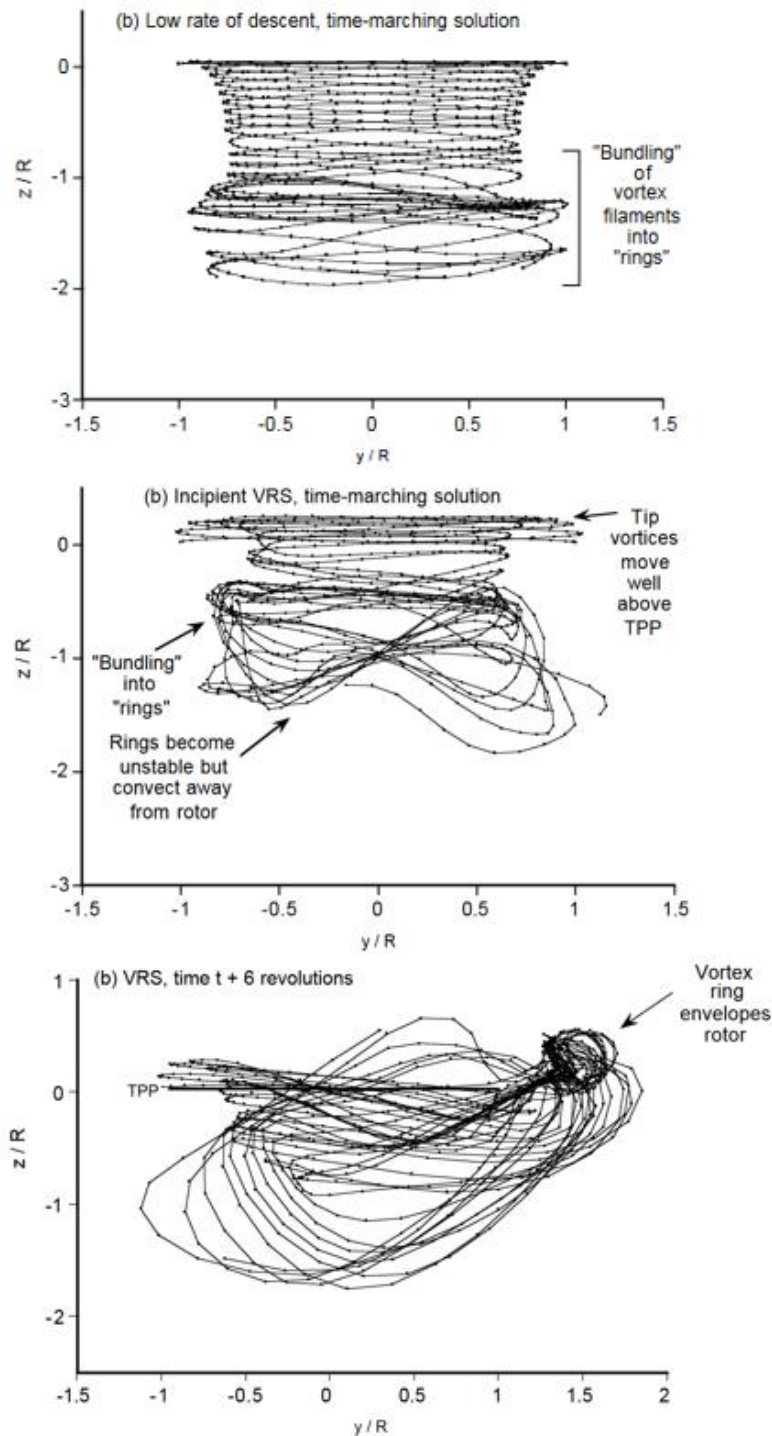
When the helicopter descends, it enters into its own downwash. The airflow of the inner blade sections is upward relative to the disk while the opposing mass of still air does not allow the downwash to move downwards freely (Figure 2-1 (B)).

Increasing the rate of descent, the opposing mass of still air will effectively block the rotor downwash. When the descent speed of the rotor is in a certain range, the pairing of the vortices starting downstream propagates upstream up to the rotor.

Figure 2-2, based on a numerical study [1], gives a good representation of the pairing of vortex filaments in the rotor airflow at low rate of descent, incipient VRS and developed VRS. This figure shows the wake structure at a series of different times when the rotor is operating close to the VRS.

As the rate of descent is increasing, the wake begins to recirculate in the plane of the rotor. The blade tip vortices bundle together, and essentially form a series of vortex rings. Once in VRS, the rings lie close to or pass through the plane of the rotor, and the blades can intersect large concentrated regions of accumulated vorticity.

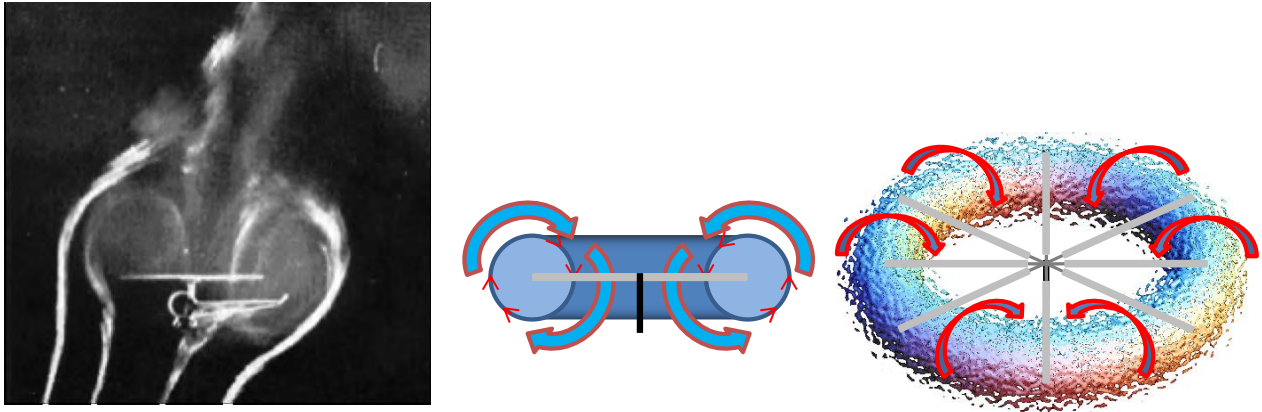
► Figure 2-2 Rear view of the wake geometry generated by a 4-bladed rotor using free-vortex numerical method – taken from [1]



This spatio-temporal aerodynamic instability starting locally downstream turns into a global instability transforming suddenly the whole helicoidal rotor wake into a huge vortex torus encircling the rotor as illustrated in Figure 2-3.

This aerodynamic instability of the rotor wake has been studied numerically and experimentally leading to numerous publications such as [1] or [2].

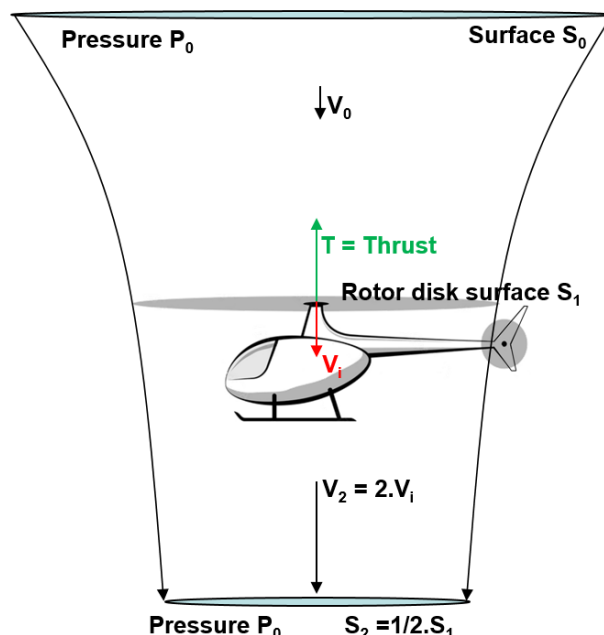
► Figure 2-3 Visualization with smokes of the airflow recirculating in a vortex ring torus through the rotor of a helicopter in descent flight [3] and 3D schematic view of the vortex torus around a rotor.



From the theoretical viewpoint, the simplest theory to assess analytically the thrust, mean induced flow and power of a rotor is the well-known momentum theory (also called Froude’s theory). A perfect fluid flow accelerated through a rotor can be seen as a fluid tube having for section the rotor disk of area S_1 at the rotor plan (see Figure 2-4). As the velocity in the airflow is increased downstream, the section of this fluid tube is decreasing downward.

In hover (out of ground effect), climbs and descents at low vertical speed, the rotor is working in a normal regime which can be called “helicopter mode”, accelerating the airflow in a downwash from the initial speed V_0 to V_i at the rotor disk level and to $V_2 = 2.V_i$ in the infinite downstream. This airflow being subsonic, the increase of the air velocity within the air tube produces a decrease of the pressure with respect to the ambient pressure outside the rotor wake and thus resulting in its radial contraction. Downstream where the induced flow is the double ($2.V_i$) of the mean induced velocity at the rotor level, the wake section is divided by two with respect to the rotor disk surface ($S_1/2$).

► Figure 2-4 The air flow tube through an open rotor working in “helicopter mode” as assumed by the momentum theory.



The momentum theory says that within this close surface corresponding to this fluid vein, the variation of the outgoing momentum (at a speed V_2 downstream) with respect to the incoming one (at a speed V_0 upstream) is equal to the resulting force applied to the air fluid and by reaction to the rotor thrust T :

$$T = D \times (V_2 - V_0)$$

with D being the air mass flow rate through the rotor disk:

$$D = \frac{dm}{dt} = \rho \cdot S_1 \cdot V_i$$

With these assumptions, the momentum theory provides a quadratic form of induced velocity evolution versus helicopter's vertical and longitudinal speed.

The demonstration can be easily found in the literature, such as in [4].

$$1 = \bar{v}^2 [\bar{\mu}^2 + (\bar{v} + \bar{n})^2]$$

With

$$\bar{v} = \frac{V_i}{V_{i0}}; \quad V_i: \text{induced velocity}; \quad V_{i0}: \text{induced velocity in hover} = \sqrt{\frac{mg}{2\pi\rho R^2}}$$

where m = helicopter mass; g = gravitational constant; ρ = air density, R = rotor radius

$$\bar{\mu} = \frac{V_x}{V_{i0}}; \quad V_x: \text{longitudinal speed along the rotor disk}$$

$$\bar{n} = \frac{V_z}{V_{i0}}; \quad V_z: \text{vertical speed on the rotor disk}$$

For example, the induced velocity in hover for the Fenec helicopter (Mass=2250Kg, $\rho = 1.225\text{Kg/m}^3$) is equal to:

$$V_{i0}(\text{Fenec}) = \sqrt{\frac{2250 * 9.81}{2\pi\rho 5.345^2}} = 10 \text{ m/s}$$

The induced velocity in hover for the AS365N helicopter (Mass=4000Kg, $\rho = 1.225\text{Kg/m}^3$) is equal to:

$$V_{i0}(\text{Dauphin}) = \sqrt{\frac{4000 * 9.81}{2\pi\rho 5.965^2}} = 12 \text{ m/s}$$

Figure 2-5 shows the momentum theory analytical solutions for the particular case of the vertical flight. The right side of these solutions is relative to the normal climbing flight (vertical velocity $V_z > 0$).

The left side is associated to the vertical descent. Referring to this part of the figure, it's easy to see that for descent rates higher than 2 times the induced velocity in hover ($V_z/V_{i0} < -2$), there are multiple solutions to the momentum theory equation. This multiplicity of solutions leads generally existing flight mechanics codes to instabilities at very high rates of descent.

► **Figure 2-5** Non dimensional momentum theory solutions in vertical flight

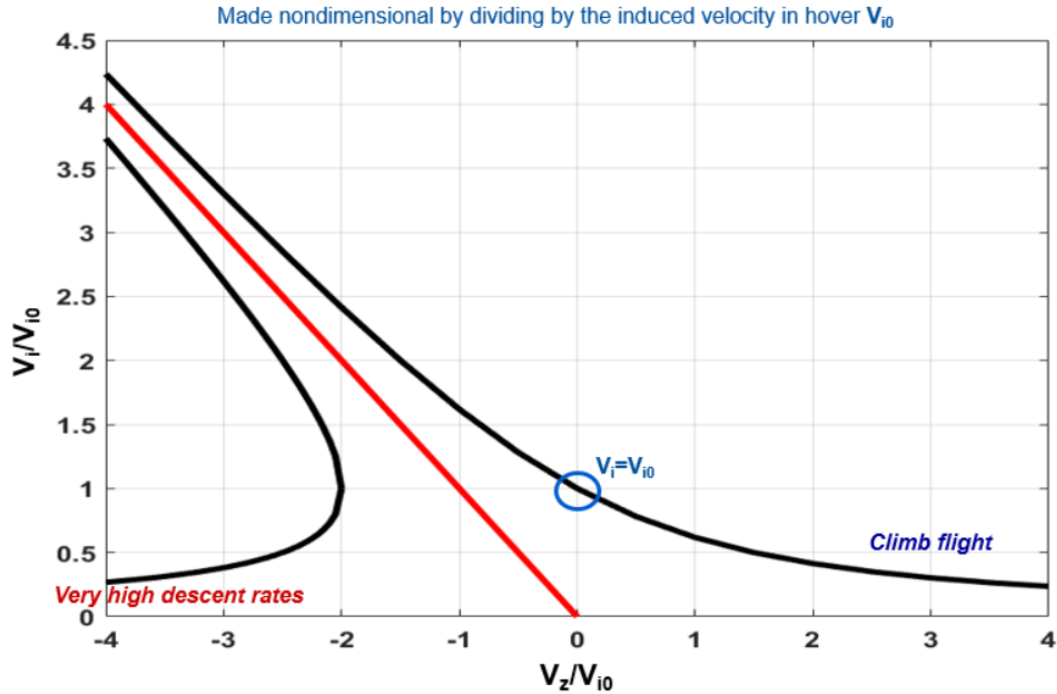
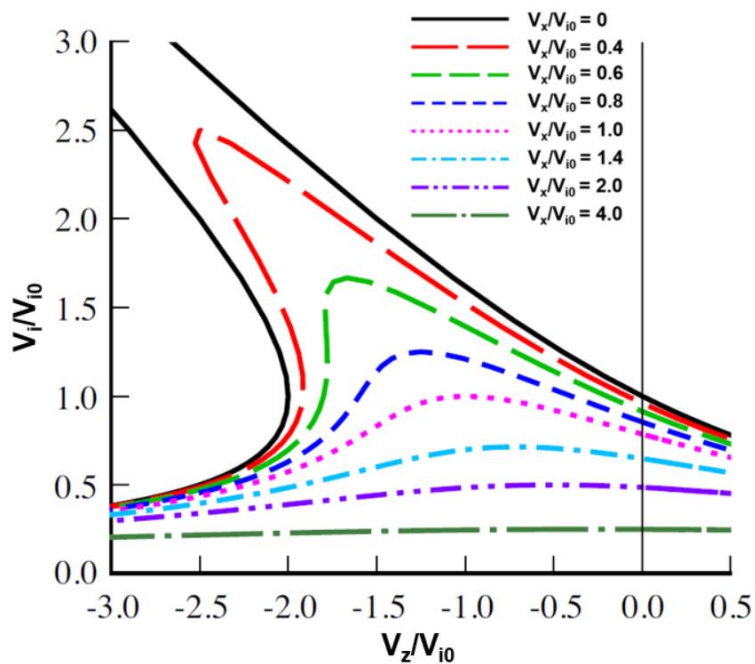


Figure 2-6 illustrates the momentum theory solutions in forward flight for the particular case of the descent. The solutions are shown at different non-dimensional forward speeds $\bar{\mu} = \frac{V_x}{V_{i0}}$. Once again, it can be seen that for non-dimensional forward speeds lower than 0.6, there is a multiplicity of solutions.

► **Figure 2-6** Non dimensional momentum theory solutions in descent – taken from [5]

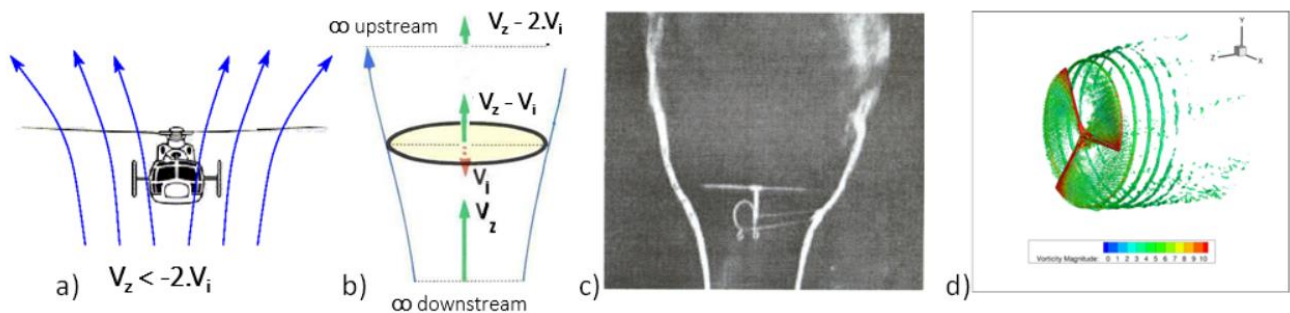


As the main assumption used in this theory is the air-wake continuity equation (describing the continuity of the downward airflow from infinite upstream to infinite downstream, in terms of mass flow rate conservation), the

momentum theory can also be applied to the other well-known rotor regime called “wind-mill mode”. Indeed the airflow through the rotor of a wind turbine or of a helicopter rotor in high descent rates corresponding to the wind-mill working regime is also well-defined. In this case the rotor is absorbing the kinetic energy of the air flow passing through the rotor from downstream to upstream. Thus the air velocity is decreased through the rotor disk and the air flow tube is enlarged going upward, as it can be seen in Figure 2-7.

The air passing upward through the rotor provides the power to turn the blades at a rotation speed (RPM) close to the nominal one as in auto-rotation or at higher RPM in “wind-mill brake mode”. Although it is theoretically possible for a helicopter to enter into this stable regime at high descent rates ($V_z/V_{i0} > 2.5$), in practice this working rotor regime is mainly used for wind turbines and autogyros.

► **Figure 2-7** Rotor wake air tube enlarging in “wind-mill mode”, a) and b) schemes of the airflow through of a helicopter rotor, c) picture from Meijer Drees wind tunnel experiment [3], d) CFD simulation of the air wake behind a wind turbine.

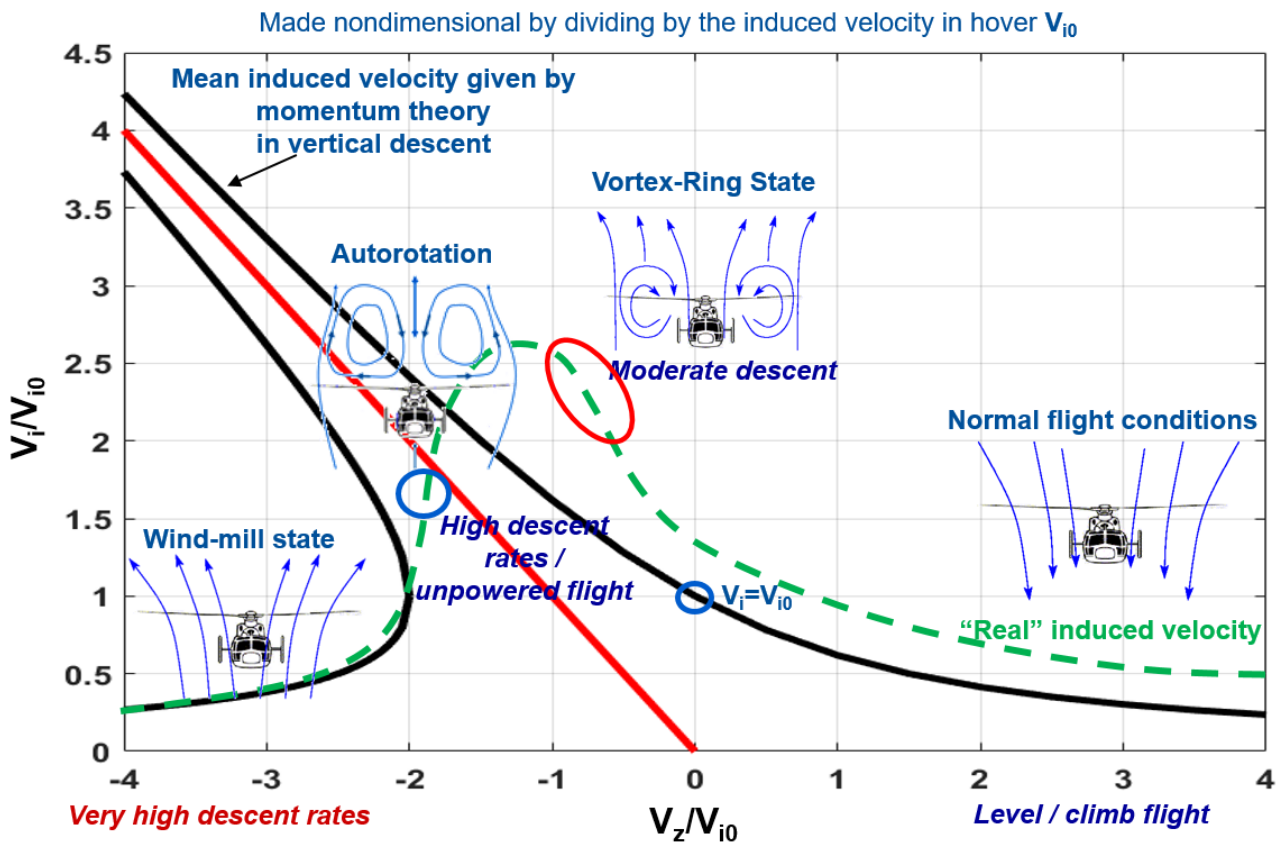


Between these two working regimes (“helicopter mode” and “wind-mill mode”), the momentum theory can no longer be applied because its fundamental assumption of a well-defined airflow vein collapses.

Besides this impossibility to apply this principle (and the associated conservation laws of mass flow rate and momentum), even when considering the simple expression given above ($T = D \times (V_2 - V_0)$), it can be seen that the rotor thrust would be null because the air velocity ($V_2 - V_0$) becomes null either above or below the rotor (which makes the air flow tube collapse) and because the mean air mass flow rate D can also be considered as null in this intermediate regime where the airflow recirculate around the rotor periphery. Indeed in the VRS, the rotor wake being no more a well defined vortex tube but a vortex torus concentrated only at the rotor level, there is no induced velocities far downstream or upstream and thus $V_2 = V_0$. Therefore the variation of the momentum is null both because the net airflow rate D is null and because the rotor wake has no more effect on the global variation of the air speed between upstream and downstream ($V_2 - V_0 = 0$).

Figure 2-8 represents the different working regimes of a rotor. They are positioned here with respect to the non-dimensional speeds $\frac{V_i}{V_{i0}}$ and $\frac{V_z}{V_{i0}}$, considering a pure vertical flight. The autorotation, which is a also a stable aerodynamic regime is outlined in the figure.

► **Figure 2-8** The three stable working regimes of a rotor (helicopter / autorotation / wind-mill) and the unstable VRS.



Autorotation is a stable aerodynamic regime of the rotor, operating with no net power requirement from the engine system. The descent velocity upward through the rotor disk supplies the power to make turn the main rotor blades.

In ideal autorotation, the helicopter would descend at a rate equal to the rotor downwash, thus with no flow through the disk. The ideal autorotation would thus occur when $|V_z| = V_{i0}$. Actually the flow state presents considerable recirculation and turbulence, similar to the one that would be experienced by a circular impermeable disk of the same area. The operational autorotation occurs at a higher rate of descent, around $|V_z| = 1.8 \times V_{i0}$. Remember that V_{i0} is the mean induced flow in hover according to the momentum theory which sees this induced velocity as being uniformly distributed through all the rotor disk. But in reality there are different aerodynamic phenomena, like blade lift losses at the root and the tip of the blades, that make the induced velocity non uniform as the lift over the entire surface of the rotor. Therefore, in practice, the mean induced velocity through the rotor disk V_i is higher than V_{i0} (see the green curve on Figure 2-8). Hence the actual required induced power is higher than the theoretical one ($T \times V_{i0}$). The required power to make turn the blades includes also a part to overcome the profile drag of the blades. Thus, these different losses of energy explain that in the autorotation mode in order to make turn the blades more power is required from air than just the one given by a descent speed $|V_z| = V_{i0}$.

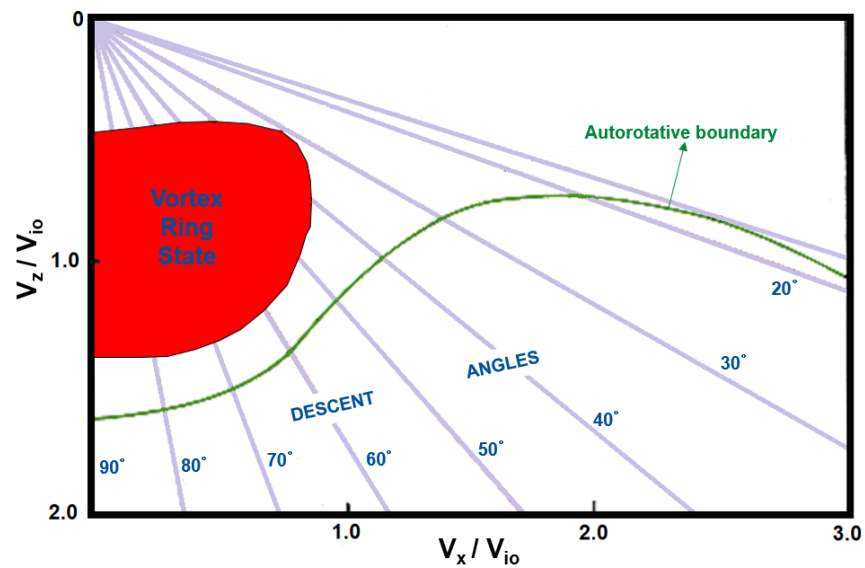
As shown in Figure 2-9, for a given forward speed, Vortex Ring State occurs at lower rates of descent than the autorotation regime.

It has to be noted that the vertical velocity reached in autorotation can be approximated by the following equation:

$V_{Z \text{ autorotation}} = -\frac{P_{\text{level}}}{m \times g}$ where P_{level} is the required power in level flight at the considered forward speed, m the helicopter mass, g the gravitational constant.

In vertical descent, VRS can be roughly considered occurring between vertical speeds of $-1.5 \cdot V_{i0} \leq V_z \leq -0.5 \cdot V_{i0}$. In descent with forward speed, as the rotor airflow and vortices will be blown away from the rotor disk as the speed is increasing, the VRS is limited to horizontal speed $V_x \leq V_{i0}$.

► **Figure 2-9** Vortex Ring State domain with respect to autorotation in terms of helicopter non-dimensional forward speed (V_x/V_{i0}) and vertical speed (V_z/V_{i0}).



Only few data are available on induced velocity measurements (mainly in vertical descents). These experimental data, collected during a PhD thesis performed at ONERA in 2002 [6] are shown in Figure 2-10. These experimental data can be found in [7], [8],[9], [10].

► **Figure 2-10** Experimental data of the induced velocity – taken from [6]

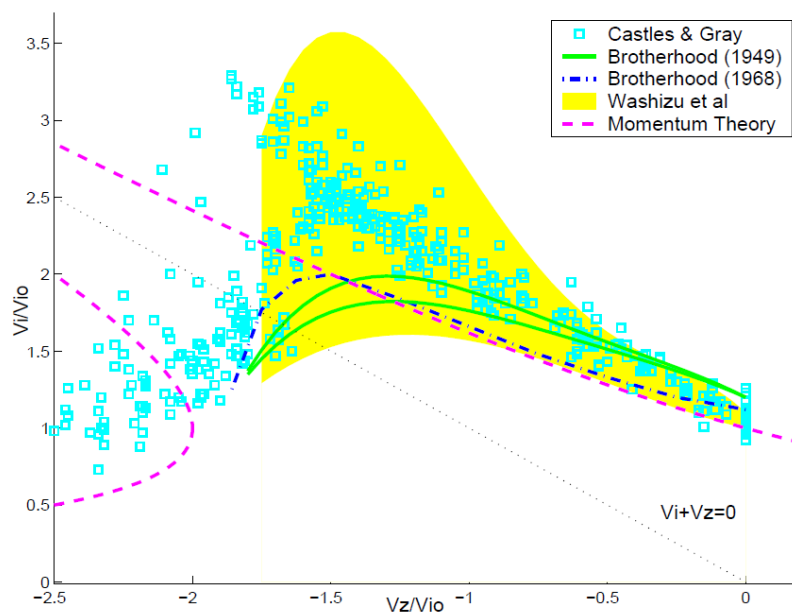


Figure 2-10 confirms that for negative vertical rates weaker than $-2V_{io}$, the momentum theory is no more valid. However, for higher rates of descent ($V_z < -2V_{io}$) the experimental data tends towards the lower branch of momentum theory solutions. This configuration of V_z corresponds to the rapid wind-mill state, for which the theory is applicable.

VRS symptoms will be highlighted in the next chapter but, from the practical standpoint, when entering into the VRS, the pilots feel some vibration and a lack of reactivity to the controls especially on the collective. But undoubtedly the most significant and unmistakable sign of the VRS is the unwanted sudden increase of the rate of descent.

This brutal downward acceleration is due to the collapse of the rotor lifting thrust no more compensating the aircraft weight. On a rotary wing in normal operation, the strongest lift forces are produced near the blade tip simply because the blade airfoil speeds relative to the air increase with their radial position. Therefore, the resulting overall lift thrust center on a rotary wing is located near 75% of the blade radius, whereas on a fixed wing, the lift distribution along the wing span is more symmetrical with an elliptical shape and the lift center located close to the middle of a rectangular wing. As exposed above, the vortex torus surrounding the rotor induces high rotor inflow near the blade tip. This strong downwash at low forward speed results in negative angles of attack on this tip quarter part of the blade making fall apart the lift. The rotor can no more take support on the air which is shrinking beneath the blades into this huge vortex torus in which the rotor wake has merged.

2.2 VRS symptoms, description and characterization

For the case of a main rotor VRS condition, the symptoms are generally excessive vibrations, large unsteady blade loads, thrust/torque fluctuations, and loss of control effectiveness and above all, an uncontrolled sudden increase of the rate of descent leading to excessive loss of altitude. Hence flight in the VRS is a dangerous flight condition, especially if entered at low altitude.

Thrust and/or torque fluctuations are part of the early sign of VRS. For **thrust oscillations**, the following results were reported in [11]:”

- They are more pronounced at oblique descent, with the rotor disk angle of attack α_D such that ($\alpha_D = 60^\circ - 70^\circ$) rather than at vertical descent ($\alpha_D = 90^\circ$);
- The loss in thrust indicates the most turbulent region of the VRS $-0.8 \leq V_z/V_{i0} < -0.6$;
- The period of the thrust fluctuations measured on a model rotor lies in the range 0.3 - 0.6 sec;
- Thrust oscillations appear to be independent of the disk loading;
- The range of variations of thrust oscillations lies in the order of 12 - 15 to 20% of mean thrust.”

A loss of average lift and severe lift fluctuations (similar to flying in heavy turbulence) are mentioned in [12]. This is recognised as sudden lightness in the seat (low g sensation) [12].

VRS boundary can be derived from rotor thrust fluctuations, especially during experimental tests where rotors are set in wind/water tunnels or numerical investigations using CFD methods as this will be detailed in next chapters.

As indicated in [13]:

“the VRS boundary can be determined from the magnitude of $\Delta T/T$ with two reference values set at 0.15 and 0.30, where ΔT and T are the amplitude of fluctuation and the mean value of the thrust respectively. When $\Delta T/T = 0.15$, the corresponding boundary extended from axial descent to inclined

descent with a forward velocity component of $V_x/V_{i0} < 1$. When $\Delta T / T = 0.30$, the corresponding boundary mainly covered the inclined descent region with descent angle (defined as the angle between the resulting airspeed vector and the rotor disk) ranging from 45° to 80° ."

"A significant **mean thrust reduction** can also be observed in VRS. As a result, thrust ratio C_T/C_{T0} was used as an indicator, where C_T and C_{T0} represented the mean thrust coefficient and the thrust coefficient in hover out of ground effect, respectively. It was shown that the lowest thrust ratio centered at about $\alpha_D = 75^\circ$ and $V_x/V_{i0} = 0.3$, and extended from $\alpha_D = 60^\circ$ to $\alpha_D = 90^\circ$."

From a more aerodynamical point of view and based on numerical computations as described in [14]:

"the fundamental characteristic of the Vortex Ring State is that the vorticity produced by the rotor in a descent configuration is not evacuated from this one. Moreover, the vortices tend to organize in vortex rings around the rotor plan, causing large thrust fluctuations and vibrations".

"The main event of the Vortex Ring State is the transition of vortex rings from a position below to a position above the rotor which is accompanied by a large thrust drop that characterizes the entry in the state. The establishment of the state is described by steadier vortex structures organizing in larger rings above the rotor. Instabilities that can develop in the flow pattern break the stable structures and vortices are thrown in the wake and through the rotor. Settling of the Vortex Ring State consists of the succession of stable vorticity accumulation and development of instabilities that force the breakdown of the ring which then moves through the rotor inducing thrust fluctuations. The development of steady vorticity windings around the rotor leads to a reduction of the effective angle of attack that decreases the thrust production."

For **torque fluctuations**, which may lead to directional (yaw) control problems, the following results were reported in [11]:"

- The increase in torque indicates the beginning of the VRS, $V_z/V_{i0} \approx -0.4$;
- The period of the torque fluctuation measured on a rotor model is about 3.7 sec;
- The torque fluctuation of a rotor with lower disk loading is larger than that of a rotor with higher disk loading;
- Compared with changes in rotor thrust, rotor torque variations are less significant;"

As reported in [13], "irregular variations of the rotor torque can be observed at about $V_z/V_{i0} = -0.28$. Torque fluctuations were more severe for $\alpha_D = 60^\circ$ and $\alpha_D = 75^\circ$ than in axial descent. As the descent angle decreased, torque fluctuations also diminished and finally disappeared below $\alpha_D = 40^\circ$."

Blade Flapping Fluctuations : The free-vortex wake method was applied in the VRS study by Leishman [15]. Besides thrust and torque fluctuations, it was suggested that blade flapping fluctuations may also be a concern as a result of unsteady airloads found near or in the VRS. An excessive blade flapping angle (greater than 10% of the mean) may lead to piloting difficulty.

Loss of control effectiveness is a widely experienced and documented symptom of VRS [16], [17], [18].

As indicated in [12], the helicopter may experience a reduction of control power (loss of effectiveness of cyclic and yaw control inputs) and/or sluggish rotor response in VRS.

This slow control response is caused by the reduced efficient length of rotor blade which is producing thrust and, therefore, able to respond to control inputs. [19]

If the control power is reduced on longitudinal and lateral cyclics, the loss of collective control effectiveness is certainly the most well known symptoms of the VRS.

It should be noted here that the term "Settling With Power" or "power settling" are often used as an alternative to Vortex Ring State to describe the condition. Settling With Power is actually a subtly different condition and

should be more accurately described as “Settling With Insufficient Power.” This latter condition can occur when attempting to arrest a low speed rate of descent but the power demands cannot be met by the engines within correct power limits; this is not true Vortex Ring State, but Vortex Ring State may develop from this condition if there is insufficient power to prevent the rate of descent increasing.

In addition to previous symptoms, **erratic fuselage movements** are commonly observed in VRS [12], [20].

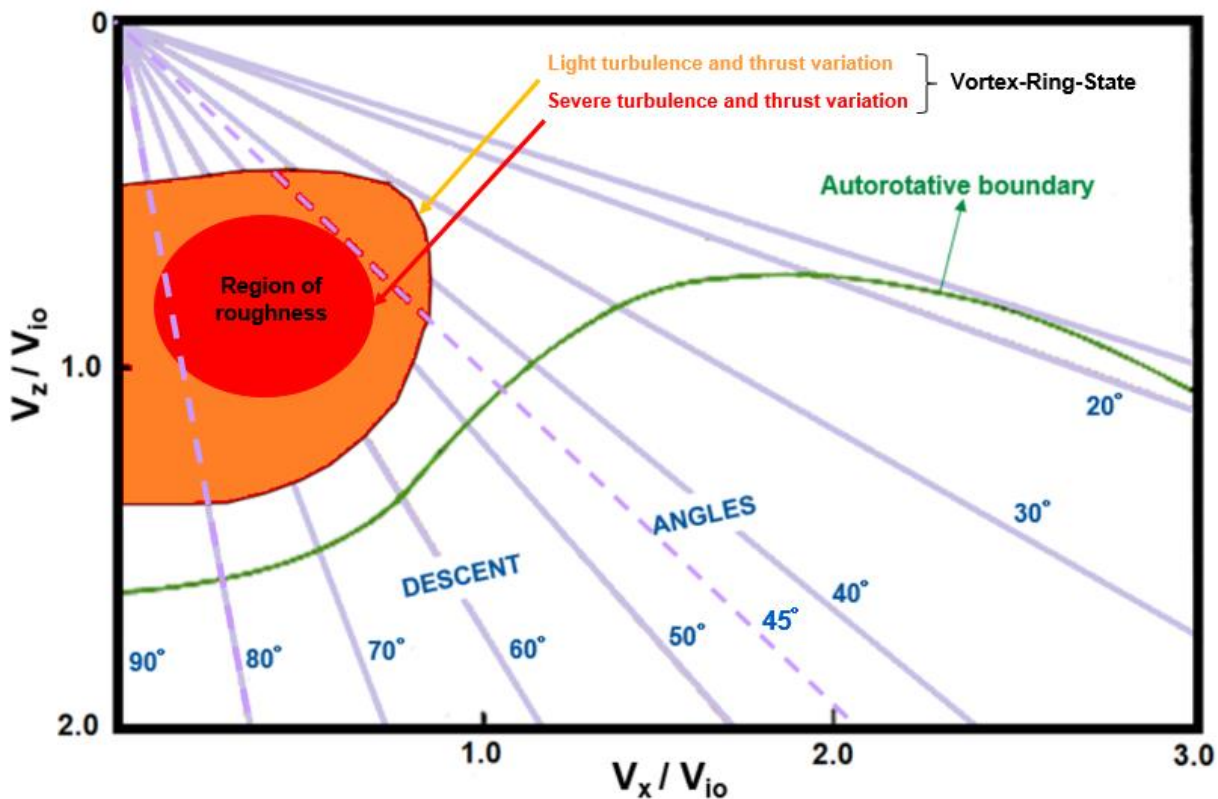
“Random pitching and rolling due to the complex airflow causing the rotor blades to flap without control inputs are also experienced as well as random yawing caused by the tail rotor being in the unstable airflow from the main rotor blade tip vortex region” [19].

These erratic pitch or roll moments are often described as “**region of roughness**”. In this region, the helicopter behaviour is rough with respect to attitude and control. Extreme nose-down pitching motion are also observed.

According to [21], “roughness and loss of control occur due to turbulent rotational flow on the blades and unsteady shifting of the flow along the blade span”.

While the region of roughness, also corresponding to severe turbulence and thrust variations, seems located “at the heart” of the VRS domain, VRS is characterised by an increase of turbulence and thrust variation. The region of roughness is entered for a flight path angle of about -45° for a certain speed range as it can be represented on the following Figure 2-11.

► **Figure 2-11** Speed envelope with respect to the VRS



Another commonly observed symptom of VRS is the change of the **vibration** spectrum felt in the helicopter. It can be found in [17] a large bibliographical review on VRS symptoms, and vibration increase as VRS is approached is largely documented. Thus,

- “The resulting flow is unsteady, hence a source of considerable low frequency vibration”;
- For some helicopter types, a considerable increase in vibration level can be observed while it is less noticeable on others;
- “The vibration measured in vortex ring state was characterized by large irregular pulsing of the vibration envelope at a random frequency, which probably indicated shedding of vortices”.

It can also be found in [19] that “significant vibrations are caused by vortices forming and breaking away, and the stall at the blade root increasing the pitch control forces.”

More generally, as outlined in [12], a change in rotor vibration can be observed in VRS. A more detailed analysis of the vibration experienced in VRS is presented in chapter 3.1.3

Finally, probably the most noticeable symptom of VRS consist in the **sudden and uncontrolled increase in rate of descent**. If the previous depicted symptoms can differ from one helicopter to another, the sudden increase in rate of descent is the common denominator in all VRS occurrences and could be used as a definition of the phenomenon.

As already mentioned, [17] provides a large overview of the influence of vortex ring state on rotorcraft flight dynamics and presents a review of experimental studies. VRS symptoms are described for different types of helicopters.

It is thus reported that:

“typically cues begin around 700-800 ft/min rate of descent. The cues include increased roughness followed by rapid buildup in rate of descent, and loss of control effectiveness.”

“For H-60 helicopter, VRS effect is measurable at descent rates above 700 ft/min and airspeeds from 0 – 20 kts and is worst at descent rates of about 1500 ft/min with airspeeds of 5 - 10 kts. Fully developed VRS is characterized by an unstable condition where the helicopter experiences uncommanded pitch and roll oscillations, has little or no cyclic authority and achieves a descent rate which may approach 6000 ft/min.

For H-46 helicopter, VRS is not restricted to high gross weights or high-density altitudes. It may not be recognized and before a recovery is performed considerable altitude may be lost. Helicopter rotor theory indicates that it is most likely to occur when descent rates exceed 800 ft/min during vertical descents initiated from a hover and steep approaches at less than 40 knots. Indications to the pilot are rapid descent rate increase, increase in overall vibration level, and loss of control effectiveness.

For MH-53E helicopter, the decreased rotor efficiency due to VRS will cause a loss of lift, increased roughness, and poor control response. A recovery may not be effected until considerable altitude has been lost. VRS is most likely to occur during conditions of high gross weight, high density altitude, low airspeed, downwind landing, and descending powered flight. Flight conditions causing VRS should be avoided at low altitudes because of the loss of altitude necessary for recovery. Recovery is best made by increasing forward speed and decreasing collective pitch. Increased collective pitch may further worsen the condition. According to the field manual, pilots tend to recover from a descent by applying collective pitch and power. If not enough power is available for recovery, applying collective pitch may aggravate VRS. This results in more turbulence and a higher rate of descent.”

Contrary to the common assumption (and previous observations), it was found during the ONERA/DGA-EV VRS flight tests that collective increase did not amplify VRS effects. The helicopter in fully developed VRS is generally insensitive to collective inputs. These observations, and more details, are reported in [16].

It can be found in [22] a description of the VRS symptoms occurring on Kaman K-1200 K-Max:

“If VRS occurs, the helicopter begins to be shaken with a frequency that assumes a sort of rhythmic vibration of the cabin. Observing the variometer the pilot can read unusual rates of descent, which can

increase when the pilot instinctively activates the collective step, worsening the situation. The loss of altitude is important, so it is necessary to act correctly on the controls.”

“...The K-MAX gives almost no warning signs. You realize you are in a vortex situation when you read on the variometer descent values in the order of 3000-3500 ft/min! In this case the helicopter stops more easily than other models: it is sufficient to pull the collective adding at the same time a bit of cyclic. In certain phases of the flight, the pilot when operating the pedals has to expect different reactions, especially when the helicopter is not carrying loads, the response is slow. For this reason in close proximity to the ground, you have to be very careful and manoeuvre with great caution”.

VRS symptoms observed on other helicopter types are described in [17] and [20].

2.2.1 Summary of VRS symptoms, description and characterization

The main characteristic symptoms of VRS are summarized hereafter:

- Thrust fluctuation;
- Torque fluctuation;
- Blade flapping fluctuation;
- Loss of control effectiveness;
- erratic fuselage movements;
- Region of roughness;
- Vibrations;
- Sudden and uncontrolled increase of the rate of descent;
- Loss of collective effectiveness .

These symptoms differ depending on the closeness of the phenomenon, when the helicopter is in the vicinity or already in a fully developed vortex.

Even though the VRS symptoms are more or less always the same, their amplitude, effects, feeling and perception by the crew differ from one helicopter to another.

This may be explained by the influence of the rotor technology, vibration absorber devices, overall fuselage architecture, on the way how VRS settles and how its symptoms (vibrations, control response, etc.) are propagated or felt.

The impact of a collective increase once entered VRS seems also very correlated to the helicopter type. It can be found that applying collective pitch may aggravate VRS (MH-53, K-Max, and indicated in [20]) while it was found during the ONERA/DGA-EV VRS flight tests (on semi-rigid rotors helicopters) that collective increase did not amplify VRS effects. Nevertheless, it is most generally observed the loss of collective efficiency once entered into VRS.

The most common and general symptom corresponds to a sudden increase in the rate of descent, which is observed for all helicopter types while the rate of descent reached during VRS will depend on the disk loading of each machine.

2.3 Review of the main parameters influencing VRS onsets

2.3.1 Rotor disk loading – downwash

VRS is characterized by the entry the rotor into its own downwash. The rotor induced velocity concerns the air being "pumped" downward and depends on disk loading (gross weight/rotor disk area) and air density:

$$DL = \frac{m \cdot g}{S}; \quad \text{while } V_{i0}: \text{ induced velocity in hover} = \sqrt{\frac{mg}{2\pi\rho R^2}} = \sqrt{\frac{DL}{2\rho}}$$

As mentioned in chapter 2.1, horizontal and vertical speed at which VRS occurs can be expressed by

$$V_z(\text{VRS}) \leq -0,5 \cdot V_{i0}$$
$$V_h(\text{VRS}) < V_{i0}$$

So It can be easily understood that as the vehicle disk loading is increased, the size (in terms of horizontal/vertical speeds) of the VRS domain, shifts downwards and grows dimensionally with the hover induced velocity V_{i0} .

2.3.2 Flight parameters

If the VRS boundaries were plotted in terms of dimensional values (V_h and V_z), then they would differ for varying atmospheric conditions. This effect is caused by the impact of air density on the induced velocity. For example, as density increases for the same gross weight, V_{i0} decreases so the vertical velocity must decrease in absolute value to remain outside the boundary. The onset of VRS is expected at lower rates of descent when operating at higher air density conditions.

In the literature, if disk loading (which deals with main helicopter characteristics and that is very simple to calculate) is commonly associated with VRS Domain size, it doesn't take into account air density. In [23], ONERA carried out an assessment of VRS occurrence (in terms of vertical speed, noted hereafter $V_{z\text{limit}}$) during helicopter steep descents. The assessment of VRS occurrence was performed on a generic helicopter (class 2 to 4 tons), using the fast time simulation environment. Simulations were realized by computing a VRS onset criterion (from [16] described in chapter 2.4.2.) with a set of various helicopter and atmospheric parameters (helicopter mass, temperature, pressure altitude) contributing to the proposal of a chart showing the influence of main helicopter and atmospheric parameters on the speeds at which the VRS may occur. Figure 2-12 gives an example of utilization of this chart. Starting from a temperature of 15°C (noted $T^\circ(c)$) at sea level and at 3000 ft of pressure altitude (Z_p), the corresponding point in plot 1 gives -1040 ft/min. In the second plot, the mass of 3700 kg gives approximately -987.5 ft/min. Finally, using the iso-airspeed curves of the third plot and selecting a 10 kts airspeed, the maximum vertical speed corresponding to VRS onset in these conditions is -887.5 ft/min.

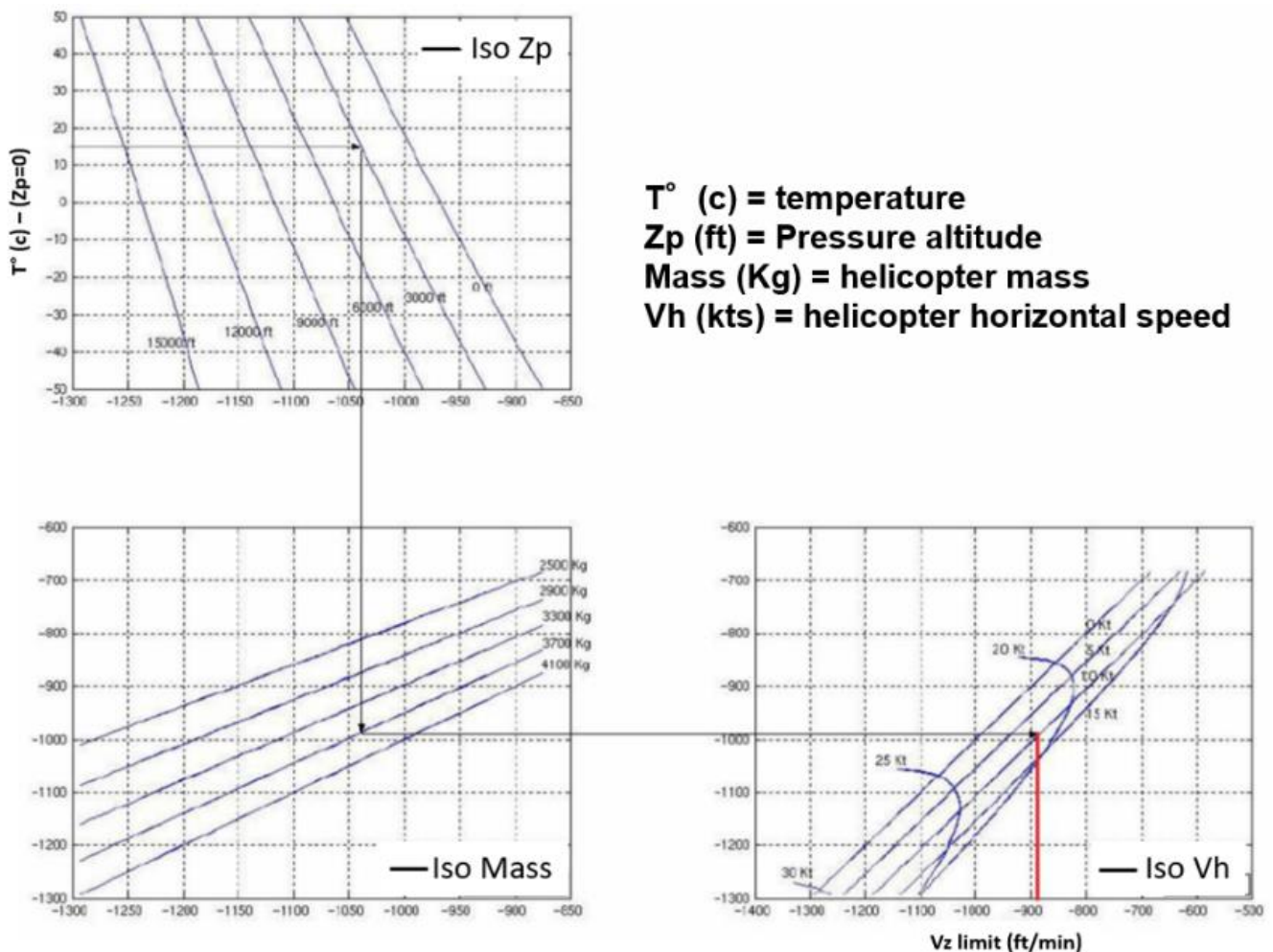
Nevertheless, we have to keep in mind that this chart is based on an empirical VRS onset criterion. In addition, as it can be seen, the potential variations of VRS vertical speed due to parameter variations are relatively small as outlined hereafter:

- Altitude effect: for the same temperature of 20°C at sea level, the same mass of 4100 kg, altitude variations between 3000ft and 12000ft provides interesting results. At 15 knots the maximum admissible rate of descent increases from -900 ft/min (3000ft) to -1050 ft/min (12000ft). At 25 knots this trend is reversed. The VRS rate of descent reduces from -1130 ft/min to -1050 ft/min.
- Temperature effect: starting with an altitude of 3000 ft, two different temperatures of -20°C and +20°C and a mass of 3300 kg, the maximum rate-of-descent seen at 15 knots changes from -750 ft/min to -800 ft/min. It corresponds to an increasing VRS entry V_z with increasing temperatures. At 20 kts the VRS onset descent rate is the same for both temperatures (-825 ft/min). At 25 kts, there is no VRS risk at this altitude and mass.

- Mass effect: at 20°C temperature (sea level) and 3000 ft altitude, increasing the mass results in an increase of VRS entry rate of descent. At 4100 kg VRS onset can occur for airspeeds below 25 kts and vertical speeds varying between -900 and 1150 ft/min. At 2500kg, the airspeed limit becomes around 18 kts for rates of descent between -700 and -900 ft/min.

Considering smaller range of variation of the input parameters, for example from -10 to +40° C for the temperature and altitude pressure less than 3000 ft. Then for a mass of 2500kg, VRS occurrence exists for airspeeds below 18 kts and vertical speeds between -700 and -900 ft/min. When the mass increases to 4100 kg, the minimum airspeed out of VRS occurrence grows to 25 kts. VRS entry rates of descent will then be located between -900 and -1150 ft/min. Any deceleration at these airspeeds should be done with a particular attention on the varying VRS onset limits.

► **Figure 2-12 VRS Vz limit assessment chart – taken from [23]**



As it will be discussed in the next chapters, the formation of VRS is a flight-path dependent phenomenon. This is to say that the onset of VRS is not only dependent on whether the instantaneous flight condition falls inside some VRS boundary; rather, it is also affected by the temporal evolution of the maneuver.

Additional considerations on flight parameters that may affect the onset of the VRS can be found in [24]:

Rate of descent:

“Basically the rate of descent in absolute terms is less important than the non-dimensional vertical speed V_z/V_{io} .”

As a first and rough approximation, boundaries to avoid the VRS are: $-1.5 < V_z/V_{io} < -0.5$.

Rate of descent at which the helicopter can meet VRS conditions is detailed in the next chapters.

Airspeed and measurement limitations:

“The uncertainty of VRS boundaries identification is not the only factor of danger for flights in steep descents”.

The limit of airspeed measurement system reliability depends on helicopter type and system installed. Modern helicopter types usually have this threshold at a value as low as 20 KIAS. (CS 29.1323 defines airspeed calibration requirement from 20 kts).

“The absence, or poor reliability, of airspeed measurement below 20 knots is a major factor of aggravation.

Indeed, as the pilot has no reliable information on its airspeed at low-speeds, he can lead the helicopter to the dangerous situation of VRS which depends on the relative airspeed between the main rotor and the air mass. This is mainly the case when a steep descent is performed in tail-wind conditions. Presently, pilots know that they must avoid descending at low speeds with a wind coming from the rear. However, this solution limits considerably helicopter’s operational envelope and the benefits operators can realize from its flight capabilities. Moreover, the current limitations during operations don’t efficiently prevent from the occurrence of accidents due to VRS phenomenon. In such conditions, the ability to predict the VRS onset and to warn the pilot of its limits approach appears as a necessity.

This lack of low-airspeed measurement capability is a non-event in IFR conditions. For an IFR approach, the approach may not to be flown at a speed lower than the minimum IFR speed. The minimum IFR speed is determined by the capability of the on-board equipment in determining airspeed, controlling the vehicle, etc., so the lack of airspeed measurement should never occur during an IFR approach. If low speeds are called for then the on-board equipment should be able to handle it, otherwise the aircraft is not allowed to proceed with the approach.”

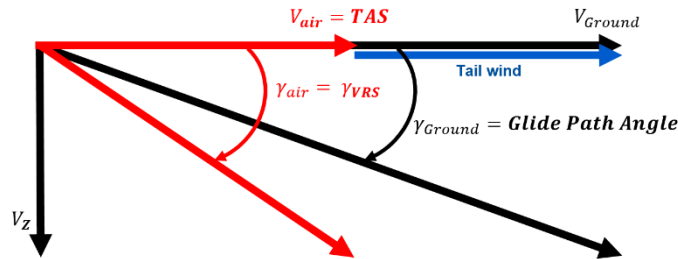
When transitioning from either an IFR approach or from a visual approach to hover over a helipad (FATO), the speed is reduced constantly, while the pilot usually is trying to maintain a constant glide path angle. As this will be discussed in the next sub-section “Accelerated flight (load factor) & Dynamic vortex”, while the pilot will still have an airspeed indication between the minimum IFR speed and 20 kts, this deceleration leads to increase the rotor disc angle of attack and thus, modifying the airspeeds seen by the rotor, especially the vertical component in rotor frame.

Head or tailwind:

In case of a non-zero wind the horizontal wind component V_{wind} , the horizontal air velocity V_{air} and the inertial horizontal velocity V_{Ground} are related to one another as follows: $V_{Ground} = V_{air} + V_{wind}$

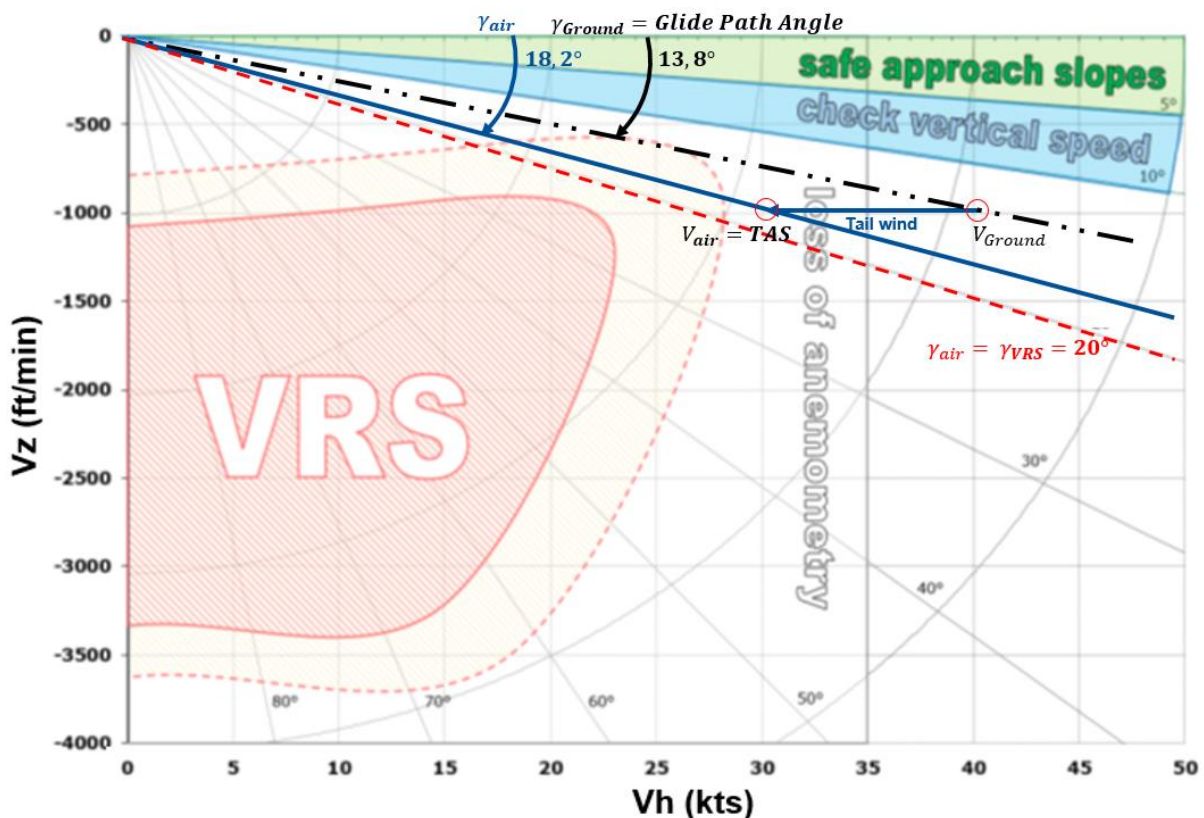
If there is a tailwind, i.e. $V_{wind} > 0$, then for a “fixed” ground speed to follow a prescribed glide path angle, the horizontal air velocity V_{air} becomes less than for the no-wind case as illustrated in following Figure 2-13.

► Figure 2-13 Speed components with tailwind



As shown in following Figure 2-14, based on [12], a tailwind would bring the flight point (40 kts of ground speed, $V_z = -1000 \text{ ft/min}$) closer to the region of VRS, as VRS domain is determined through forward airspeed and vertical speed. So decelerating on the approach to hover in case of a tailwind, or an increase in tailwind component on the approach, will result in an increased possibility of entering the vortex-ring state than with a headwind condition.

► Figure 2-14 Effect of tailwind on closeness to VRS - based on [12]



As described in [24]:

“To estimate the effect of tailwind on closeness to VRS, the horizontal wind component V_{wind} required to enter the region of the VRS, for two glide path angles γ_{Ground} and three rates of descent (RoD) has been computed.

Results are given in Table 2.1. The formula used is given hereafter:

$$\tan(\gamma_{Ground}) = \tan(\text{Glide Path Angle}) = \frac{RoD}{V_{Ground}}, \text{ thus } V_{Ground} = \frac{RoD}{\tan(\gamma_{Ground})}$$

And, considering a smaller “air glide path angle” γ_{air} at which VRS can be encountered equal to -20° :

$$TAS = \frac{RoD}{\tan(\gamma_{air})} \quad \text{thus} \quad TAS_{VRS} = \frac{RoD}{\tan(\gamma_{VRS})} = \frac{RoD}{\tan(-20^\circ)}$$

$$V_{wind} = V_{Ground} - V_{air} = V_{Ground} - TAS_{VRS}$$

These tailwind values are quite large, and under operational conditions, a runway change would long have been made. One issue could be in visual flight conditions where no TAS measurement is available (usually below 20 kts). In these conditions, the pilot has no precise indication of his airspeed while he focuses on a ground reference point. Consequently, a tailwind will decrease the airspeed while the pilot won’t notice it. If the airspeed becomes too low (below 20 kts), glide path corrections could generate rates of descent higher than VRS onset conditions. The situation is all the more prone to happen as usually helicopters handling qualities are degraded at low speeds and have been quoted as a source of large flight deviations.”

Table 2-1 Tailwind needed to enter the VRS

Parameters	Flight regime					
	VRS ($\gamma_{air}=20^\circ$)					
	Nominal Glide Path Angle γ_{Ground}					
	6°			9°		
	RoD (ft/min)			RoD (ft/min)		
	600	800	1000	600	800	1000
V_{Ground} (kts)	56.3	75	94	37.4	50	62.3
TAS_{VRS} (kts)	16.2	21.7	27	16.2	21.7	27
V_{wind} (kts)	39.8	53.3	67	21.2	28.3	35.3

Nevertheless, it has to be noted that the constraint raised by tailwind is mitigated by a strict monitoring of the rate of descent. As it can be seen in Figure 2-14, high aerodynamic glide angles can be reached as long as the rate of descent remains higher than -1000ft/min . Performing a vertical descent, with $\gamma_{air}=90^\circ$, is possible without entering VRS if the rate of descent is moderate.

Accelerated flight (load factor) & “Dynamic vortex”:

The impact of an accelerated flight is depicted in [24]:

“Under this heading fall the normal acceleration n and the (longitudinal) deceleration A_x . In case of accelerated flight the rotor thrust relates to the rotorcraft weight (W) roughly as:

$$T \cdot \cos(i_{mr}) = n \cdot W$$

Where i_{mr} is the rotor mast tilt angle with respect to the vertical to the fuselage waterline. From this equation, one can derive the expression for the induced velocity in hover:

$$v_{i_0} = \sqrt{\frac{T}{2\rho\pi R^2}} = \sqrt{\frac{nW / \cos i_{mr}}{2\rho\pi R^2}}$$

So in level turning flight, for example, the induced velocity V_{i0} increases with \sqrt{n} , and hence the non-dimensional velocities V_z/V_{i0} and V_h/V_{i0} decrease, i.e. bringing the rotorcraft closer to the VRS boundary.

Another important acceleration aspect is the longitudinal deceleration A_x . When the rotorcraft is decelerating in level flight, the rotor disc angle of attack increases more or less linearly with the deceleration rate. From equilibrium of forces one can write for the longitudinal & vertical force balance:

$$\text{Equation (1)} \quad \left. \begin{array}{l} T \cos i_{mr} \sin \theta = mA_x \\ T \cos i_{mr} \cos \theta = W \end{array} \right\} \Rightarrow \tan \theta = \frac{mA_x}{W} = \frac{A_x}{g}$$

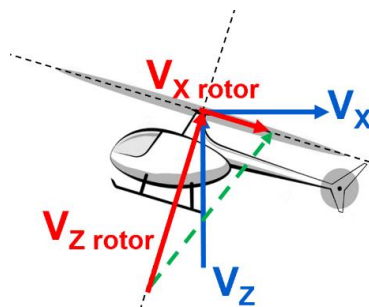
If the deceleration is 0.1g for example, then the increase in pitch angle, which also equals an increase in rotor disc angle of attack, is $\tan^{-1}(0.1) = 5.7^\circ$. This value has to be added to the current glide slope followed by the helicopter. It is obvious that any increase brings the rotorcraft closer to the VRS boundary.”

The effect of a maneuver distorts the rotor wake, and hence may affect wake stability, and may potentially affect the VRS boundary [11]. Acceleration or angular rate are indeed known to affect the onset and development of the VRS [25], [26]. For example for pull-ups or for other types of maneuvers that increase the rotor disk angle of attack, VRS onset conditions could be attained at a lower rate of descent and/or at higher forward speed, than predicted by the VRS boundary [1], [15].

In [27], the theoretical aspects of the vortex phenomenon are reviewed, showing their limitations and the important aspects for the pilots. The dynamic vortex is discussed and the main characteristics presented hereafter:

Quasi-vertical descent is a very rare flight condition to enter VRS. It is therefore most probable to enter VRS during final approach or tailwind. The particularity of conventional helicopters is that there is no determined relationship between pitch attitude and slope. With a nose-down attitude, one can be in descent, level or climb. When approaching to brake, especially on modern aircraft for which parasite drag has been minimized, the only way is to take a high pitch attitude. And in order not to climb, to reduce the power. In general, pilots do not look in the cockpit and it is the ground scrolling and the height that are used to control the trajectory. Considering the velocity decomposition (in earth frame) shown in the following Figure 2-15, with a $V_x = 12.8$ m/s (25kts) and $V_z = -4$ m/s (-787 ft/min), the total aerodynamic velocity is 13.4 m/s, but the V_z of the rotor depends on the pitch attitude as shown in Figure 2-15.

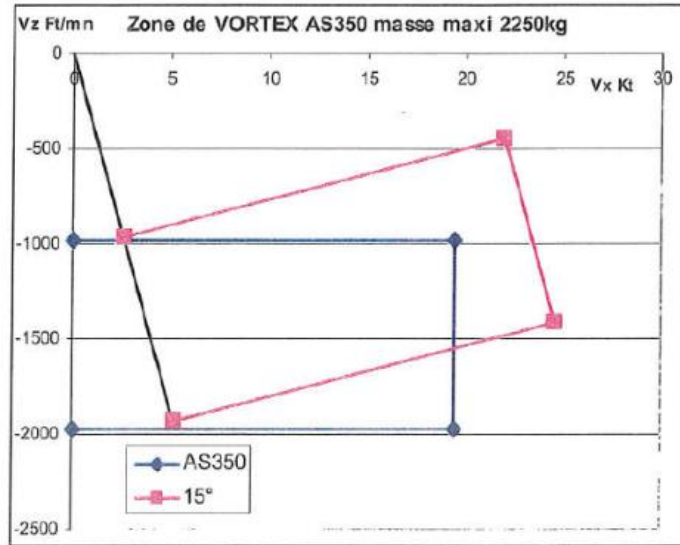
► **Figure 2-15** Decrease of the rotor longitudinal speed and increase of the rotor vertical speed with nose-up attitude



Thus, considering a 10° pitch up attitude, $V_{x \text{ rotor}} = 11.9$ m/s (23 kts) and $V_{z \text{ rotor}} = -6.17$ m/s (-1214.6 ft/min - in rotor frame), leading the rotor closer to VRS.

This change of axis can be represented more simply by drawing the critical VRS zone in the earth axes in Figure 2-16, taken from [27].

► **Figure 2-16** Critical VRS zone affected by nose-up attitude - taken from [27]



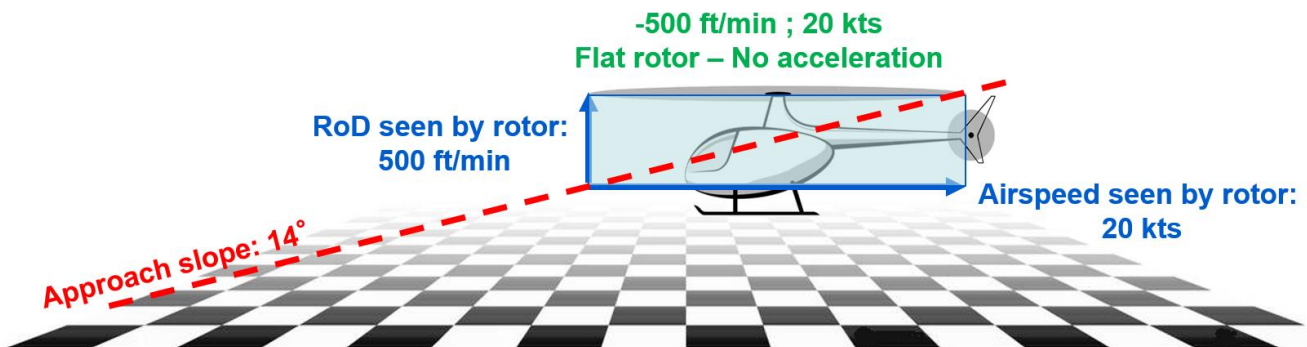
Considering a rough estimation of the VRS domain, from -1000 ft/min to -2000 ft/min in Vz, and up to 20 kts in forward speed, then with a 15° pitch-up attitude, VRS could be entered at a Vz=-500 ft/min. With Headwind, the pitch down to zero will be performed at around 30-40kts of indicated airspeed, but with a tailwind of 15 kts, a late pitch-down maneuver will lead into VRS domain, while the ground scroll will not indicate to the pilot that he is already almost in vertical descent.

It is also the case, mainly for light helicopters, during a turn with a high headwind: In order to keep the same ground speed, the pilot will have a tendency to reduce the airspeed, potentially leading to VRS domain.

More examples are available in [12]:

“In low-speed descending flight the horizontal component of the airspeed (say, 20 kts \cong 10 m/s) will be combined with the vertical rate of descent (RoD). The angle formed by the two speeds (forward and vertical) is the flight path angle, also called the approach slope in the final approach. For example, 20 kts combined with a 500 ft/min rate of descent gives a flight path angle of 14° (see Figure 2-17). Contrary to the 3° approach slope of fixed-wing aircraft, it is not unusual for a helicopter to conduct approaches at much steeper angles of 10°, even 15°.”

► **Figure 2-17** Classical helicopter flight path – based on [12]

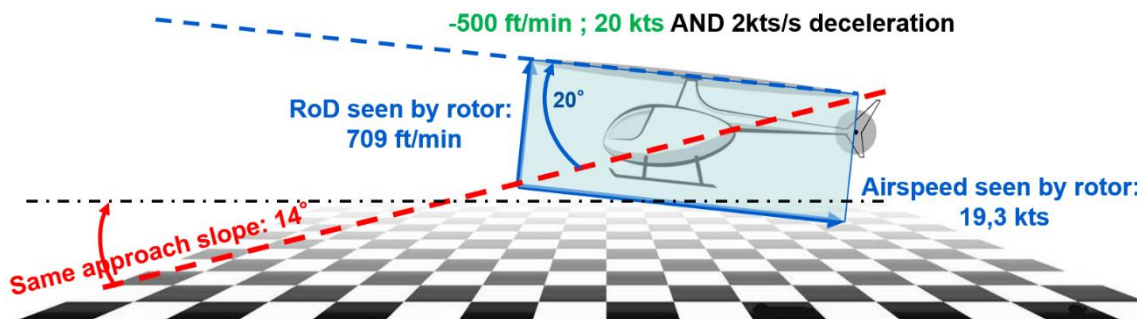


“As previously shown in Figure 2-14, we may be approaching or entering VRS at -1000 ft/min in vertical descent. The onset of VRS (i.e. -1000 ft/min) does not significantly change at low speeds, up to 20 kts. Above 25-30 kts there is almost no chance of VRS. If we combine a RoD of 1000 ft/min with 20 kts we obtain a 26° approach slope, which is much higher than the usual 5°- 10° slope of everyday helicopter operations. However, two basic elements that separate low speeds from hover should be taken into account, with regards to VRS:

1. In final approach, low speed is only a transient phase of a decelerating flight, from 60-80 kts of steady descent towards the near zero of landing. The deceleration rate is not perfectly monitored by the pilot, and the wind direction and strength are not always known. Therefore flying at 30-40 kts (outside VRS) can be quickly transformed into flying at 10-20 kts in a matter of seconds in terms of airspeed seen by the rotor.”

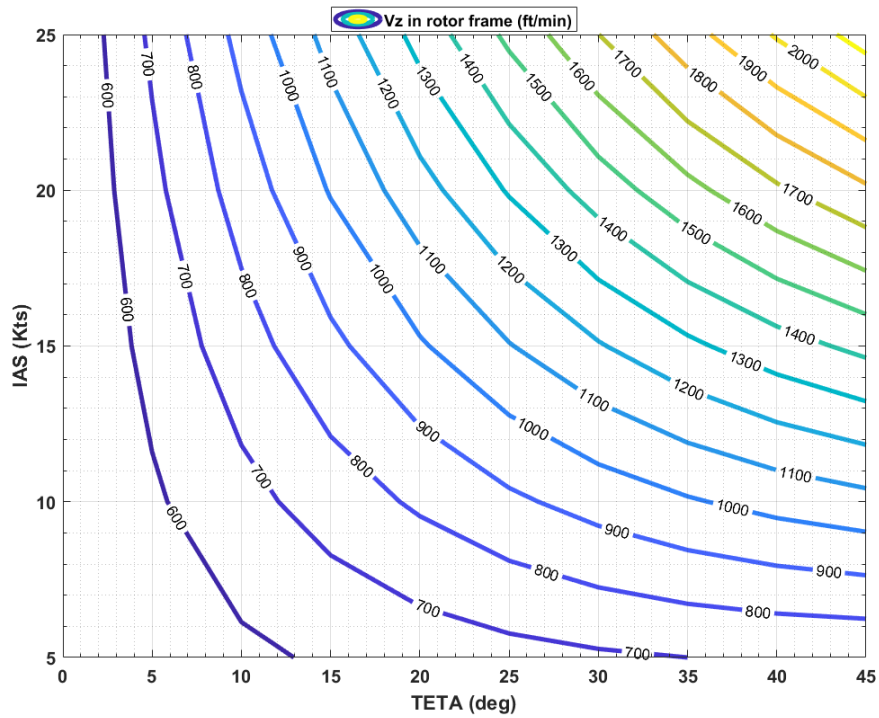
2. As highlighted in Figure 2-15, when decelerating the helicopter, the rotor maintains a positive tilt angle of 5°, possibly 10°. The rotor tilt angle is not to be confused with the helicopter pitch attitude. Sometimes, inadvertently, the rotor tilt angle can raise above 15°. A reasonable approximation regarding deceleration is that the rotor must tilt upwards (pitch-up) by 3° for every knot-per-sec of deceleration. For instance, if we decelerate smoothly from 40 to 20 kts in 10 sec, then the deceleration rate is 2 kts/sec, and the rotor tilt is +6° as this can be calculated thanks to Equation (1). Now, in the previous example of 20 kts and 500 ft/min (=approach slope of 14°), if we add the 6° of rotor tilt coming from deceleration, we obtain a total angle between rotor disc and approach slope of 20°. It is as if the rotor was effectively seeing a RoD of 709 ft/min, which is much closer to the 1000 ft/min VRS threshold in our example (See Figure 2-18).”

► **Figure 2-18** Classical helicopter flight path in deceleration – based on [12]



In the same way, considering a constant vertical speed of -500 ft/min in earth frame and the transformation between the earth frame and the helicopter frame, it is possible to plot (see Figure 2-19) the rate of descent seen by the rotor depending on the helicopter airspeed (IAS) and pitch angle (TETA). The previous values can be found again, when looking at an IAS of 20 Kts and a pitch angle TETA of 6°.

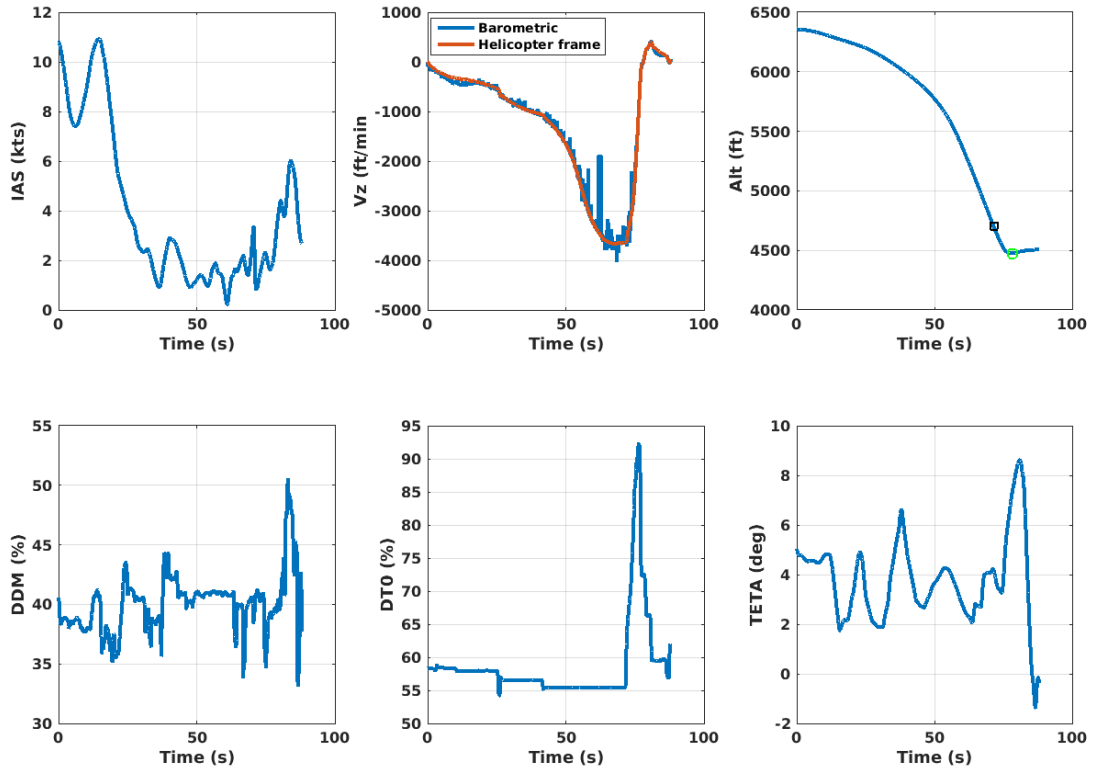
► **Figure 2-19** RoD seen by rotor depending on IAS and Pitch angle



Another example of the difference between the barometric vertical speed monitored by the pilot and the vertical speed seen by the rotor is given in the following figures. Some VRS trials were performed by a French Army helicopter pilot in the real-time ONERA’s simulator in July 2022. The helicopter model was an EC225, at a weight of 6000 Kg. ONERA’s simulator runs the flight mechanics code HOST (Helicopter Overall Simulation Tool) from Airbus Helicopters, integrating the VRS model implemented by ONERA in 2003 that will be described in next chapters, and that is detailed in [6], [16], [28], [29].

In Figure2-20 the pilot entered VRS by successive collective reductions (DT0) while maintaining a low indicated airspeed (IAS).

► **Figure 2-20** VRS entry during steady maneuver in ONERA’s simulator

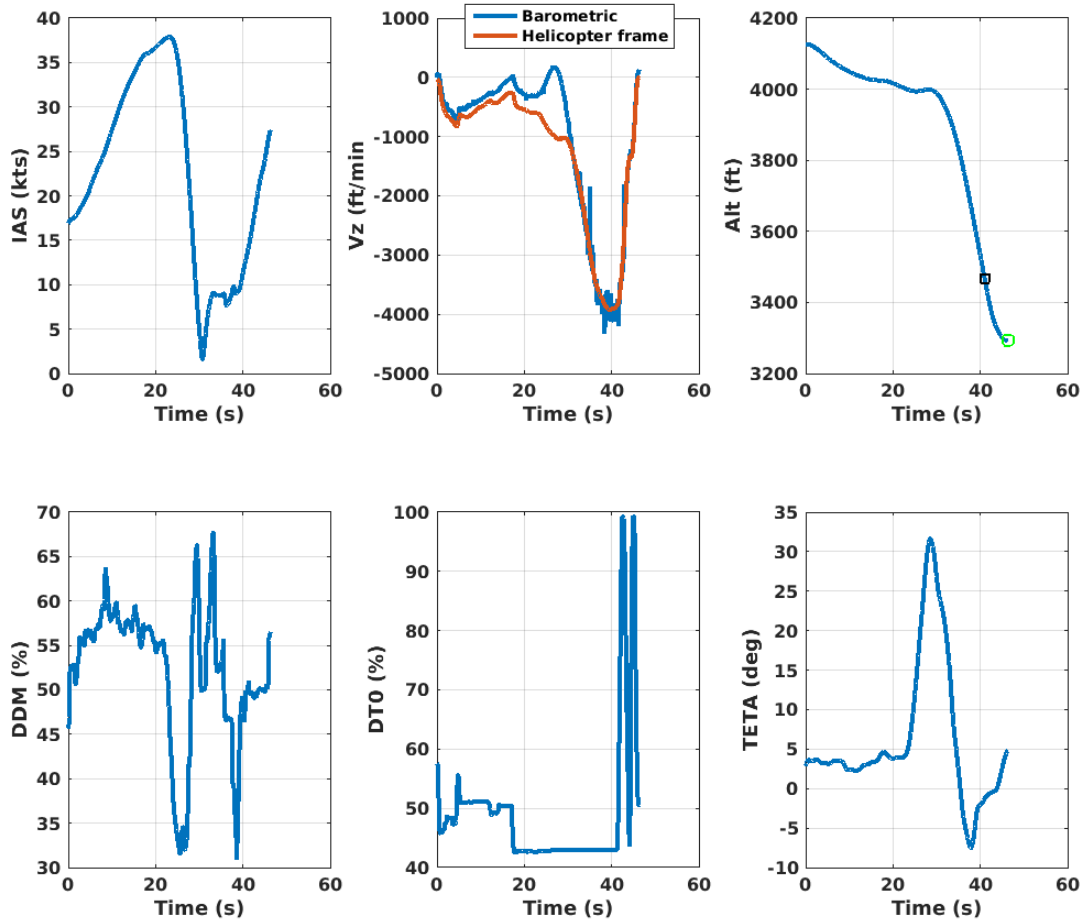


The maneuver was done smoothly, the pitch angle TETA showing very light variations around 3°. On the vertical speed graph (V_z), the barometric vertical speed (based on the altitude derivative) is shown in blue, while the vertical speed in helicopter frame (i.e. rotor frame) is shown in red. In this maneuver, vertical speeds are very similar and the VRS occurred after the last collective decrease at around -1000 ft/min.

In Figure 2-21 the pilot entered VRS by a collective decrease (DTO) associated with an airspeed reduction (IAS) through a pitch-up attitude (TETA) started at 22s. The pitch angle was increased up to 30° leading to a large difference between the barometric vertical speed (in blue) and the vertical speed in helicopter frame (in red). The VRS entry is relatively difficult to precisely determined, as the both vertical speeds decrease with the pitch-down attitude performed before 30s. Nevertheless, it can be clearly observed that barometric and vertical speed in helicopter frame can highly differ (here the maximum difference is higher than 1000 ft/min).

It can be seen on both figures that the pilot exited the phenomenon by a large increase of collective (DTO) while being in a fully developed VRS. The simulator doesn’t integrate a realistic engine model, so power is always provided, rotor RPM is always maintain, and there’s no limitations due to the engine or main gear box. It is thus possible to pull 100% of collective.

► Figure 2-21 Dynamic VRS entry on ONERA's simulator

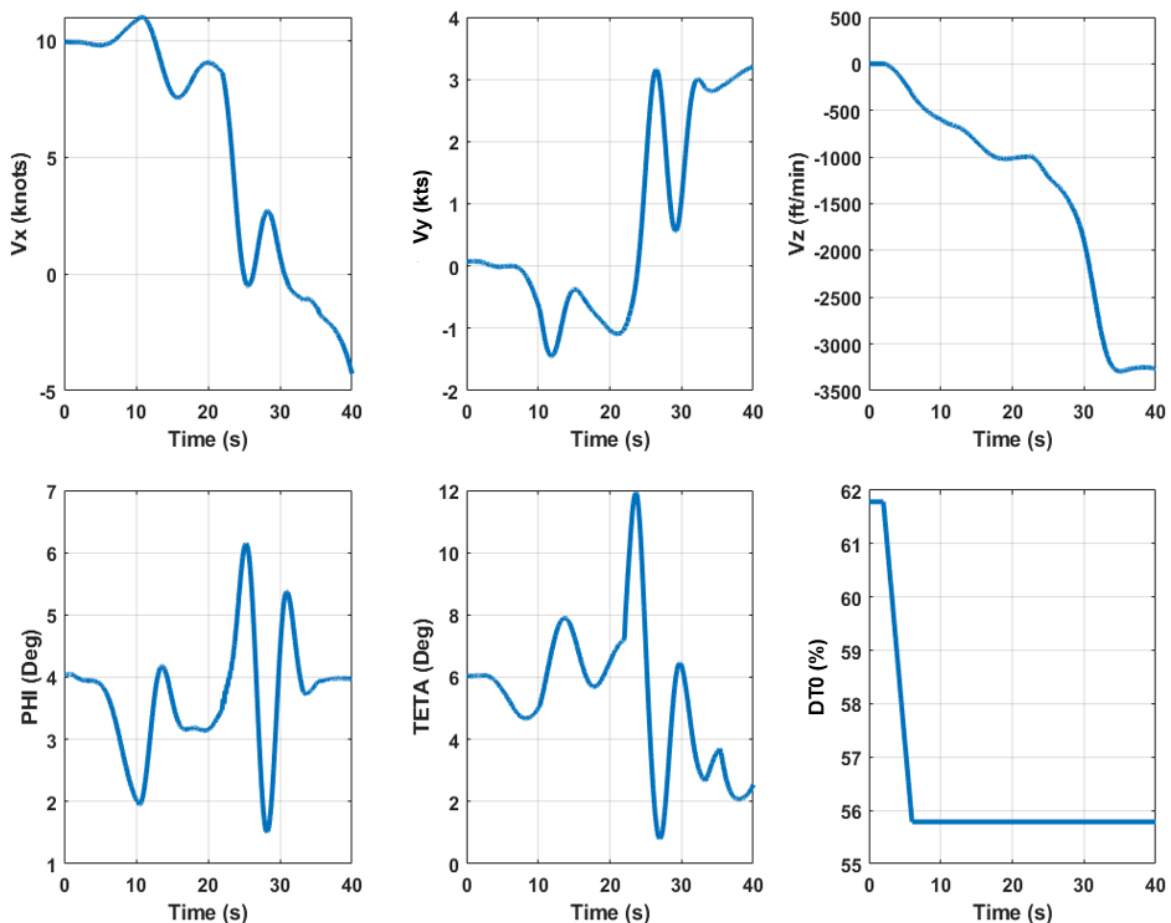


As shown later (sub-chapter 3.1.1, 3.1.2), it can be seen a change in the relation between collective pitch and the vertical speed in VRS. The relation $DT0/V_z$, monotonous in normal flight conditions (meaning that, at a constant forward speed, a vertical speed corresponds to a collective value) is no more valid around VRS. On the boundaries of the VRS domain (in terms of vertical speed), one collective value corresponds to two very different vertical speeds. The ONERA model consists in a modified induced velocity model in steep descent that, as a consequence, changes the relation between collective pitch and the vertical speed. The large increase of the rate of descent is the result of a kind of hysteresis in the relation $DT0/V_z$. Slight decreases of the collective can lead to large rate of descent but on the other hand, it is possible to recover from these high descent rates by a large increase of the collective.

In real flights, as observed during flight test and show in next chapters, it would certainly not be possible to exit VRS by a unique increase of the collective pitch. In addition, the pilot would take care about engine/MGB limitations (at least during training/test flights) and the collective increase would be very limited compared to what was done in the previous figures.

Other examples of dynamics vortex entry are given hereafter. Figure 2-22 represents the result of a simulation performed with the HOST code through off-line simulation. The helicopter model is a Dauphin AS365N and serie of automatic modes enables to stabilise and control the helicopter model. Starting from a 10 kts airspeed (V_x), a collective decrease (DTO (%)) is done at 2s, leading the helicopter to a rate of descent (V_z (ft/min)) of around -1000 ft/min. While close to the VRS, the RoD stabilises. Then, at 22s, a quick stop maneuver is initiated at constant collective pitch by an increase of the pitch angle. The change in airspeed seen by the rotor lead to VRS, easily seen on the rate of descent. The rate of descent finally stabilises at around -3250 ft/min.

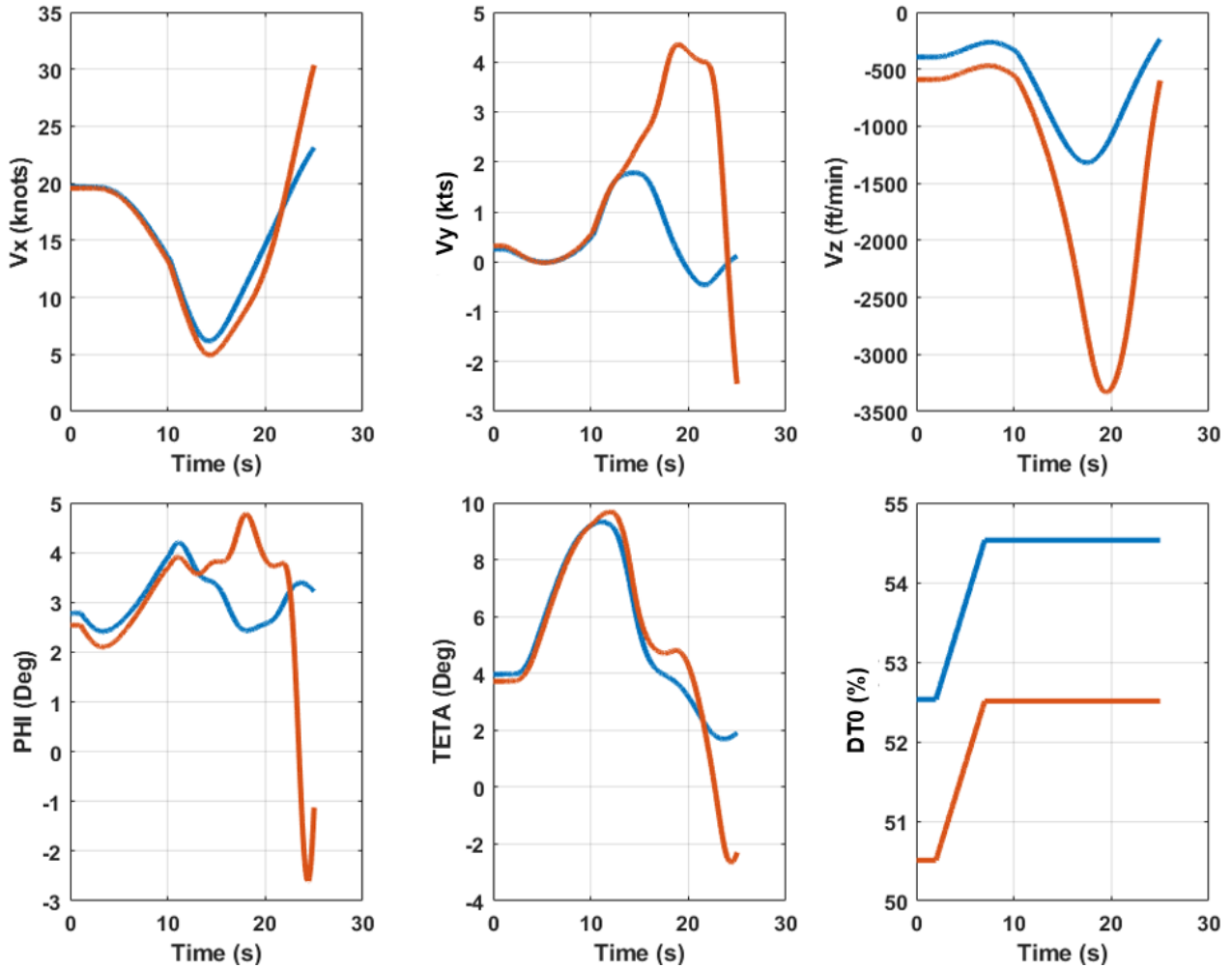
► **Figure 2-22** Dynamic vortex through off-line simulation of pitch attitude variation



Another HOST simulation of a dynamic vortex is given in the following Figure 2-23, where a “level-off” is done from a pitch-up attitude realised from an initial airspeed of 20 kts and an established rate of descent of around -400 ft/min for the blue curve, -590 ft/min for the red curve. At the transition from nose-up to level, the resulting rate of descent reaches -1250 ft/min in the first case, while the helicopter enters VRS in the second case, before existing it by an increase of the forward airspeed. The same behaviour would be observed in rear flight, from a nose-down attitude to level.

This clearly demonstrates that performing pitch variation at low speeds can lead to VRS even if the rate of descent seems safe with respect to VRS, here around -500 ft/min. These kind of maneuvers are sources of number of VRS accidents.

► **Figure 2-23** Nose-up to level attitude variation through off-line simulation



As previously stated, acceleration or angular rate affects the onset and development of the VRS by increasing rotor disk angle of attack, and thus, modifying the airspeeds seen by the rotor, especially the vertical component in rotor frame. Dynamic vortex can occur when speeds in rotor frame are different from anemometric and barometric speeds monitored by pilots. VRS onset conditions can thus be attained at a lower rate of descent and/or at higher forward speed than predicted by the “static” VRS boundaries, where it is assumed that rotor and fuselage have the same airspeed components.

2.3.3 Rotor/blade design parameters

Some guidelines related to rotor and blade design considerations are presented in [11]: “

- There are no substantial differences in VRS inflow curves due to variations in rotor RPM and rotor radius;
- The effect of blade taper on VRS is weaker than the effect of blade twist;
- For moderate blade twist, blade stall has no effect on the descent rate for VRS onset. It is still possible however that stall could influence the subsequent development of the VRS;
- For moderate blade twist, the influence of twist on the behaviour of the rotor is relatively minor;
- For high blade twist, the influence of twist on the behaviour of the rotor is more pronounced. Such rotors with high blade twist seem to be more susceptible to VRS onset [1], [15]. But the appearance of blade stall on the inboard parts of a rotor, with highly twisted blades, was also shown to reduce the violence of the VRS;
- Thrust settling is associated with a considerable fall in blade loading but only at the outboard sections of the blade. The inboard sections of the blade play only a small role in the thrust settling phenomenon.”

In [30]:

- “it is suggested that, in addition to the disk loading effects, the high levels of blade twist may expand the VRS regime to a wider range of operational descent velocities and to higher forward speeds than is the case for rotors with more lightly-twisted blades.”

“The onset of the VRS is related to the unstable growth of disturbances in the structure of the rotor wake. The VRS is encountered when the net convection of these growing disturbances away from the rotor becomes low enough for vorticity to accumulate near the plane of the rotor, significantly affecting blade loads and rotor performance. The onset of VRS, as well as the behaviour of the rotor within the VRS, is not solely determined by the operating conditions of the rotor, such as descent rate and forward speed, but is also dependent on details of the design of the rotor such as the degree of twist incorporated into the blades. The work presented in [30] suggests that blade stall also plays an important role in governing the behaviour of the rotor in the VRS.”

Additional aspects that may also influence the VRS are rotor/fuselage aerodynamic interference [31], rotor disk angle of attack [15], blade stall [25], blade root cut out location, blade planform taper [25], and blade spanwise loading distribution. On the other hand however, it appeared that the VRS region was insensitive to tail rotor interference [31].

2.3.4 Aggravating factors

In this section, largely based on [12], it is presented some conditions or situations where the helicopter can be found even closer to the VRS boundaries, whether intentionally or unintentionally. Thus, besides the general knowledge of VRS provided previously, special attention must be also given to the following information.

1. Flying light

As already shown in the sub-section 2.3.2 and Figure 2-12, a reduction of the helicopter mass reduce the RoD at which VRS may be encountered.

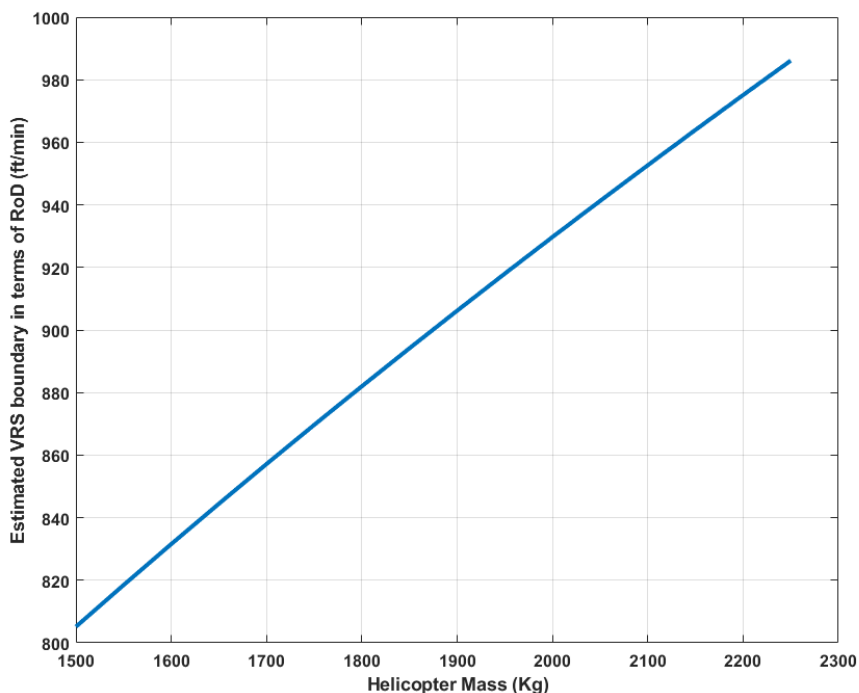
When a helicopter flies relatively light, the average speed of its rotor downwash is also reduced. As the VRS range is roughly determined as one-half of this downwash speed, the VRS boundary, in terms of RoD, will be reduced as shown in the following Figure 2-24. Using the simple formulation of the induced velocity in hover:

$$V_{i0} = \sqrt{\frac{mg}{2\pi\rho R^2}}$$

the helicopter mass is varied from 1500 Kg to 2250 Kg, leading to a variation of the VRS boundary from -800 ft/min to -1000 ft/min as shown in this Figure. Rotor Radius R used here corresponding to an AS350, ρ being equal to 1.225 Kg/m³

One can note that a variation of 10% of the helicopter mass lead to a variation of about 5% of the estimated rate of descent at which VRS can occur. This is also the case for a variation of the air density, but the effect is inversed. A decrease of 10% of the air density leads to an increase of around 5% of the VRS onset's rate of descent.

► **Figure 2-24** Evolution of the estimated VRS upper limit w.r.t helicopter (AS350) mass



“Of course, the required margins must be adjusted accordingly. On the other hand, flying light generally means a greater power margin available to cancel out an excessive RoD.

2. Flying with tail wind close to the surface

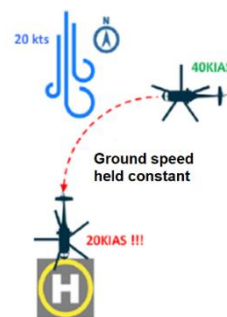
This paragraph is applicable to all evolutions close to the surface, including landing when no head wind option is possible (tail wind landing not recommended). While tailwind effect on VRS entry has been already outlined in the previous chapter, some operational flight cases and considerations are presented hereafter.

When flying close to the ground the pilot uses the ground speed to pilot the trajectory (instead of airspeed when higher). In doing so, when turning tail wind, the pilot reduces the airspeed to maintain (or even decrease) ground speed. As a consequence the necessary power for level flight is increased. If the pilot is not attentive, a significant RoD appears. This RoD is even more important in the event of a tail wind approach due to the necessity to maintain the approach slope.

When the helicopter descends at 40 kts (ground speed) with a tail wind of (say) 20 kts at that moment, then the airspeed becomes 20 kts and we are approaching the VRS danger zone, depending of course on the RoD. In mountainous terrain or urban areas especially, where the speed direction and strength may vary significantly, additional attention has to be given to the low airspeed phases of the flight.

Another potential case is approaching to land after a turn (as shown in Figure 2-25). Supposing a 20 kts wind coming from the north with a helicopter approaching at a 270° heading (westbound), with 40 kts of airspeed. Then, just before landing the helicopter performs a 90° left turn (new heading is now 180°). On exiting the turn the helicopter will find itself again with a tail wind of 20 kts, and thus its airspeed will drop suddenly to 20 kts. In that case the helicopter is approaching the VRS danger zone and if power is not adjusted this will result in increased RoD, with the aforementioned consequences.

► **Figure 2-25** VRS potential flight case – taken from [12]



3. Small power margins

Although small power margins are not directly linked with the VRS range (airspeed, RoD, deceleration) they can become a strong contributing factor when combined with poor management of the sink rate (RoD). When a helicopter is heavy and/or in high-density altitude (i.e. hot & high), and reduces its speed then the power required to sustain flight increases rapidly. The pilot has to pay special attention to the power management through the collective, because an intended RoD of 300-400 ft/min can easily take on higher values in these conditions (above 500 ft/min, thus approaching the VRS boundaries).

4. Flying in a degraded visual environment and at night

When visual cues are degraded (fog, clouds, dark night) and the crew is in its final approach (descending flight, low speed, deceleration) it may be difficult to determine the altitude, airspeed, RoD, and pitch attitude, without continuously scanning the instruments. Even the deceleration rate (roughly proportional to the pitch attitude increase as shown previously) cannot be felt as a longitudinal force (similar to braking inside a car) because of the helicopter's specific mechanics. Moreover, under these conditions but with some minimal visual cues (i.e. helipad lights only) sensory illusions (spatial disorientation) can lead to a false understanding of the position and speeds of the aircraft. To make matters worse, there have been numerous incident & accident reports where both pilots during final approach, in their intense search for visual references, neglected instrument scanning for a short period of time, finding themselves with unacceptable RoD and/or pitch attitudes close to or within the VRS boundaries.

5. Rapid deceleration

As previously mentioned, the deceleration rate during final approach, roughly proportional to the increase of pitch attitude (3° more for every 1 kt/sec), changes the effective RoD of the rotor disc. Sometimes pilots, from fear of overshooting the platform or helipad, decelerate hard in the last seconds before landing, combined with an already established RoD. In this case, the helicopter comes

closer to the VRS boundaries. Thus, hard decelerations are to be avoided, especially during descent. It should be noted that rapid decelerations (quick stops) might be inadvertently combined with other aggravating factors, such as tail wind. The combination of two aggravating factors can lead the helicopter closer to VRS conditions.

6. Confined environment

Small helicopters often operate and land inside city blocks and other confined environments. In this case, pilots usually choose steep approach slopes, which can bring them close to the VRS boundaries. Moreover, wind through big city buildings, and recirculation of the downwash of the helicopter itself can make the conditions even more complicated. The RoD must then be carefully monitored and held at less than 500 ft/min.

7. Collapsing updrafts at low speed or hovering out of ground effect

Updrafts can either have thermal or dynamic origins. Thermal winds are usually less constant than dynamic ones. Consequently, thermal winds have a stronger tendency to collapse suddenly, which can have a major negative effect on the helicopter in certain operations.

Typical situations where this phenomenon arises are, for example: approaches in the mountains, or in hot deserts, or near a cliff, or an elevated heliport on buildings or on ships. This phenomenon is generally less present on elevated helidecks where the wind can flow under the platform due to the construction.

The updraft will reduce the power required at low speed or in hover. If this updraft suddenly collapses, the helicopter will fall into a descent due to the missing power. The conditions for developing VRS might therefore be encountered.

Collapsing updrafts may also occur in deserts (particular atmospheric conditions due to excessive heat and winds).

8. Incorrect or insufficient use of AFCS

The knowledge and the correct use of AFCS, when the aircraft is equipped with one, can assist the crew in maintaining the aircraft in the nominal flight envelope, and thus reduce the probabilities of approaching the VRS boundaries. Particular attention should be given to 3-axis AFCS management that implies a manual management of the vertical axis.”

Therefore, [19] reports that “the following stages of flight should be carried out with great care:

- Vertical descent, because when descending vertically into a confined area from above the level of the obstacles, it is difficult to judge height and a high rate of descent can develop.
- Steep approach: in light winds, a misjudged steep approach can cause the conditions for vortex ring.
- Downwind maneuvers, resulting in low or negative airspeeds.
- Quick Stop Flares: when a helicopter is flared in a quick stop, the horizontal airflow past the rotor comes more nearly from below as the disc is tilted back. If a rate of descent develops, the airflow directly opposes the induced airflow, potentially leading to VRS. This situation was detailed previously as the dynamic vortex.”

In [32], VRS-related accidents from the 13 biggest helicopter-operating countries have been gathered and analyzed. Steep approaches with aggravating factors such as tailwind, high weight, and high density altitude were found to be the most prominent VRS-inducing situation.

2.3.5 Summary of the main parameters influencing VRS onsets

If design parameters, such as blade twist, can have an impact on the development and the onset of VRS as well as the behaviour of the helicopter within the VRS, it is almost impossible to estimate the influence of a single parameter through the realization of flight tests, as VRS occurrence is dependent on many parameters. The influence of a single parameter can only be estimated through numerical methods or wind tunnel tests where everything is controlled and mastered.

Pilot actions on controls have also a large impact on the development of the phenomenon. Indeed, some patents are based on the generation of control inputs to delay the VRS development, as indicated later in Chapter 5. Nevertheless, there is no way of guaranteeing that the actions done will not contribute to the VRS entry.

As influencing the rotor induced velocity, flight parameters such as air density (temperature and altitude) or helicopter mass have an impact on VRS generation and onset. Variations of such parameters have to be considered in flight, but these variations have a smaller impact on VRS onset's rate of descent compared to the impact of dynamic maneuvers and more globally the way the helicopter approaches the VRS domain.

Whatever the flight case, the main challenge is to have an estimation of the airspeeds seen by the rotor. VRS domain is traditionally shown in terms of airspeeds, but in earth frame. However, it is clear that depending on helicopter attitudes, the rate of descent seen by the pilot (generally based on barometric measurement) will be different from the vertical airspeed component seen by the rotor. If taking into account the airspeeds in rotor frame is mandatory, it is certainly not sufficient during dynamic maneuvers (i.e.: maneuvers leading to large helicopter attitude variations, angular speed variations, etc.). In these situations, the dynamics of the wake, how the vortex is generated and blown away (or not) highly influence the occurrence of VRS.

2.4 Analysis of the current available analytical and simulation methods for prediction of the VRS

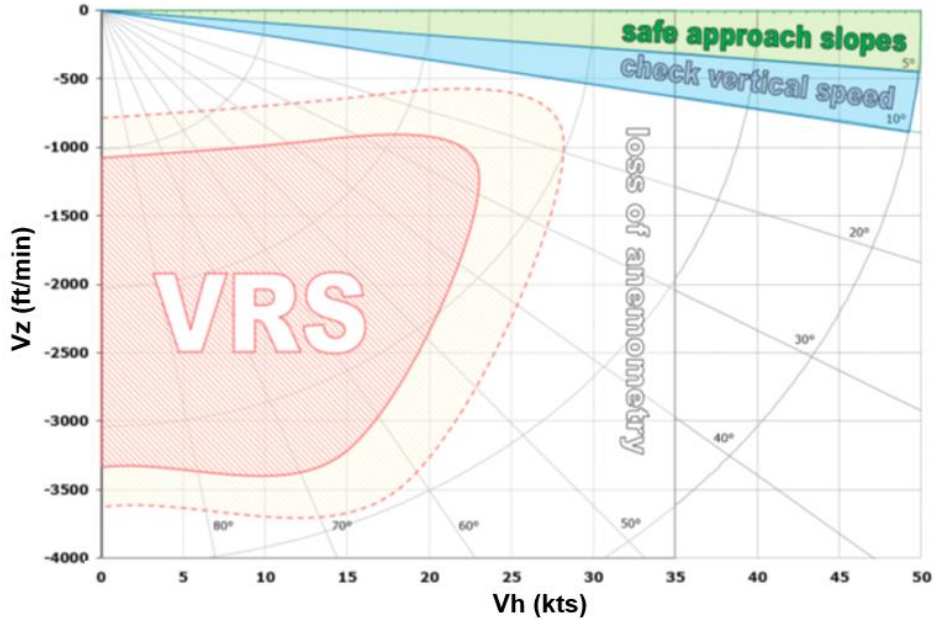
2.4.1 Example of VRS domain mapping

As indicated in [12]:

“Many studies have been carried out in the past in order to determine the boundaries of the VRS domain, using both experimental (flight, wind tunnel) and numerical means (simulations). The VRS mappings that can be found in the literature are numerous and differing. Nevertheless, they all give a very similar message when it comes to the RoD where the helicopter can meet VRS conditions at very low speeds (<25-30 kts): the RoD of VRS is about half of the downwash velocity the helicopter would have in HOGE. As a reminder, a 2250 kg light helicopter with 10 m/sec of average downwash velocity in hover (10 m/sec \cong 2000 ft/min) will meet VRS conditions at about 1000 ft/min. This should not mean that one can descend safely at (say) 900 ft/min just because the limit is 1000 ft/min. For various reasons (see previous section about aggravating factors) and most importantly in order to conserve safety margins as a general rule, one should never conduct an approach below 25-30 kts with a RoD greater than 500 ft/min .”

In the VRS mapping Figure 2-26 below, taken from [12], an example of the VRS range (red) with associated margins (amber) is plotted as a function of airspeed and rate of descent (RoD). An indicative threshold of the loss of reliable anemometry (IAS) is also given. Based on airspeed and RoD we can also add several approach slopes in order to compare with VRS boundaries. It is observed that for a 5°-10° approach slope the helicopter stays away from the VRS range. However (see example in the previous sections) the pitch-attitude due to deceleration must be monitored.

► Figure 2-26 VRS mapping - taken from [12]



“NOTE: A steep approach at low airspeed is possible but requires a very specific attention to vertical speed. [12]”

It is also well known that the VRS onset boundary is significantly influenced by the specific criterion used to define it. Indeed, a boundary based on torque fluctuations may be slightly different from the classic boundaries predicted using thrust fluctuations, blade flapping or vibration level increase. A good review of various researched criteria, such as thrust or torque fluctuations can be found in [13], [17], [33].

2.4.2 Criteria defining the envelop of the VRS domain

A first simple criterion is based on the following scheme considering the convection speed of the blade tip vortices. In a rough approximation, this displacement speed of the tip vortices relative to the rotor is the average between the external airspeed V_z due to the descent and the airspeed through the rotor ($V_z + V_i$), therefore:

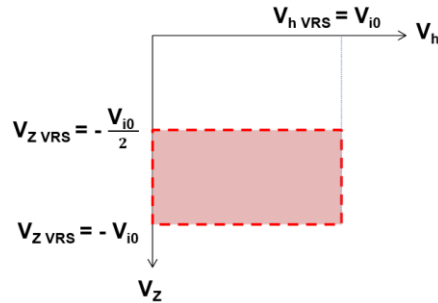
$$\frac{V_z + V_z + V_i}{2} = V_z + \frac{V_i}{2}$$

When this airspeed relative to the rotor becomes null, that means that the blade tip vortices remain close to the rotor agglomerating together to form this huge vortex torus making collapse the rotor lifting thrust. The vortex torus absorbs all the kinetic energy blown by the rotor (V_i) preventing him from generating the air momentum between the upstream and downstream faces of the rotor.

Thus in this first rough assessment, the VRS envelope in the airspeed domain (horizontal speed: V_h , vertical speed: V_z) has a rectangular shape as shown in Figure 2-27 with :

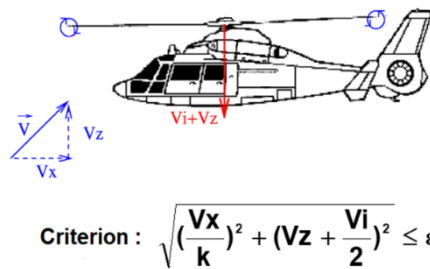
- an upper limit given by : $V_z = -V_i / 2$
- a lower limit given by: $V_z = -V_i$
- a front limit given by: $V_x = V_i$

► **Figure 2-27** First quick and rough approximation of the VRS domain



A more careful study has been performed by ONERA based on helicopter flight tests done with the DGA-EV Flight Test Centre in Istres and that will be detailed in the next sections. In parallel, a Ph.D thesis [6] was dedicated to the development of a rotor inflow model providing an extension of the momentum theory able to give a reliable assessment of the mean rotor induced flow including through the VRS. In addition, a criterion was developed [16], enabling the estimation of the VRS domain and displayed in Figure 2-28.

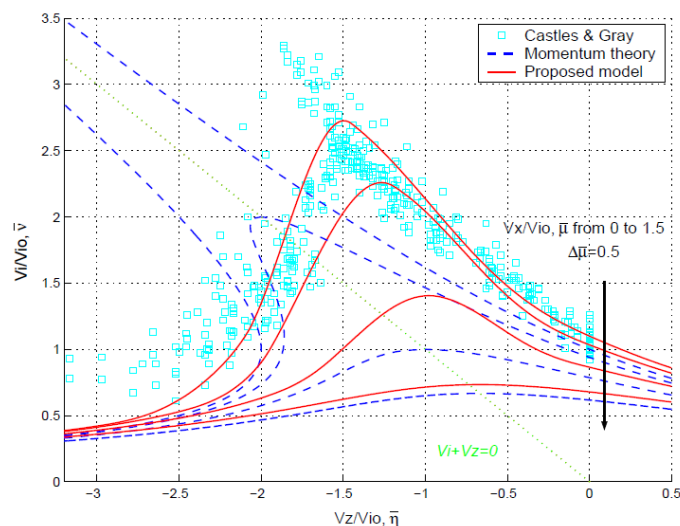
► **Figure 2-28** ONERA VRS domain criterion



This criterion is dependent on horizontal speed V_x and vertical speed V_z in rotor frame, as well as the induced velocity V_i .

Thus, a specific induced velocity model adapted to steep descent was developed. In Figure 2-29 the proposed model is plotted, showing the evolution of the induced velocity and different forward speed.

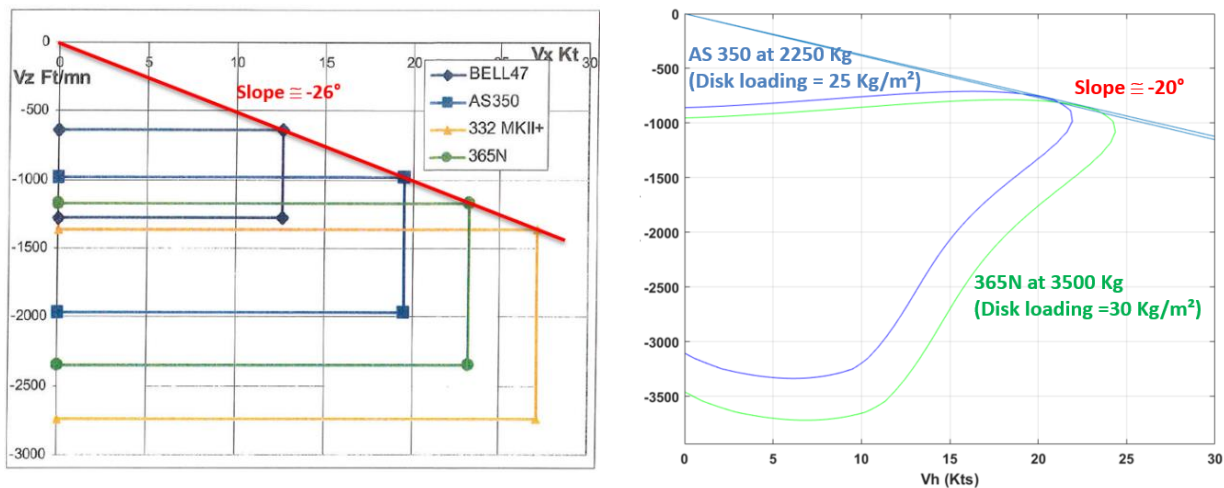
► **Figure 2-29** ONERA induced velocity model in steep descent – taken from [16]



Once this induced velocity model and criterion are combined, it is then possible to estimate VRS domain of different types of helicopter as represented in Figure 2-30. These domains correspond to a criterion (see Figure 2-28) where $k=4$ and $\epsilon=0,25$.

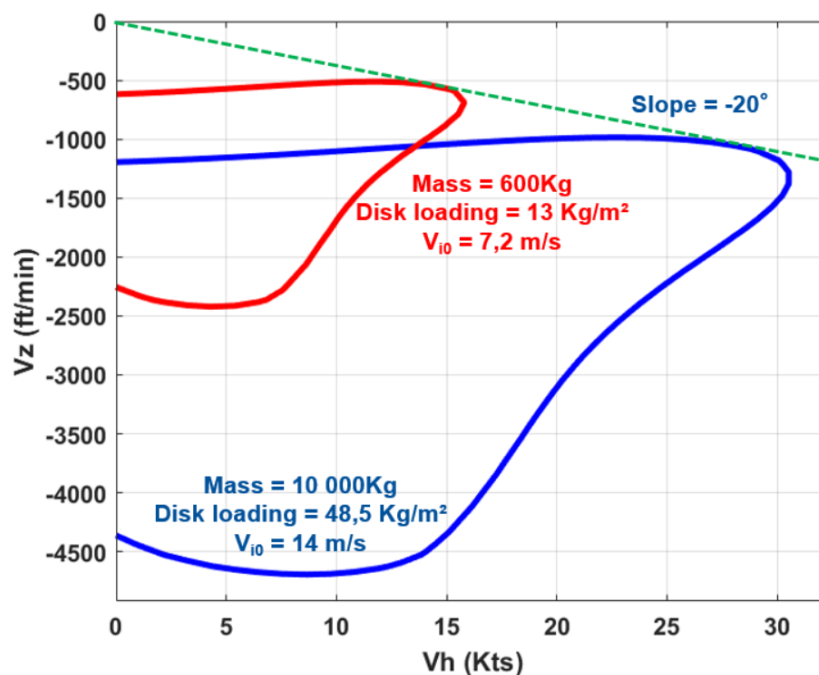
ONERA criterion is a bit more conservative. It has to be noticed that the expected “lower boundaries” are also much higher.

► **Figure 2-30** ONERA VRS domain estimation (Right) compared to VRS domain estimation – left figure taken from [27]



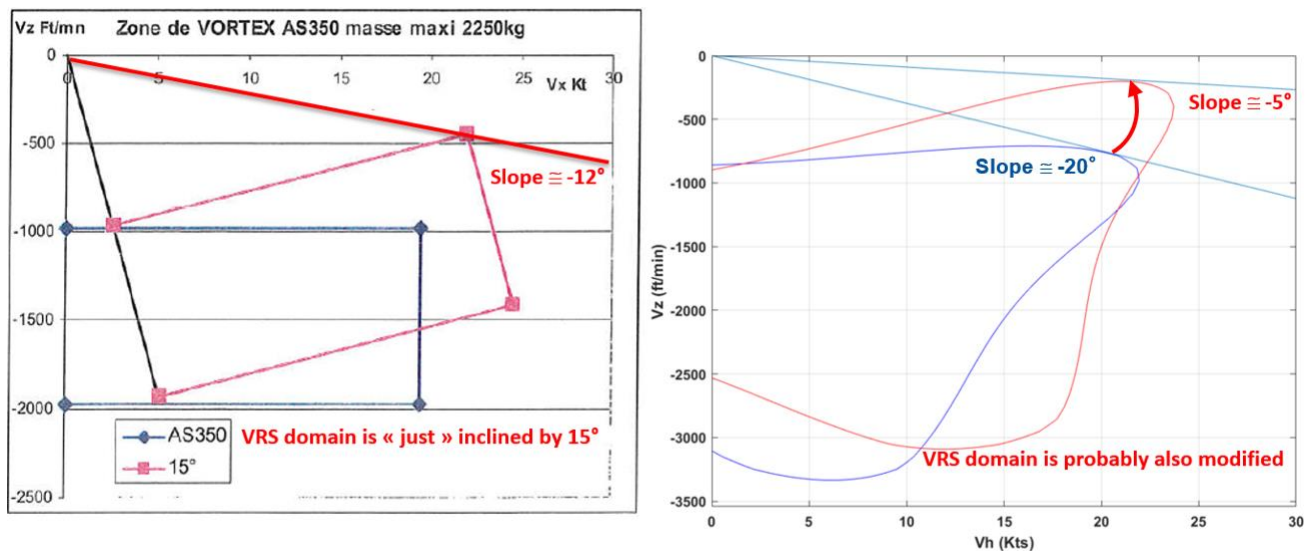
On the following Figure 2-31, the ONERA criterion provides the VRS domain estimation for two helicopter masses of 600Kg and 10000Kg, corresponding to a R-22 and H225 helicopter types.

► **Figure 2-31** ONERA VRS domain estimation for two helicopter masses



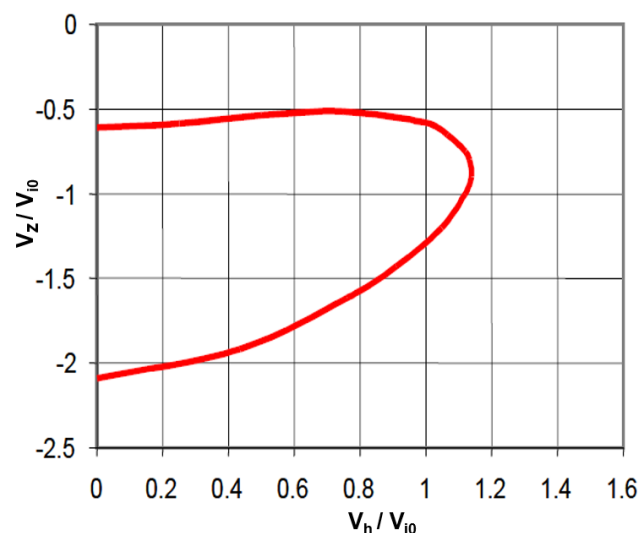
If VRS domain is generally represented in terms of horizontal and vertical speed in earth axes, computing the speed seen by the rotor (i.e. in rotor frame) with pitch attitude variation is possible. This change of reference axis has an impact on VRS domain as shown in Figure 2-32 and already discussed in sub-section 2.3.2.

► **Figure 2-32** ONERA VRS domain estimation (Right) compared to VRS domain estimation with 15° nose-up attitude – left figure based on [27]



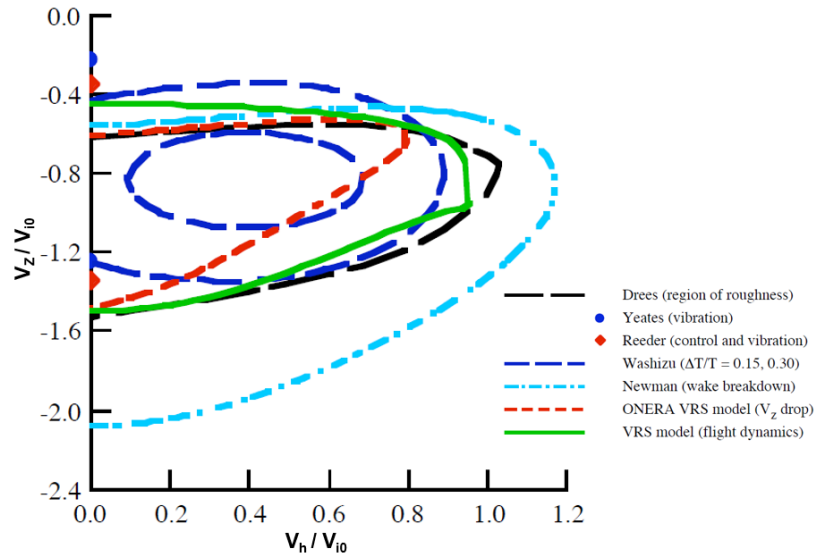
In [34], a similar approach was followed to develop a wake transport criterion for assessing VRS conditions. The wake transport velocity consists of the vector sum of forward speed, climb (descent) speed, and the rotor induced velocity at the tip path plane. The wake transport velocity components tend to separate the tip vortex filaments. Inflow and climb speed provide vertical separation, while forward speed provides some horizontal separation. Therefore, Newman et al. developed the “effective” wake transport velocity term, leading to the predicted VRS boundary curve shown in Figure 2-33.

► **Figure 2-33** Newman et al. analytical prediction of the VRS boundary with non-dimensional speeds



A number of other VRS boundaries estimation methods and criteria have been proposed and are presented in [17] and shown in Figure 2-34.

► **Figure 2-34** Various VRS boundary estimation criteria – taken from [17]

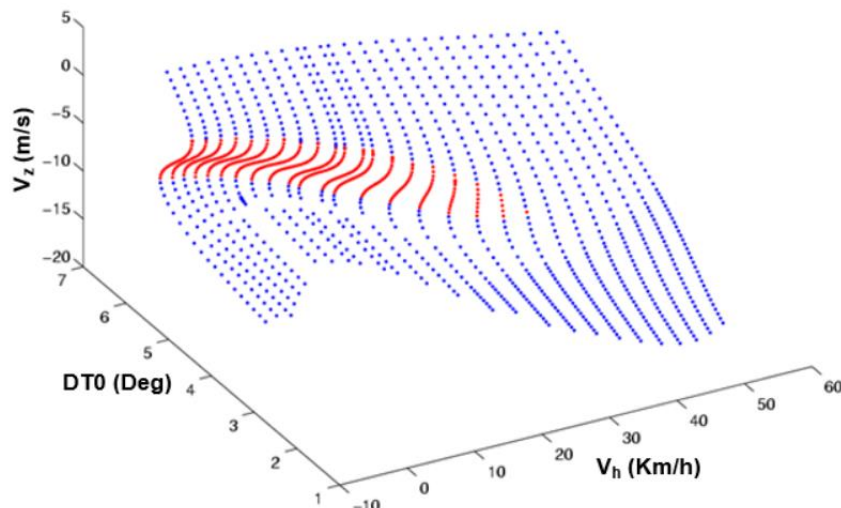


The ONERA criteria is based on the V_z drop encountered in helicopter flight tests. The boundary for the VRS model is based on the flight dynamics stability of helicopters and tiltrotors. The other boundaries are based primarily on the vibration and roughness that a helicopter encounters in VRS. Of particular note are the boundaries that Washizu constructed for $\Delta T/T = 0.15$ and 0.30 [10], where ΔT and T are the amplitude of fluctuation and the mean value of the thrust respectively (see sub-section 2.2), which are found in numerous documents on VRS.

Another example of criterion is based on the bifurcation theory.

This was studied in a Ph.D thesis at ONERA [35], following the work initiated in [36]. The fundamental idea of this approach is that the system of equation governing the rotorcraft flight dynamics is a non-linear system.

► **Figure 2-35** Folding of the equilibrium surface of the helicopter flight dynamics in descent at low forward speed (in red the unstable solution, i.e. the VRS, in blue the stable trim solution, i.e. the helicopter and wind-mill branches) – taken from [35]



Therefore its behavior is better rendered by bifurcation theory than by any method relying on linear assumption.

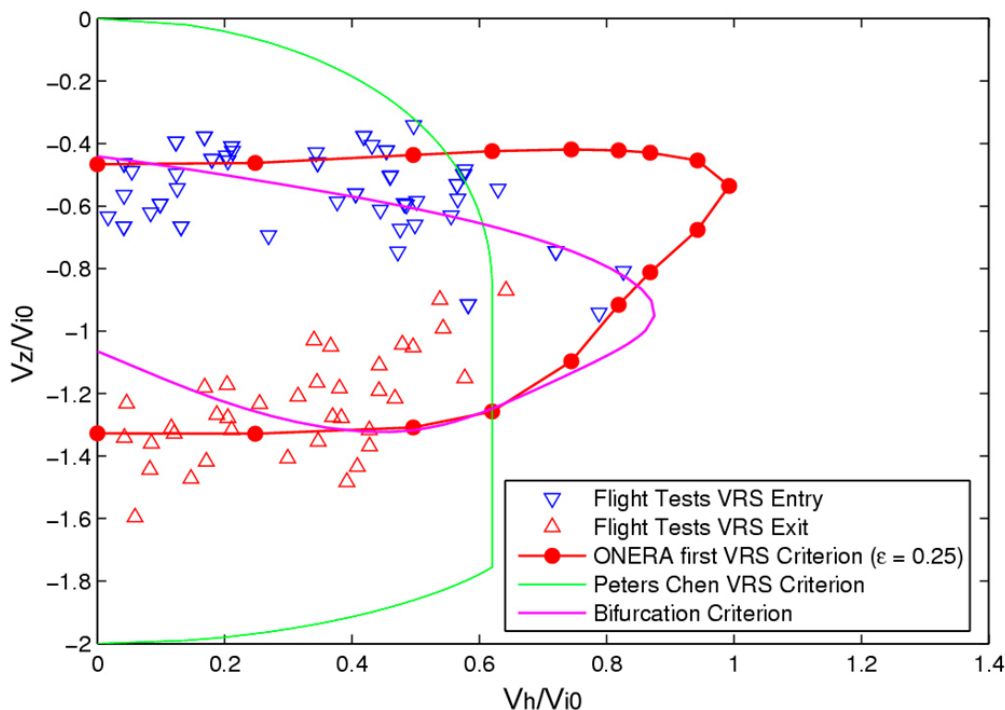
In this approach, the VRS is explained as a folding of the trim surfaces meaning that for a certain set of flight and control conditions, several trim solutions co-exist. They can be stable (in blue on Figure 2-35), that is the case of the trim in “helicopter” or “wind-mill” modes, or unstable and that is the case of the VRS (in red on Figure 2-35).

It is also clearly seen that for certain flight conditions (V_h , V_z) and control (here $DT0$ is the collective blade pitch angle, in deg), there is a folding of the equilibrium surface with three trim solutions for the same (V_h , $DT0$): in red the VRS unstable solution, in blue the “helicopter” and “wind-mill” stable solutions.

In [35], an algorithm of continuation for calculating all the trim solutions and their stability has been implemented in the Airbus Helicopters code HOST. When used with the rotor induced velocity model developed in [6], the trim solutions including the VRS unstable one are obtained (Figure 2-35). Within this approach based on the non-linear system dynamics theory, the VRS frontier are mathematically defined as being the bifurcation points between these stable branches. At these bifurcation points, the value of a real eigen-mode of the helicopter flight dynamics changes of sign, so by calculating the locus of the trim points where a real eigen-mode is null, we get the frontier of the VRS domain.

In summary the model is the same as in the previous approach based on helicopter flight tests [6], [16], [28], but the mathematical method for defining the VRS frontier is different leading to different VRS domains as can be seen on Figure 2-36.

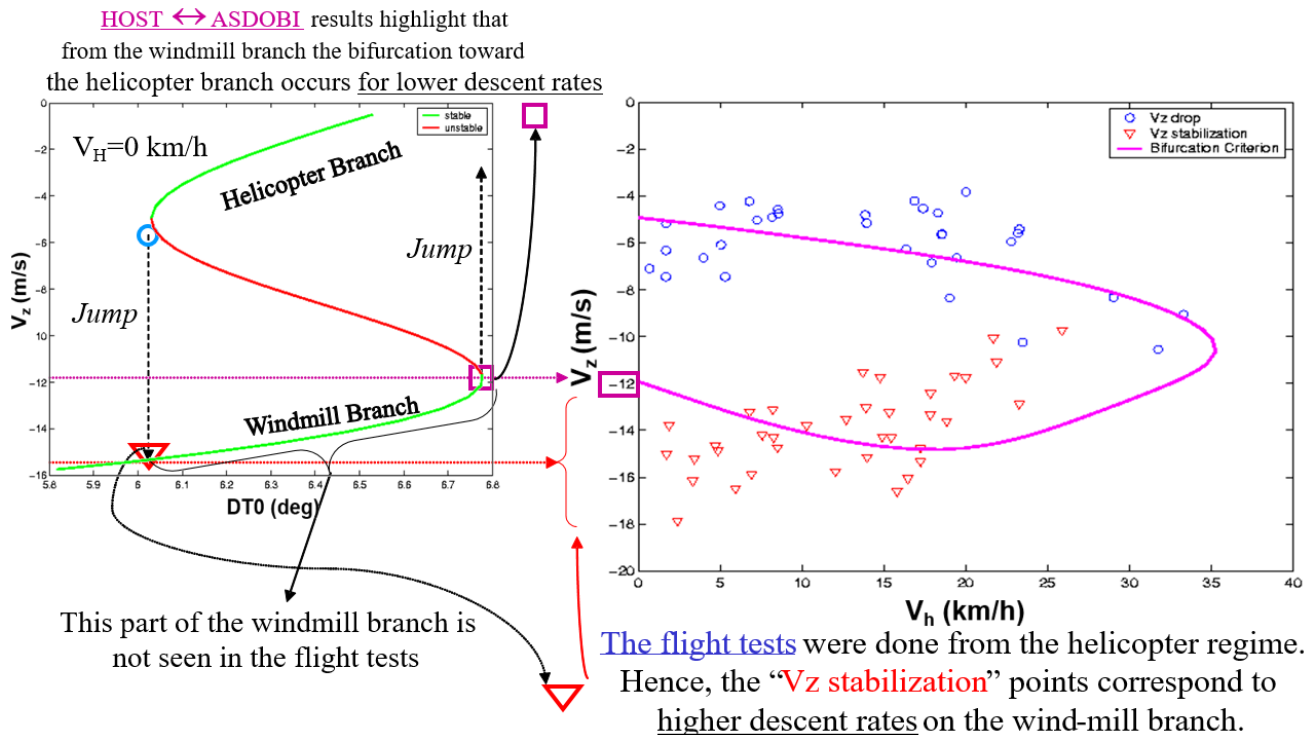
► **Figure 2-36** Comparisons of different VRS criteria defining the limits of the VRS domain w.r.t. the Dauphin Flight test data – taken from [35]



The “Bifurcation Criterion” gives a good assessment of the VRS upper and front limits giving a better prediction of the “knee” of the domain w.r.t. the other criteria. It could seem that the lower limit is not so well predicted especially at low forward speeds, but that is because the reflex is to compare with the red triangles which correspond to the vertical speed stabilization. Indeed the Figure 2-37 hereafter clearly explains that starting from the “Helicopter stable branch” when the pilot reaches the upper bifurcation point (“blue circle”), the

helicopter enters into an unstable dynamics so a very small change in collective makes “jump” the trim toward the “Wind-mill branch” and therefore the helicopter stabilizes at a high descent speed corresponding to these “Vz stabilization points” (i.e. “red triangles”). The actual bifurcation point from the Windmill branch to the Helicopter stable branch occurs at lower descent speed (“purple square” on Figure 2-37).

► **Figure 2-37** Bifurcation locus giving the actual frontier of the VRS unstable domain



The robustness and generality of this mathematical interpretation of the VRS frontier in terms of bifurcation points has been demonstrated with another rotor inflow model based on vortex rings (see [33])

2.4.3 VRS phenomenon simulation

Numerous rotortorcraft wake modeling methods have been developed for simulating flow over rotorcraft, as reviewed in [37], [38], [39], where state of the art of rotorcraft inflow and wake modeling developments are presented.

The mathematical modelling of the VRS phenomenon depends on the intended application of the model which can be either for its prediction, analysis or for training simulations. A model is always a simplified representation of a physical phenomenon with a compromise between accuracy and rapidity which must be adapted to its application. Classically three groups of models can be distinguished:

- Fast models: the priority is on the timeliness with very fast execution time. This term “Fast models” is preferable rather than “Low fidelity” models, because this kind of models can provide more accurate results than more complex models if the available input data are too few to inform a so-called “High Fidelity” model ;
- Mid-fidelity models: they provide a trade-off between accuracy / rapidity suited for performing repeated simulations in a reasonable time for engineer analysis ;

- High-fidelity models: their purpose is to simulate with the highest accuracy the phenomenon whatever the computational time.

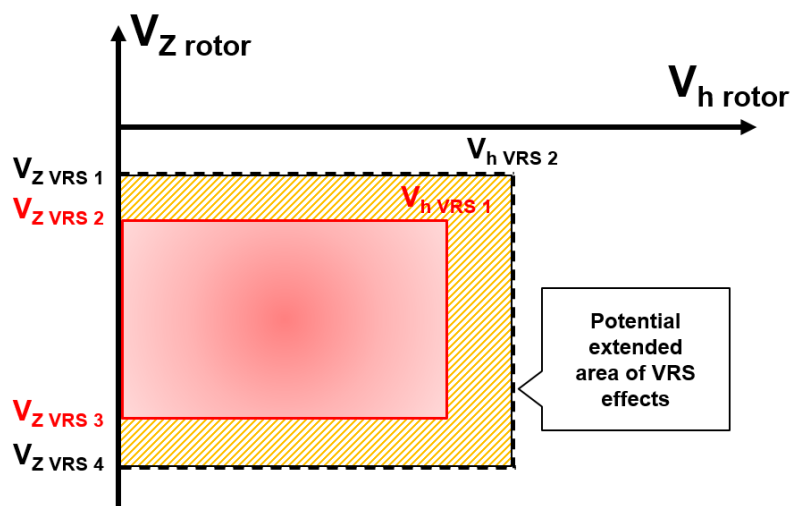
2.4.3.1 Fast models

For the training simulations, the computation must be rapid enough for allowing a real time simulation of the VRS effect on the rotorcraft flight dynamics. The “Fast models” are thus focus on rendering the main effect of the VRS. They can be qualified as “behavioural models”.

The most simple way to render the VRS is to impose a law of rotor thrust loss in a preidentified VRS region. Therefore this kind of models are based on rather simple analytical expressions with empirical parameters tuned for the simulated helicopter.

An example of this direct thrust reduction method based on predefined forward and vertical speed values is shown on Figure 2-38 . This approach is generally the one adopted in training simulators.

► **Figure 2-38** Predefined VRS domain for loss of lift generation



A percentage of lift loss is set and applied depending on the speeds seen by the rotor with respect to a predefined VRS domain.

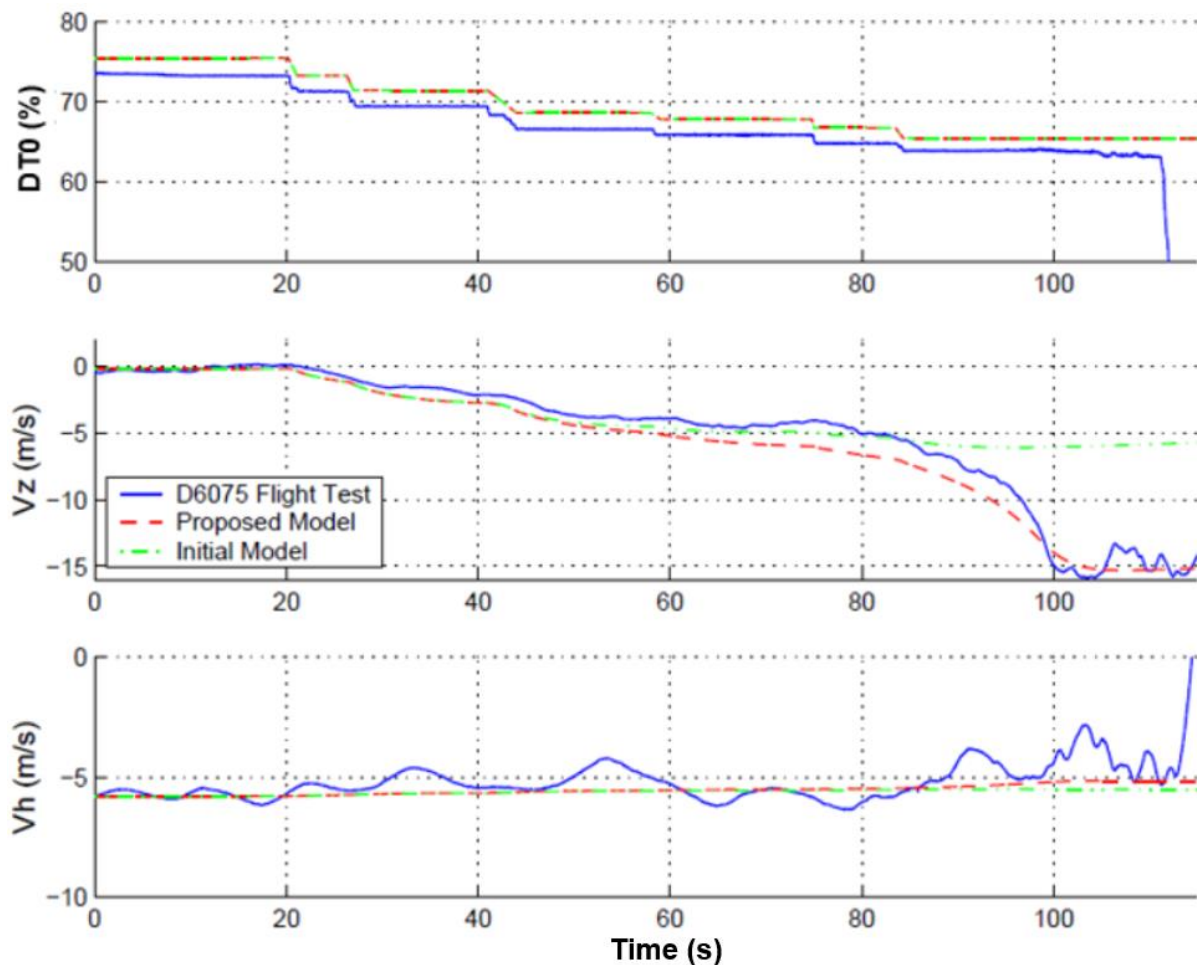
The major disadvantage of this approach is the need of experimental data and/or pilot evaluations to tune the different parameters defining the VRS domain. In addition, there is also the question of how representative VRS occurrences in dynamic maneuvers are, as well as the representativeness of recovery techniques.

Another “Fast” analytical approach closer to the physics represent the effect of the VRS on the rotor inflow itself in a global way by correcting the momentum theory. A good example of this kind of models is the one presented in chapter 2.4.2. and detailed in [6], [16].

Indeed, ONERA developed and implemented in the Airbus Helicopters flight mechanic code “HOST” an induced velocity model adapted to steep descent, enabling the simulation of VRS. One can see on Figure 2-39 a simulation where the flight mechanic code is fed with the pilot collective inputs (DTO in %) of a flight test performed on a Dauphin (blue curve) [6], [16]. It can be seen a comparison in terms of forward speed (V_h) and vertical speed (V_z) of the proposed VRS model (red dashed curve) with respect to a simulation with no VRS modelling (green dashed curve).

The collective is gradually decreased, each time leading to a stable response of the vertical speed while the forward speed is maintain constant. At around 85s, a slight decrease lead the helicopter in VRS. The proposed model is then able to correctly simulate the helicopter behavior in VRS. The simulated responses match well the flight data, such as the VRS entry time and Vz variation (from -5 m/s = -984.25 ft/min to -15 m/s = -2952.75 ft/min).

► **Figure 2-39** Simulation of VRS entry – taken from [6]



This model was used in the simulations presented in Figure 2-18, Figure 2-19, Figure 2-20, Figure 2-21, Figure 2-22, Figure 2-23.

As outlined in sub-chapter 2.3.2., while this model is able to correctly capture the drop of vertical speed, questions arise about the representativeness of the vertical speed response due to a collective pitch increase. This project will also be the opportunity to verify the ability of this model to represent the helicopter behaviour during recovery techniques.

2.4.3.2 Mid fidelity models

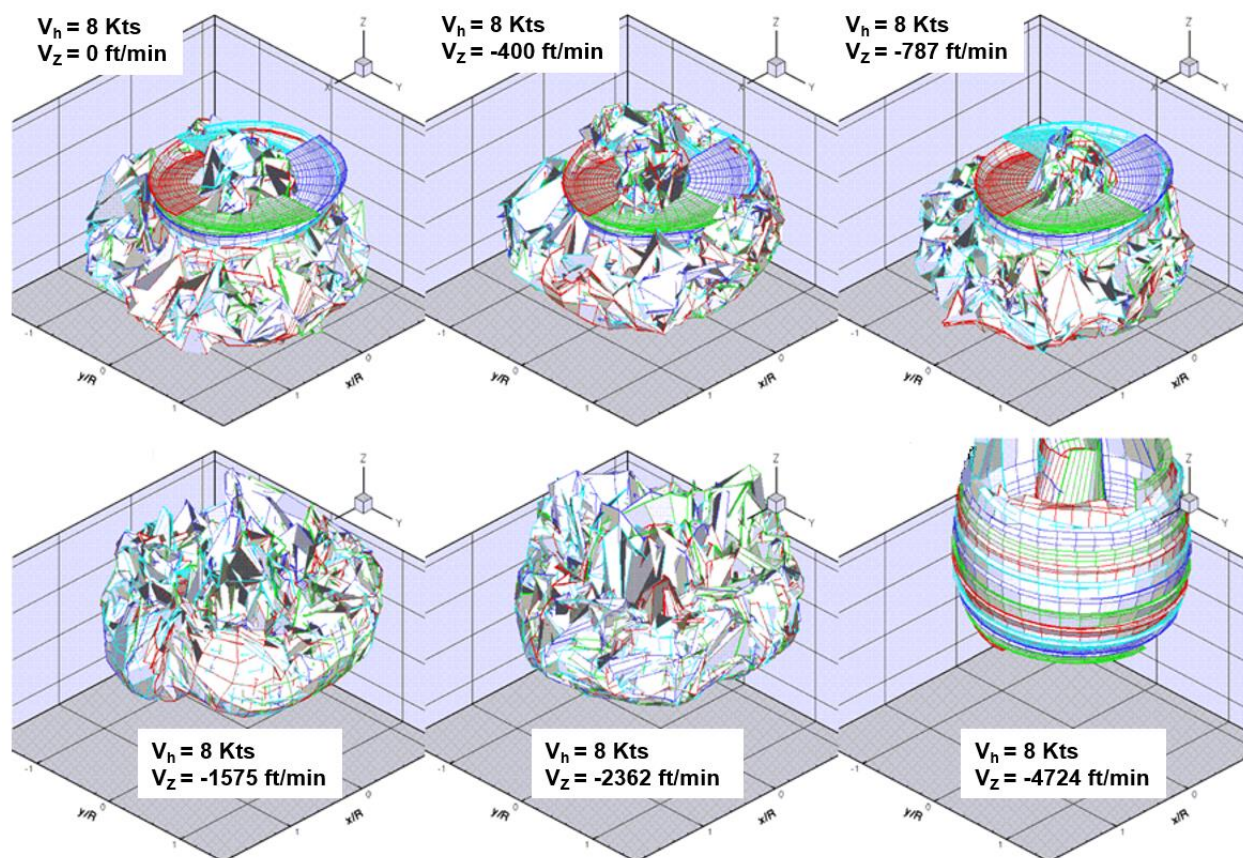
Low fidelity methods or models are not able to describe the dynamics of the wake and its interaction with other bodies. Medium fidelity method resolve this problem by modelling the rotor wake.

Among the intermediate methods between low and high fidelity modelling of the underlying physics causing the VRS, two groups can be distinguished.

On the one hand, lagrangian approaches using vortex singularities for representing the rotor wake. They must be based on a free-wake formulation in order to let the wake geometry settles freely under the action of all vortices. With the Biot & Savart law, the induced velocities by each vortex on the blades and on the other vortices are calculated thus influencing both the aerodynamics seen by the blades and the rotor wake geometry. The vortex singularities can be points, segments or surfaces.

An example of application of that kind of approach applied to the VRS simulation is with a time marching free-wake model using vortex panels : MINT [40], [41] implemented by ONERA in the Airbus Helicopters code HOST and its stand-alone version PUMA. It suits with a lifting line approach for representing each blade and is based on an unsteady wake modelling (Mudry theory). Each blade deploys its own wake represented as a potential discontinuity surface discretized in panels of constant gradient of potential jump. Thanks to that kind of “spread singularities” dealt with a numerical integration performed by a 4 points Gauss integration, the method is less sensitive to the regularization distance than other vortex methods. Indeed the other vortex methods often use a more or less empirical “viscous core radius” of the vortex in order to avoid that the induced velocity goes to infinity for a point closer and closer to the vortex (in the Biot-Savart law, the induced velocity is inversely proportional to the distance between the vortex and the calculation point reaching infinity when this distance is null).

► **Figure 2-40** Four bladed rotor wake simulation with MINT at a low forward speed and different rate of descent



This is a time-marching approach with a Runge-Kutta scheme with sub-iteration to converge the circulation on the blade and the emission conditions of the wake at each time step.

In order to capture the VRS, a lot of rotor revolutions must be simulated and kept within the rotor wake. That is why a fast-multi-poles approach has been adopted for decreasing the computational time. In most of these

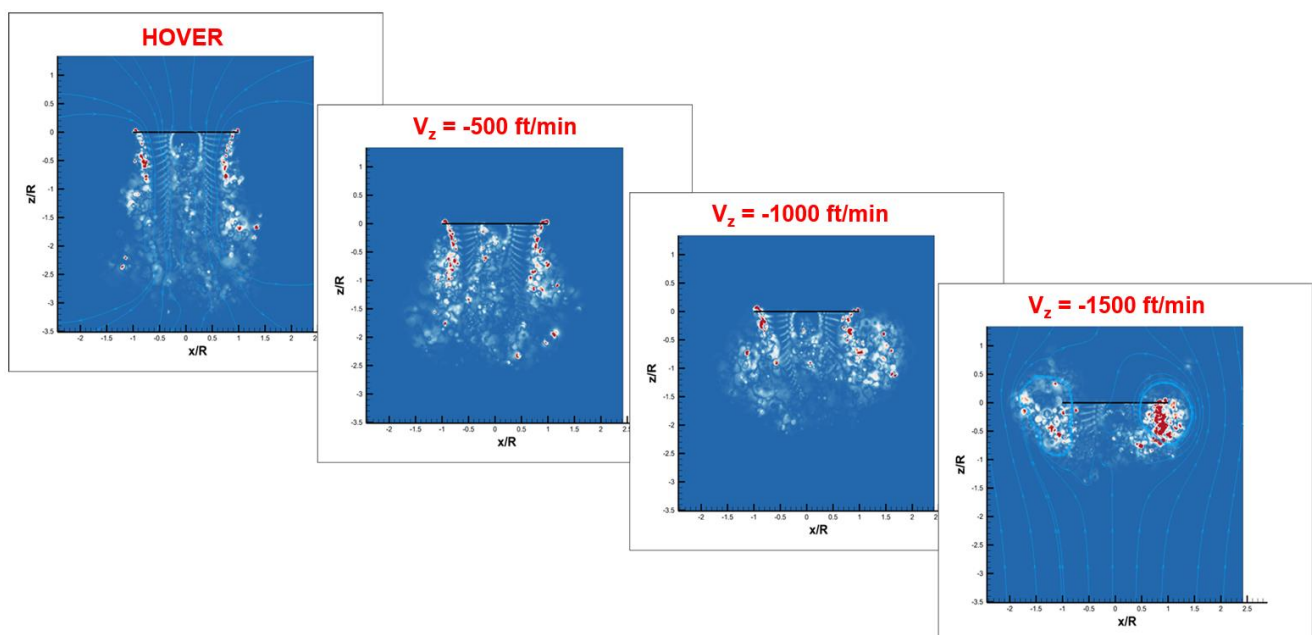
free-wake models, a wake roll-up appears rapidly below the rotor even in hover if the rotor wake is not simulated with enough rotor revolutions.

A very first application of this free-wake MINT model to the VRS simulation at the time it was not coupled with the HOST flight dynamics code is shown in previous Figure 2-40.

The VRS with its typical torus-shaped vortex structure can be observed for $V_z = -1575$ ft/min and $V_z = -2362$ ft/min.

A more recent simulation of the VRS with this free-wake model using the ONERA stand-alone PUMA version has been tested by Airbus and is shown on following Figure 2-41.

► **Figure 2-41** Main rotor wake visualisation with fixed collective pitch and zero cyclic pitch angles performed with PUMA



The wake modelling is finer with this last version PUMA (Figure 2-41) compared to the initial rough first assessment with MINT (Figure 2-40). But a strength of MINT which was not exploited, is that it is strongly coupled with the blade kinematics and helicopter flight dynamics thanks to its implementation into the HOST rotorcraft flight dynamics code.

Another lagrangian approach is the viscous vortex particle method (VPM), solving the vorticity-velocity form of the incompressible Navier–Stokes equations with a Lagrangian description for obtaining the wake vorticity field. Therefore, consideration of viscous effect utilizing the VPM, which directly simulates the viscous flow and avoids artificial numerical dissipation, is crucial for solution accuracy.

The VPM simulation can accurately predict both the downwash magnitude and variation trend for various rotor configurations, including single main rotor, co-axial, tandem, tiltrotor, etc. In addition, it has been validated for a broad range of flight conditions, such as hover (in or out of ground effect), forward flight, climb and descent, autorotation (including vortex ring state), as well as steady and maneuvering flight. Examples of the use of the vortex particle method in rotor wake modeling can be found in [42], [43], [44], [45].

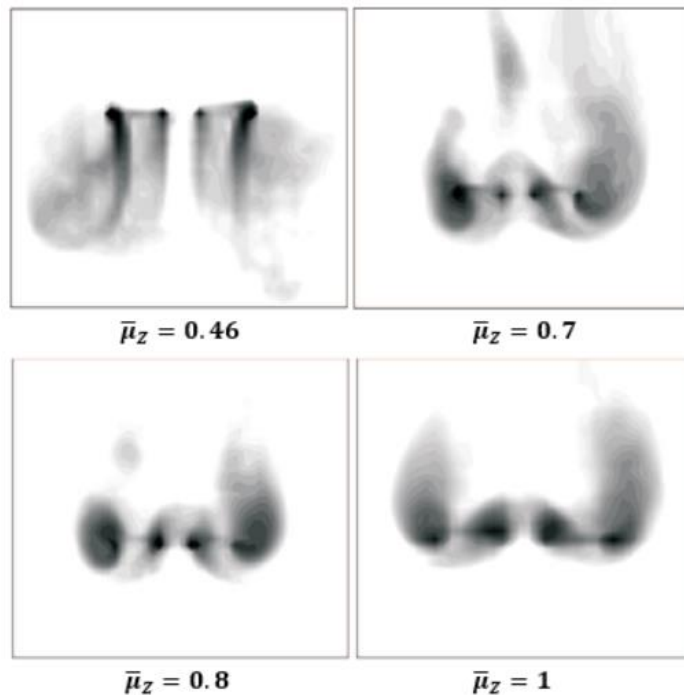
On the other hand, some eulerian approaches propose mid-fidelity modelling with interesting features for the VRS simulation. The Vorticity Transport Method (VTM), developed by Dr R. Brown and his students at Glasgow University (and earlier at Imperial College London), is a good example of such approaches. Developed and applied successfully for years, this model has been applied to a large number of different rotor wake problems

with exceptional success to date. These applications include near-field wake modeling for airloads and aeroacoustics, mid-field rotor-fuselage interaction and rotor-rotor interaction, and far-field helicopter-aircraft wake interaction, ground effect, brownout and vortex ring state [46], [47].

For example, taken from [46], the following Figure 2-42 shows a contour plot of the vorticity in the rotor wake at different rates of descent, averaged over several rotor revolutions.

These simulations confirm that the toroidal flow of the fully developed VRS is not finally established until a descent rate of $\bar{\mu}_Z = 0.7$.

► **Figure 2-42** Contour plot of the vorticity in the rotor wake using Vortex Transport Method - taken from [46]



Where:

$$\bar{\mu}_Z = \frac{\mu_Z}{\sqrt{C_T/2}}, \text{ with } \mu_Z = \frac{\text{rotor descent rate}}{\Omega \cdot R}, \text{ with } \Omega = \text{rotor angular velocity}, R = \text{Rotor radius}$$

And where:

$$C_T = \frac{T}{\rho \cdot S \cdot (\Omega \cdot R)^2}, \text{ with } T = \text{Rotor Thrust}, S = \text{Rotor disk surface}, \rho = \text{air density}$$

For descent rates greater than $\bar{\mu}_Z = 0.7$, the wake intensity above the rotor increases at the expense of the wake intensity below the rotor, indicating a shift in the toroidal vortex structure from below to above the rotor. Thrust recovery on the rotor begins once the toroidal VRS wake begins to lift clear of the rotor

This method has been recently applied to the study the potential VRS occurrence on eVTOL aircraft [48]. This is one of the first paper, to our knowledge, alerting on the potential risk of VRS on these new eVTOL configurations with multiple lifting propellers submitted to vertical airspeeds due not only to the aircraft descent rate, but also to its roll and pitch motions as well as to mutual aerodynamic interferences. As an example, different rotor or more precisely lifting propeller configurations are simulated to analyse the aerodynamic interaction between the rotors and their behavior in VRS.

The Figure 2-43 hereafter shows the changes which can occur on two rotors working side-by-side or in a tandem (front – aft) configuration. These changes can be appreciated from the comparisons with respect to the isolated rotor case shown for reference on the left. “Rate of climb / v_h ” means according to the notation of the present report V_z/V_{i0} . The aft rotor is clearly the most impacted one with strong interferences coming from the wake of the front rotor. Yet even the front rotor wake is altered compared to the isolated rotor case: the vortices tend to stay more below the rotor. They are less evacuated aftward due to the added vertical induced velocities by the second rotor. This induced reduction of the wake skew angle can also be observed on the case of two side-by-side rotors (on the right of Figure 2-43).

► **Figure 2-43** Comparison of the rotor wakes in forward flight ($V_x/V_{i0} = 0.5$) for different descent speeds from 0 to $V_z/V_{i0} = -0.7$ – images extracted from [48]

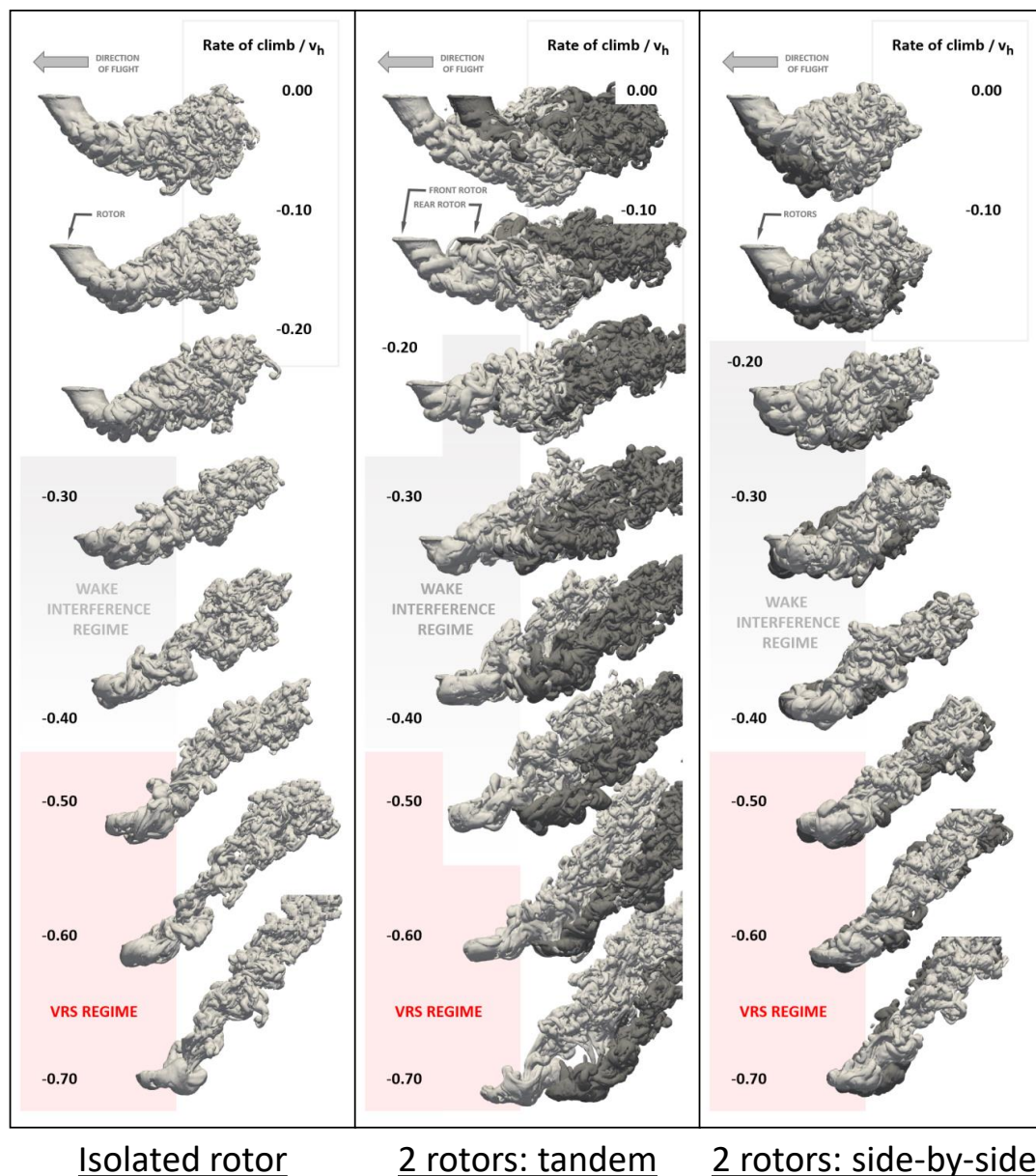
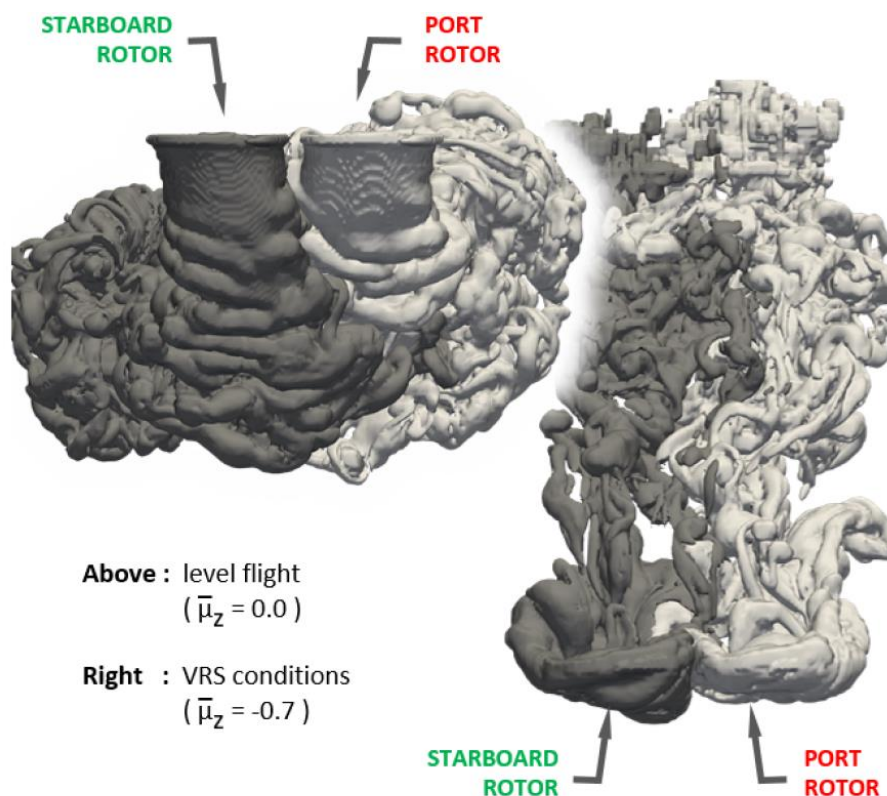


Figure 2-44 shows more in details in a front view the principal features of the interactional aerodynamics of the case of two rotors mounted closely side-by-side (and rotating in the same direction), which is a commonly encountered configuration within the design of eVTOL aircraft. The two pictures on Figure 2-44 are the same as the ones shown on Figure 2-44 for the side-by-side case both for a forward flight $V_x/V_{i0} = 0.5$: the left one in level flight ($V_z=0$) and the right one for the strongest descent rate ($V_z/V_{i0} = -0.7$).

A thrust asymmetry between rotors can be observed, causing the wake of the port rotor to lift above that of the starboard rotor. The port rotor then behaves as if the system is operating at higher descent rate than it actually is. In other words, the regime of wake interference for the port rotor begins at lower descent rates than it would have with an isolated rotor. The aerodynamic interaction between the rotors leads to a regime of highly unsteady, large-amplitude VRS-like loads on the system which extends to descent rates that are well below those at which either rotor might enter the VRS. This can be understood by the fact the rotors induce upward velocities at their external periphery (due to the strong blade tip vortices), although more complex interferences enter also into action for triggering the asymmetry. Even if the two rotors are exactly the same and rotate in the same direction, the asymmetry can be explained by noticing that the port rotor is submitted to the upwash from the other rotor on its retreating blade side, whereas the starboard rotor received more upwash on its advancing side. Less lift is produced on the retreating side and thus lower induced velocities which may explain that the total resulting downwash is weaker on the port rotor than on the starboard rotor (as can be seen even in level flight on the left picture of Figure 2-44).

- **Figure 2-44** View from forward of the wakes that are produced by two rotors when flying side-by-side, taken from the rotor wake using Vortex Transport Method - taken from [48]



With respect to FWM (Free-Wake Models) and VPM (Vortex Particle Method), the most important difference is that VTM is an Eulerian description of the airflow field whereas FWM and VPM are Lagrangian methods. This has several important advantages.

First of all in VTM, the fluid is represented by its vorticity as a 3 Dimensional volumetric field described on a mesh with adaptable accuracy. In FWM and VPM, vortex singularities (2D with vortex sheets, 1D with vortex filaments, 0D with blobs) are emitted from the lifting elements in a time marching approach. So it takes a certain time to evacuate the first vortices which have been emitted in absence of a fully developed rotor wake and thus may “pollute” the airflow with some non-physical effects. A more physical topology of the vorticity distribution is obtained from the beginning and preserved by the VTM. In practice, this means that the vortex entities within FWM and VPM representation often do not evolve properly according to the underlying physics in certain critical circumstances, because they do not interact as they should.

Secondly, the use of the underlying mesh in the VTM means that one can use rigorous metrics to make sure that the method maintains its accuracy and stability throughout a calculation. For long calculations, such is always required when dealing with the Vortex Ring State (VRS) on rotors in descending flights, this can be crucial. If errors build up in the numerics, then the representation of the physics deteriorates as the vorticity gets older and older, and if this vorticity is close to the rotor (in VRS some of the vortices near the rotor have been there for dozens of rotor revolutions) then the accuracy of the calculation suffers very badly.

This need of having a significant long description of the rotor wake in terms of rotor wake revolutions conserved within the wake is critical and recurrent in many cases, e.g. : in hover and even more in hover or low speed flights near the ground or obstacles, in descending flights and especially in VRS or autorotation. The VTM is able to keep in the rotor wake simulation hundreds of rotor revolutions while still keeping a good control over the numerical space and time steps.

Therefore the two main big advantages of VTM are:

- a direct representation of the whole flow field through the topology of its vorticity distribution;
- the mathematical control over accuracy and stability of this structure.

Another one is that the method is conservative, meaning that a calculation run at low resolution just gives low-resolution results compared to one run at high resolution, not fundamentally different answers. This can be a big problem with FWM and VPM, which are more sensitive in the sense the wake geometry can sometimes "jump" from one type of solution to another as the number of elements in the calculation is increased.

Regarding the interferences between a rotor wake and other parts of the air vehicle, some issues can raise with FWM when some vortex elements (like lines or sheets) are stretched or cut or deformed by another physical part of the aircraft (e.g. blades, wings, fuselage etc.). The advantages of the VTM come again from the grid-based representation of the vorticity (the surface of the wing or fuselage is known accurately with respect to the vorticity in the flow) and the accurate and stable treatment of the physics. For example reference [49] examined the effects of rotor wake interaction with the fuselage and tail of a compound helicopter on various issues including trim, performance, vibration and acoustics. Certain parts of the aircraft (fuselage, wings etc.) can have a significant impact on the rotor or propeller airflow. Hence on some aircraft, it can be important to account for the aerodynamic interferences between the aircraft components for a good prediction of the VRS.

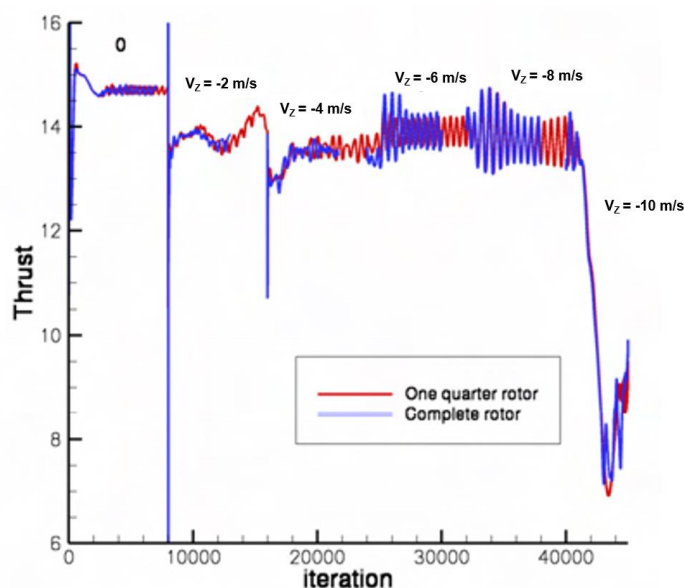
2.4.3.3 High fidelity models

Here are considered the Computational Fluid Dynamics (CFD) based on the Navier Stokes equations, the highest fidelity fluid dynamics fundamental equations. These methods are also called URANS simulation for “Unsteady Reynolds Averaged Navier-Stokes”.

A typical example of application of this kind of modelling is detailed in the PhD thesis [50] and presented in [51]. The airflow through the main rotor of the Dauphin helicopter (AS365N) is computed with the ONERA solver elsA by numerical resolution of the compressible Euler equations, (Navier-Stokes equations but without

viscosity). Indeed the VRS phenomenon appears to be dominated by large vortex structures, the “Vortex Rings”, therefore the viscosity effect is neglected for avoiding that the complex vortex wake be diffused too early in the computation. Briefly the computational process was to use, as inputs into the CFD, the blade pitch angles and blade kinematics (flapping and lead-lag motions) calculated by the flight dynamics code HOST using the ONERA modified momentum theory rotor inflow model for a helicopter weight such that $V_{i0} = 11.675$ m/s. These calculations have been done in vertical flights at different descent rates (m/s): 0, -2, -4, -6, -8, -10. The figure below (Figure 2-45) shows that the rotor thrust drop, occurring because of the VRS, appears in the CFD simulation near -10 m/s, which represents $V_z/V_{i0} = -0.857$.

► **Figure 2-45** ONERA solver elsA CFD simulations in vertical descent – taken from [51]

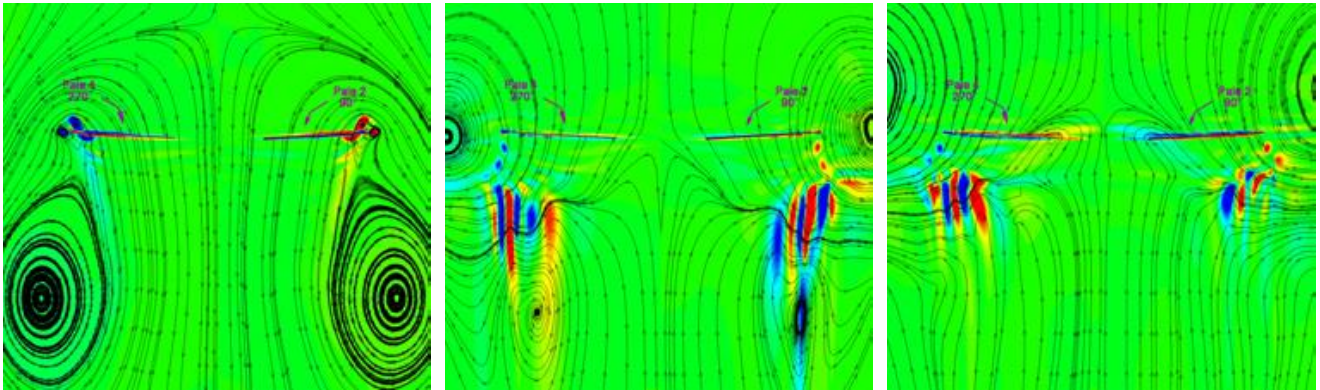


The fact that both the one quarter rotor simulations and the complete (four blades) rotor simulations remain very close means that the airflow field through the rotor stays periodic in terms of the blades positions. The symmetry of revolution of the rotor wake around the rotor hub axis which obviously exists in hover for such isolated rotor simulations is kept whatever the descent speed including those of the VRS. However, remember that these flow simulations are done for an isolated rotor with prescribed controls and blade kinematics in vertical descent. Any non axi-symmetrical perturbation would lead to a non-periodic rotor wake.

Yet, these results illustrate that the main feature of the VRS is not a non axi-symmetrical pattern of the airflow but its unsteadiness. Indeed as can be seen on the previous Figure 2-45 from an initial hover computation, both kinds of CFD simulation reach the same stable regime (for vertical speed between 0 to -8m/s, i.e. in terms of V_z/V_{i0} between 0 to -0.685) with a stabilized mean rotor thrust. At a higher descent rate ($V_z=-10$ m/s, i.e. $V_z/V_{i0} = -0.857$), there is a sudden loss thrust, the airflow can not reach a stable regime and the same divergence due to the unsteadiness of the flow field occurs with the two kinds of simulations.

The three following graphs (Figure 2-46) show this axi-symmetrical unsteady rotor airflow for the case considered in VRS ($V_z/V_{i0} = -0.857$).

► **Figure 2-46** Vorticity contours normal to the plane and streamlines for the complete 4-bladed rotor ($V_z/V_{i0} = -0.857$) – taken from [51]



At the beginning of the simulation (figure on the left), the torus formed by the wake roll-up of the blade tip vortices is below the rotor. Then this huge vortex structure comes closer and closer to the rotor because the mean induced downwash is progressively cancelled by the opposite relative speed corresponding the rotor descent speed (V_z). The authors of this study ([50], [51]) mention that the drop of thrust is correlated with the massive recirculation of the blade tip vortices through the rotor when the vortex torus is passing at the rotor level.

It should be underlined that the blades are here simulated by fine meshes suiting the real blade geometry and turning with the blades. Two different techniques of meshing have been tested: the classical structured multi-block approach matching boundaries and the Chimera overset grid approach where a child block around the blade and a background block are generated for the computation of Euler equations. The effect of the size of these grids has been studied, i.e. the fineness of the meshes with up to about 4 400 000 points for one rotor quarter for the Chimera technique for example.

As can be seen on Figure 2-46, only the profiled part of the blades is modelled. The hub and the arms connecting the blades to it are not simulated. That can lead to an overestimation of the blade root vortices. The authors observe that these blade root vortices may have an impact on the rotor thrust decrease. But again the work presented in this CFD study can not conclude about the effect of these root vortices as the sleeve connecting the blades to the hub are not modelled.

Among other improvements, they conclude that a stronger coupling of the CFD aerodynamics with the blades kinematics and rotorcraft flight dynamics is needed.

2.4.3.4 Hybrid methods

Vortex methods depicted in sub-section 2.4.3.2 are useful approaches for analyzing rotor aerodynamics and simulating a complete rotorcraft configuration but they do not consider compressibility effects (and not always viscosity). CFD methods allow us to simulate a wide range of flow regimes and to accurately capture the complex flow physics occurring in near-fields around rotor blades. However, CFD simulations suffer from excessive numerical dissipation on coarse grids; hence, wake structure and vorticity tend to dissipate rapidly after shedding from rotating blades.

It is clear that the computational methods applied to the rotor wake modelling have advantages and disadvantages. The idea to combine different methods, merging the best characteristics of each method while mitigating the disadvantages, showed promise in tackling the rotor wake simulation. This class of simulations is known as “hybrid” methods [38], [52].

The near body CFD analysis is employed to provide detailed near body flow field information which is used to obtain high-fidelity blade aerodynamic loadings. The far field wake region is simulated using vortex methods which provide accurate prediction of the evolution of the rotor wake released from the near body CFD domains.

The main idea of the approach being to divide the flow field into several regions and use appropriate flow solvers according to the dominant physical features of the flow in each region. The near body flow field (blade or aerodynamic element such as the fuselage), which is dominated by the effect of viscosity and geometry, is resolved using a 3D compressible CFD solver. The flow field outside of the CFD regions, which is primarily dominated by the vortices being shed from the aerodynamic surfaces, is simulated using a vortex/particle-based method.

A new application case of such hybrid methods consists in eVTOL aircraft studies. With their increasing number of rotor systems, vortex methods have emerged as useful tools for comprehensive analysis of eVTOL aircraft. These methods are able to provide a comprehensive solution with an affordable computational cost by combining structural, flight dynamic, and acoustic analysis solvers.

Furthermore, in the presence of complex fuselage or any other such body, a hybrid method that combines vortex methods with CFD or a generalized treatment of boundary conditions on solid walls can be used, providing an efficient and accurate way to compute flow fields around aerodynamic elements while considering the effects of the rotor wakes and interactions.

These hybrid methods could also be useful to investigate the impact of the fuselage shape, rotor/fuselage interaction on the development and the occurrence of the vortex-ring-state phenomenon.

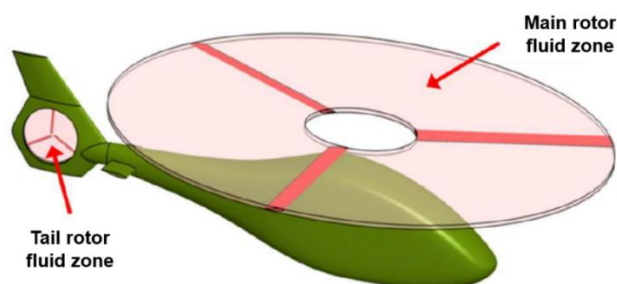
Indeed whatever CFD methods are conducted for VRS investigations on a helicopter main rotor, they almost always only consider the determination of VRS entry or phenomenon generation from the aerodynamic point of view, which is of course the fundamental cause of the VRS, but is in reality tightly coupled with the helicopter flight dynamics and blade dynamics.

Yet a counter-example is presented in [53], with a methodology based on a stronger coupling of several methods of Computational Fluid Dynamics with Flight Dynamics.

“The approach consisted of calculation of unsteady aerodynamic forces acting on the flying rotorcraft by simultaneous solution of the Unsteady Reynolds Averaged Navier-Stokes (URANS) equations, the flight dynamic equations of motion of the helicopter as well as the equations describing fluid-structure-interaction phenomena.”

Yet the airflow effects induced by the rotor blades are calculated using the actuator disk approach. In this simplified method for modelling the rotor, the blades themselves are not represented, but only their mean effect in terms of aerodynamic forces. These forces are calculated with the Blade Element Theory taking into account the airfoil characteristics of the blades. Then only the time-averaged aerodynamic effect of the blades is represented by means of momentum sources within the volume-disc zone swept by the blades, as shown on the following Figure 2-47 for the main and tail rotors.

► **Figure 2-47** Actuator disc modelling zones for the main and tail rotors – taken from [53]



Using this methodology, several helicopter flight simulations were performed in vicinity of the VRS domain. The first goal of the study was the development of a methodology of computational simulation of a helicopter flight. The methodology was directed towards simulations of strongly unsteady manoeuvres, typical for an entrance

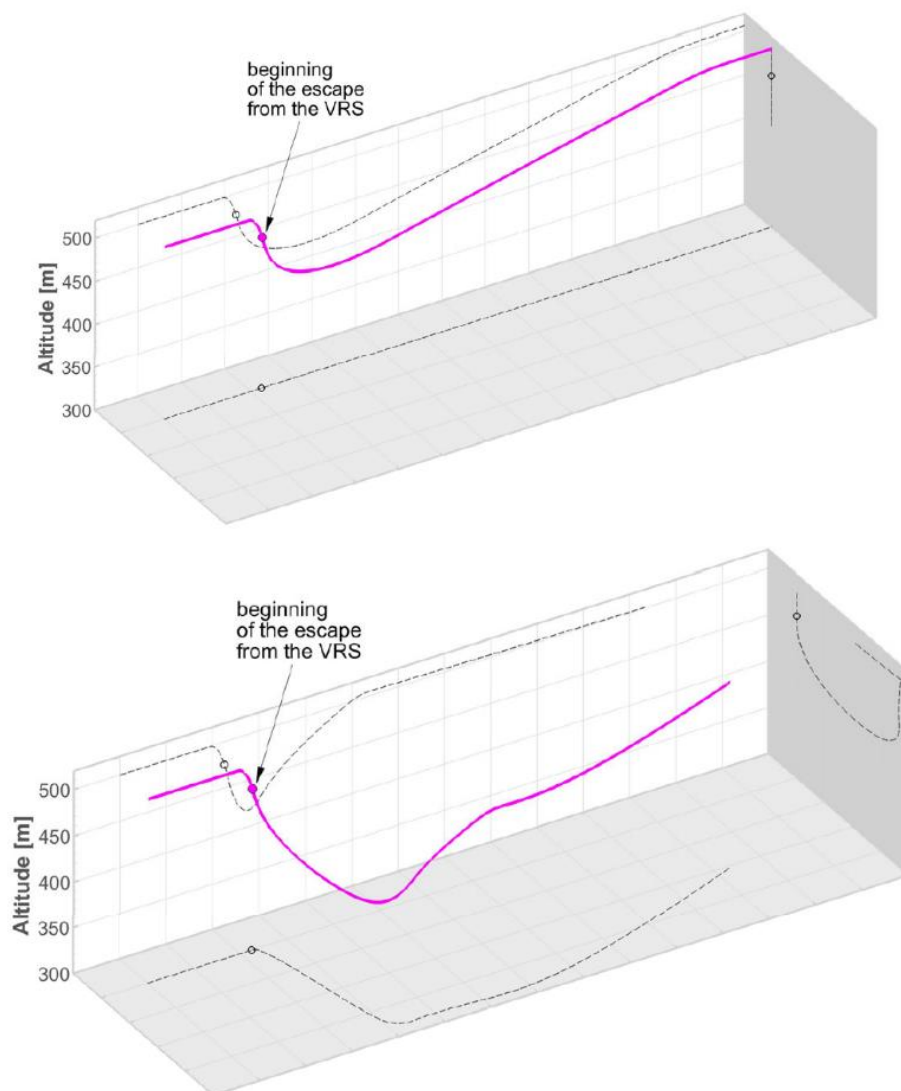
in or escape from the VRS. The second goal was the realisation of simulations of helicopter manoeuvres, focusing mainly on the identification of flight conditions leading to an occurrence of the VRS as well on the searching for “optimal” strategies to avoid or safely escape from the VRS. Simulations were performed with a light, 3-bladed, helicopter model. All simulations included the phases of an entry and a recovery from the VRS. The VRS entry was realised by the following procedure:

“Starting from the hover, the helicopter entered the horizontal flight through pitching its nose downward, thus generating an horizontal component of main rotor thrust pulling the helicopter forward. To enter the VRS, the helicopter slowed down its horizontal flight, by pitching its nose upwards. Simultaneously, the vertical acceleration of the helicopter was set to -2 m/s^2 . As a result, the helicopter entered a steep descent.”

When the first symptoms of the VRS on the main rotor appeared, the helicopter started the recovery manoeuvres. The classical recovery technique and the Vuichard technique were simulated.

Figure 2-48, taken from [53], presents the three-dimensional view of the flight trajectory and its and its two-dimensional projections on main vertical planes of the coordinate system. The position of helicopter at the beginning of the escape from VRS is marked on the trajectory by a pink circle.

► **Figure 2-48** Flight trajectory in the case of the escape from VRS through a forward-accelerated flight (upper graph) and a sideward-accelerated flight (lower graph) – taken from [53]



If, for once, both recovery techniques were simulated using high fidelity methods to compute the rotor wake, the results are quite surprising. Unfortunately, the analysis were mainly focused on the simulation of the airflow around the rotor instead of the impact of the applied recovery technique on the helicopter trajectory. Thus, in Figure 2-48, it can be seen that starting from 500 ft, both recovery techniques led to the same minimal altitude of around 420 ft while the Vuichard technique seems to allow a quicker re-increase of the altitude. But the longitudinal and lateral coordinates are not given.

The reasons why there is almost no difference between both techniques in term of loss of altitude are not discussed and the description of how the helicopter model is controlled is too limited to have a clear idea of the realism of the simulation.

Hence, the results obtained in this publication have to be considered very carefully and seem to be questionable regarding for example the rather rough modelling of the aerodynamics of the rotor blades and the control method. Nevertheless, even if it does not allow a numerical estimation of the most appropriate/beneficial procedure, this is the only publication found dealing with the simulation of recovery techniques using a rather Hi-fidelity aerodynamic CFD and flight dynamics coupled approach.

2.4.4 Summary of the current available analytical and simulation methods for prediction of the VRS

VRS domain estimation is completely linked to the criteria used to define VRS. The VRS domain estimation has been studied for a long time and numerous criteria are available in the literature. While not always based on the same methods, they generally give a domain between $-1.5 < V_z/V_{i0} < -0.4$ and $V_x < 0.8$ to $1.2 \times V_{i0}$

As already discussed and further detailed in the next chapters, these models provide an estimation of the VRS domain, but VRS onset is highly dependant of the dynamics of the helicopter when approaching the phenomenon.

For many years, inflow models have been augmented with (semi-) empirical and analytical models to remove restrictions present in dynamic inflow models. In the mean time, significant algorithmic progress have been made in the field of free wake methods.

For the transition between normal working state and wind-mill brake state, “classical” inflow models have to be extended so that they do not show false behaviour in vortex ring state. As very fast methods, they do have their use in flight simulation models, but without the use of multiple (and generally empirical) extensions, they cannot be employed with much confidence in all possible flight conditions, more especially in VRS.

Time-marching free wake models are much more promising here, as they make less assumptions about the wake; it is free to evolve under its own influence. This comes at a price however, as the computational time scales with the square of the number of wake elements.

High fidelity numerical methods are useful to assess the impact of design parameters on the knowledge of the aerodynamics phenomenon but there’s still no coupling between the airwake and the flight mechanics. It means that the airspeed is imposed on the rotor.

“Lighter” approaches (free wake computations based on different methods) are able to represent a realistic rotor airwake and the coupling to a flight mechanic code, while complex, is possible.

For real-time simulators, simple methods are still required. This generally implies adapted induced velocity model, or to artificially drastically reduce the rotor thrust on a pre-determined domain of airspeeds.

Most of the available studies are dedicated to the analysis of VRS entries and behavior of the helicopter once install in a fully developed VRS. Much less results are available regarding the recovery techniques.

An intermediate CFD approach between High Fidelity modelling with fine meshes for accounting for the blades and a coarser modelling of the global rotor effect with an actuator disc (as in [53]) could be to use an actuator line approach. In that kind of method, each blade is simulated by a line with momentum sources located along

the span (at a quarter chord from the leading edge as in a lifting line approach). This type of intermediate approach to represent rotating wings within a CFD model could allow capturing the effect of blade on the airflow at a lower computational cost compatible with a strong coupling with the computation of the blades and helicopter flight dynamics.

3. VRS Knowledge – Flight test campaigns

3.1 ONERA/DGA-EV flights test campaigns

3.1.1 Dauphin 6075

In order to improve and to validate the aerodynamic models developed during the theoretical investigations, two flight test programs were organized on the instrumented helicopter Dauphin N°6075 operated by DGA-EV. The first program was dedicated to the identification and the analysis of the Vortex-Ring State domain. During the second program, measurements of the main rotor flow airspeeds were performed. For that purpose, a specific device was designed.

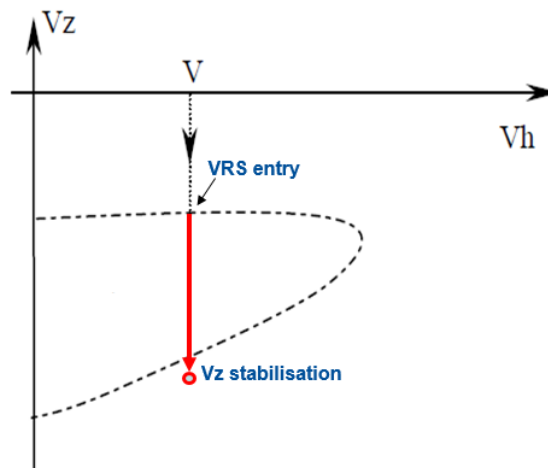
Several publications were done, dealing with the realisation of these flight tests, their analyses and the development of an adapted induced velocity model in steep descent [6], [16], [28], [29]. The main results are outlined hereafter.

3.1.1.1 VRS investigation procedures:

Two different flight procedures were defined to lead the helicopter into Vortex-Ring State.

- Method (a): from level flight at a given forward velocity, collective input was gradually decreased until the helicopter enters in Vortex-State. The maneuver was repeated for different forward velocities, determining the VRS upper limit (Figure 3-1).

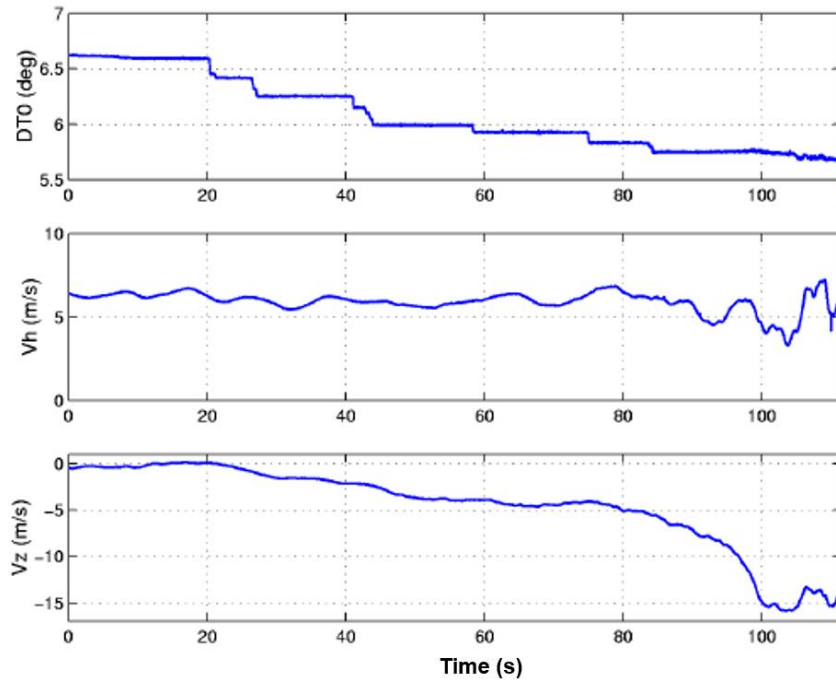
► Figure 3-1 VRS upper and lower limits determination



An example of VRS flight test with this method is shown on Figure 3-2. During the maneuver, the forward velocity (V_h) was kept constant and the collective was progressively decreased. In a first time, each collective decrease implied a light V_z decrease. The last collective decrease (DT0) at $t = 85s$ produced a vertical speed (V_z) that changes from $-5m/s$ to $-15m/s$. We assumed that the helicopter leaves the VRS when the rate of descent is stabilized (at $t = 100s$).

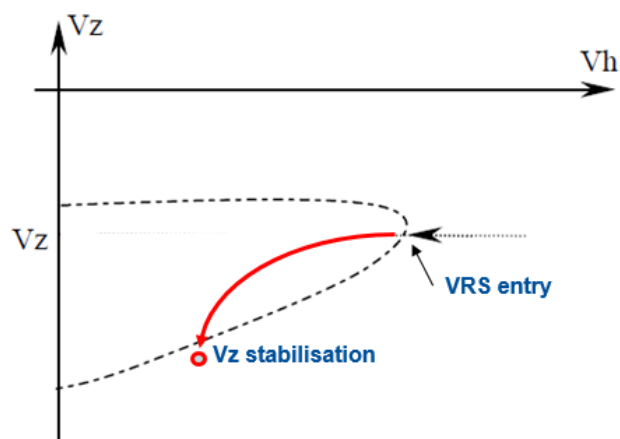
In this example the VRS boundaries are easily determined.

► **Figure 3-2** VRS Example of VRS initiation by collective decrease at constant forward speed – taken from [29]



Method (b): from a descending flight (V_z fixed), the forward velocity was gradually decreased until the VRS is reached. Repeating this operation allowed determining the “knee” of the VRS domain (Figure 3-3). As in the previous method, it was assumed that VRS is exited once the vertical speed is stabilised.

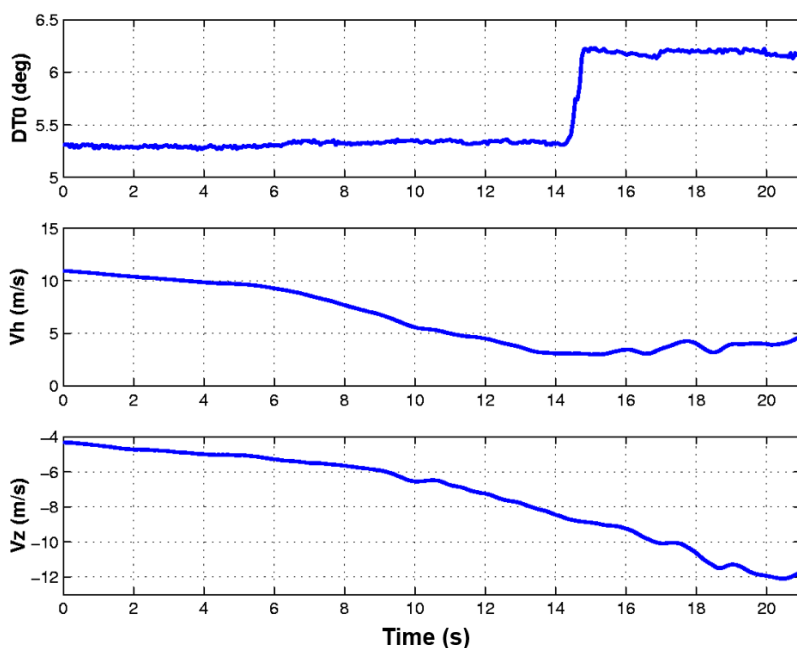
► **Figure 3-3** Determination of the “Knee” of the VRS domain



Several flight tests showed that VRS limits determination (i.e.: precise determination of VRS entry) with this method is more difficult than with the previous one. Indeed, at this region of the flight domain (low forward speeds), it was found that there is no sudden drop of V_z when the helicopter enters the Vortex regime. That is to say, VRS effects seem to be smoother when flying at the lateral limit of this region. It came out from the flight investigations that the best indicator to know if VRS is reached at low forward speeds, is a high level of vibrations.

Thus, the flight test presented in Figure 3-4 is more complex to analyse than the previous one. In this case, the helicopter entered the VRS by deceleration (method b) from the initial flight condition: $V_h=10\text{m/s}$ and $V_z=-4\text{m/s}$. As the collective was hold to its initial value, the RoD slightly increases as the forward speed decreases. The VRS limits determination with this method, if only based on a sudden increase of the rate of descent, is more difficult than with the method (a). In this case the vibration level and flight parameter fluctuations are the best indicator to determine the VRS limits. The VRS entry occurred at 10s, for a forward speed of around $V_h=5\text{m/s}$ (9.7 kts), and a vertical speed V_z of -6.5 m/s (-1279.52 ft/min).

► **Figure 3-4** Example of VRS entry by deceleration – taken from [28]



In conclusion, during type (a) maneuvers the VRS limit is easy to determine by the sudden V_z drop. For type (b) maneuvers, this analysis becomes more difficult. The best indicator of VRS being then the increase of flight parameter fluctuations such as the attitudes, required power or accelerations. However, the two methods are required to determine the whole VRS domain.

In case of a sudden increase of the rate of descent, pilot's instinctive reaction is to increase the collective level to stabilize V_z .

However, flight tests show that in VRS, rate of descent is generally insensitive to the collective. This phenomenon raises the VRS danger.

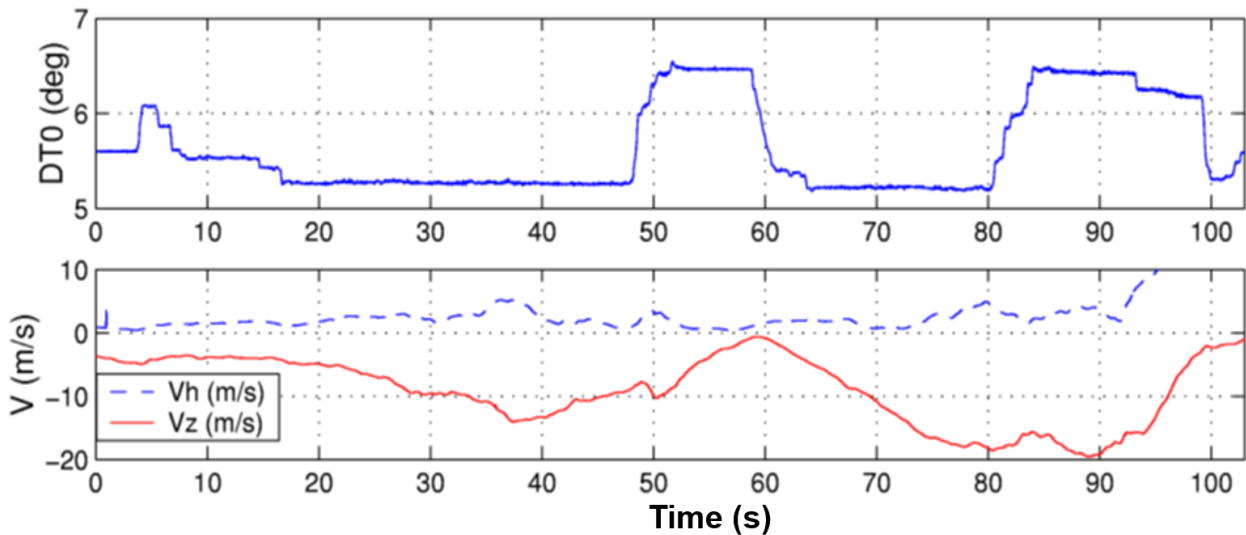
An example of the insensitivity of collective can be also seen in Figure 3-4. Once entered in VRS at $t = 10\text{ s}$, the pilot increased the collective at $t = 15\text{ s}$. But the rate of descent continued to increase. Finally, the V_z stabilization occurred at $t = 20\text{ s}$, at $V_z = -12\text{m/s}$ (-2360 ft/min).

For the majority of the tests, the collective increase, alone, didn't permit the helicopter to leave the vortex regime. Nevertheless and in contrary to the common assumption, the collective increase didn't amplify the VRS effects during these tests. The helicopter was generally insensitive to this command within the Vortex-Ring area.

However, a collective increase to a level greater than the hover value allowed the helicopter to leave VRS in a few cases, but this behavior was not predictable. For instance, the first collective increase in Figure 3-5 (at $t=48\text{s}$) resulted in a successful VRS recovery from VRS. But the second collective increase, nearly identical to the first one, didn't allow the VRS exit. The RoD finally increased when the forward velocity increased. This example illustrates again the VRS unpredictability, as discussed previously. It has to be noted that the first

collective increase was performed at a V_z equal to -10m/s (-2000ft/min ca) while the second was done at $V_z = -18\text{ m/s}$ (-3500 ft/min ca), corresponding to a fully developed VRS.

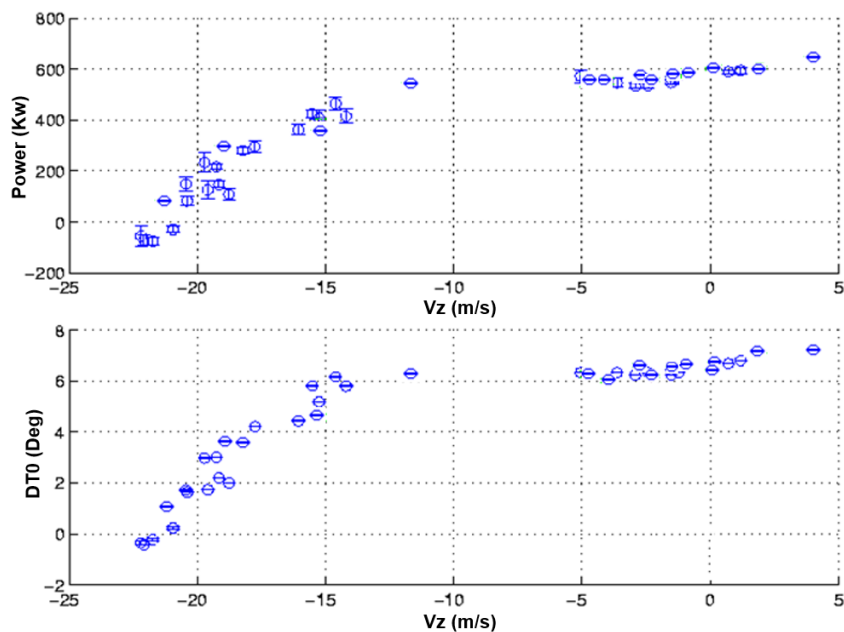
► **Figure 3-5** Second example of collective level increase during VRS – taken from [29]



To conclude, increasing the collective level is an uncertain way to leave quickly the VRS. This can help to exit VRS at the very beginning of the phenomenon, but not in a fully developed VRS.

Figure 3-6 presents the recorded collective blade pitch (DT0) and required rotor power (Power) as a function of the rate of descent (V_z), in stabilised vertical descents.

► **Figure 3-6** Required rotor power and collective as a function of vertical speed

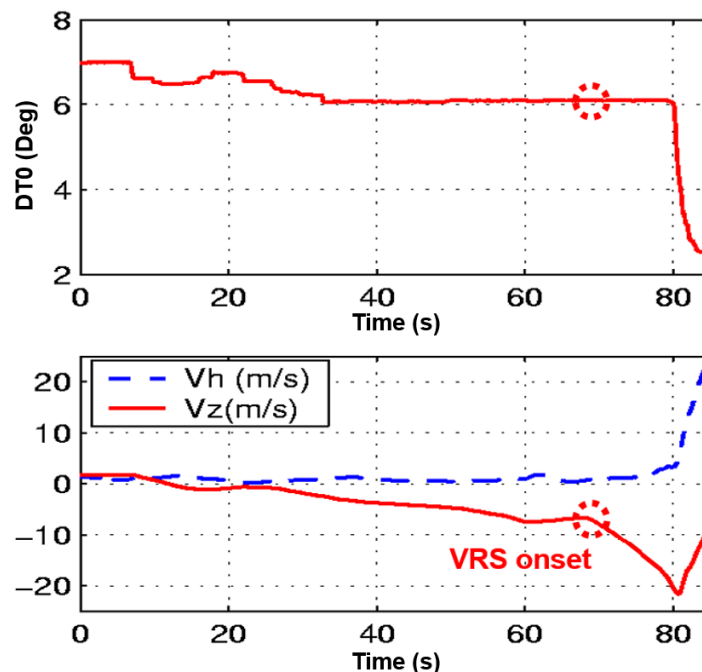


The figure shows that for a range of rates of descent corresponding to the Vortex-Ring regime (from -5 m/s to -13 m/s for the Dauphin helicopter), the required power and consequently the collective remain almost

constant. This insensitivity to the collective clearly explains the V_z drop when entering the Vortex-Ring regime in vertical descent. Indeed, when the helicopter is descending at -5m/s (flight at the right side of the insensitivity margin), any light reduction of the collective will lead to a new trim condition corresponding to a rate of descent greater than -13m/s (left limit of the insensitivity margin). It results in an abrupt fall of V_z from -5m/s to at least -13m/s .

The VRS is, for the moment, known to be an unpredictable phenomenon. Two VRS flights starting from close conditions can imply very different helicopter reactions. The turbulent flow producing VRS probably explains this behavior. Figure 3-7 illustrates the unpredictable aspect of the VRS. In this example the helicopter entered in VRS even though the flight parameters were stable in terms of forward airspeed (V_h) and no action on the collective was applied. The start was probably caused by some minor event.

► **Figure 3-7 Unexpected VRS start from stabilized conditions – based on [6]**

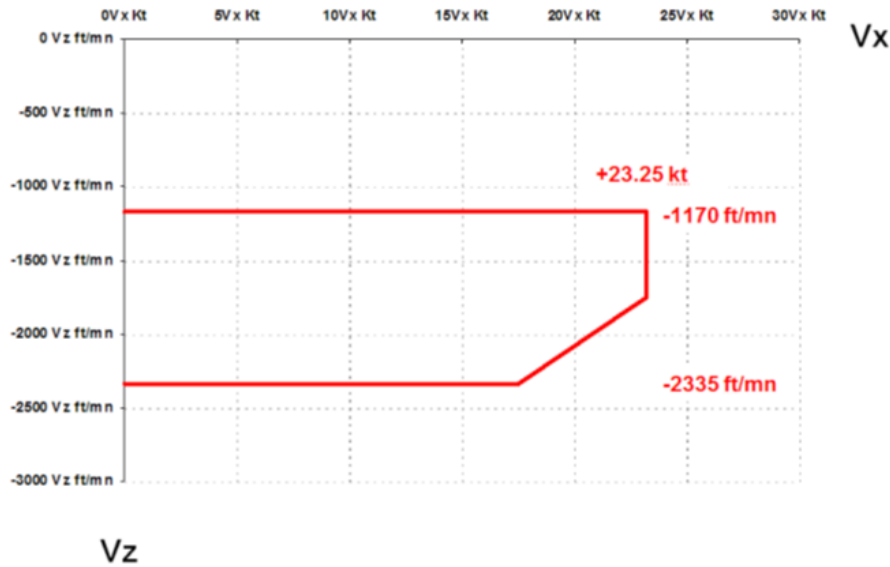


Despite several unpredictable aspects, these flights tests helped describe the VRS main characteristics. First, the crew felt an increased level of vibrations when the VRS area was approached. Then, the VRS started by a sudden decrease of the rate of descent. Increasing the collective didn't stop the V_z fall, except, sometimes, if it is apply at the very beginning of the phenomenon.

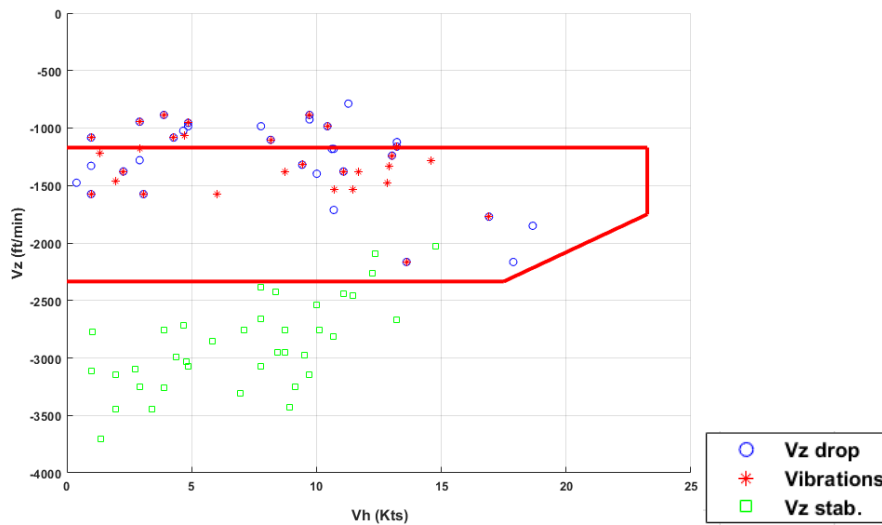
In order to determine the entry point (sudden increase of the rate of descent) and the exit point (stabilisation of the rate of descent), it was asked to the pilot to maintain a constant forward speed during the entire maneuver, thus also in VRS. During the fall, the helicopter was very unstable and hard to control, with a pitch-down tendency due to the relatively large horizontal stabilizer of the Dauphin helicopter. The crew talked about “rodeo exercise”.

Following Figure 3-8 presents the Vortex-Ring-State boundaries of a Dauphin SA365N provided by Airbus Helicopters. In Figure 3-9 is plotted the VRS domain identified from ONERA flight tests.

► **Figure 3-8** Dauphin SA365N VRS domain from Airbus Helicopters customer support at maximum mass



► **Figure 3-9** Dauphin SA365N VRS domain from Airbus Helicopters compared to flight tests



The previous limits are also plotted for comparisons. The limits are expressed in a (V_h, V_z) diagram corresponding to a given standard flight condition. The collected data correspond to the following observations:

- Beginning of V_z drop,
- Beginning of fluctuations increase (fluctuation of flight parameters such as the attitudes, required power, accelerations),
- Exit (“lower” boundary) by V_z stabilization.

When the forward velocity is lower than 20 kts, the upper limit appears at low and approximately constant rate of descent ($V_z = -1000$ ft/min).

It can be seen a large dispersion of the flight tests data (VRS entry and exit points), indicating that VRS domain is very difficult to determine, even more to predict, because of its intrinsic turbulent and chaotic nature. Two VRS runs, starting from similar flight conditions, could lead to very different helicopter behaviours.

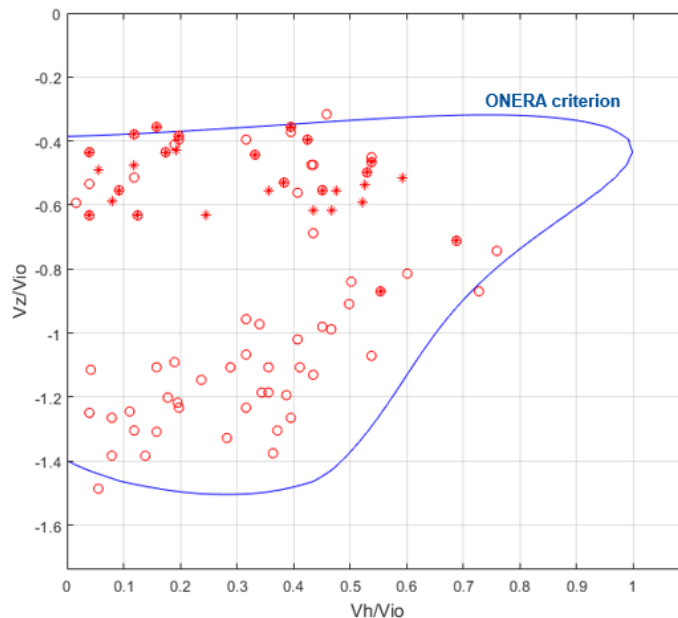
In Figure 3-10, the boundary velocities V_h and V_z are made non-dimensional by the division by the hover induced velocity V_{i0} to be compared with literature data. The limits presented are in good agreement with all the experimental data. Moreover, the comparison shows that the ONERA analytical criterion is able to predict the VRS domain.

All the data of Figure 3-10 show that VRS can not be encountered since $V_h > 0.8 \times V_{i0}$. Below this forward velocity, the pilot must keep a RoD such that $V_z/V_{i0} > -0.3$. A slope angle greater than 30° ensures, also, the avoidance of the dangerous area. It is to note that the velocities normalization by V_{i0} is particularly interesting. Indeed, it is possible to take into account several parameters:

- Helicopter weight,
- Rotor size, through S ,
- Flight conditions, through V_h/V_z

However, more sophisticated parameters such as the blade twist can not be taken into account by this normalization.

► **Figure 3-10** Non-dimensional Dauphin SA365N VRS boundaries

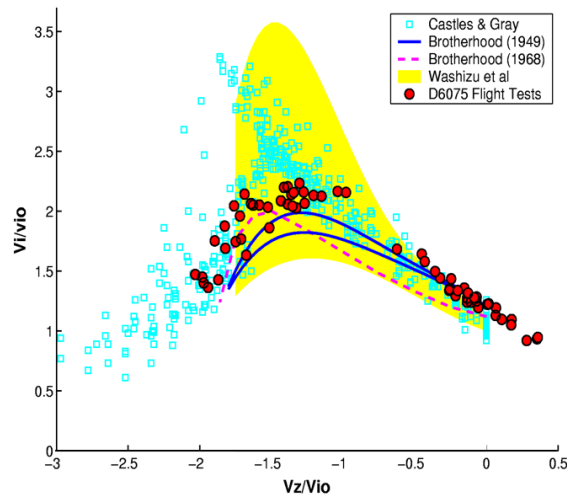


Specific configurations: Two specific configurations were included in the previous results.

- **Backward flight:**
Several VRS flights were performed during backward flights. This kind of tests would not directly appear in the previous figures because the limits are plotted as a function of the horizontal velocity modulus $V_h = \sqrt{V_x^2 + V_y^2} \geq 0$. In this case, the helicopter behavior was similar to the forward one even if it was more impressive, according to the crew. The corresponding limits are homogeneous with other data.
- **Flight without horizontal stabilizer:**
During another flight test campaign, several VRS flights were also performed without the horizontal stabilizer. In these conditions, the helicopter was more stable in the VRS. However, the VRS limits are not affected by the absence of the stabilizer.

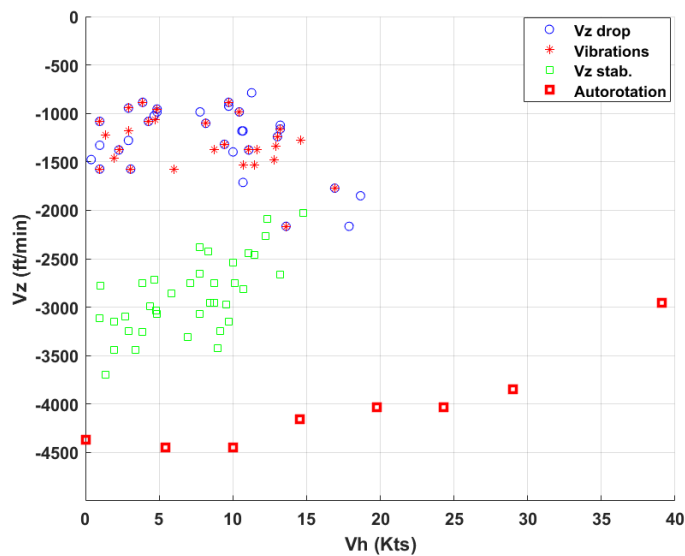
A main activity led in [6] has been to estimate the mean induced velocity during VRS flights. The method enabling this estimation is detailed in this PhD thesis and results are presented in Figure 3-11. The lack of results for non-dimensional vertical speed between -0.7 and -1 corresponds to VRS domain.

► **Figure 3-11** Estimation of the mean induced velocity based on Dauphin SA365N VRS flights – taken from [6]



Among flight test cases, some autorotations were performed at low forward speeds. The results are presented in the following Figure 3-12. It can be seen that, as already explain in the sub-section 2.1, the vertical speeds reached in autorotation are lower than in VRS.

► **Figure 3-12** Autorotation test cases on Dauphin SA365N flights



Synthesis of the Dauphin VRS domain estimation flight test campaign:

10 flights were performed to determine the VRS domain of the Dauphin.

For very low forward speeds, below 10kts, VRS manifests by a sudden increase of the rate of descent from around -1000 ft/min to -3000 or -3500ft/min.

For forward speeds between 10kts to 20 kts, a strong instability of the helicopter occurs around $V_z = -1500$ ft/min. In this case, the drop of V_z also appears but in a more moderate way than in vertical descent.

In VRS, the helicopter is insensible to collective increase, but the flights carried out show that the increase of the collective does not amplify in any way the effects of VRS.

3.1.2 Fennec flight tests at EPNER in 2004

In the framework of a thesis done at EPNER (French test pilot and engineer school) in 2003-2004, several VRS flight tests were performed to determine the VRS domain of the AS550 U2 Fennec n° 2851 of DGA-EV. As the Dauphin and the Fennec don't have the same characteristics (three and four blades, 2.0/3.8 tons), it was also interesting to validate ONERA VRS domain criterion for both helicopters.

The Fennec flight tests analysis confirmed the specific helicopter's behavior in VRS as already observed during the Dauphin flight tests. During Dauphin flight tests analysis, the VRS was mainly determined by an increase of the descent rate. But several flight tests showed that this method is difficult and doesn't always provide an accurate determination of the flight parameters at the VRS initiation.

So, in this work, other flight parameters were studied to give a better estimation of the VRS entry and to deal with the uncertain cases. The rate of descent was analyzed but also the accelerations, the heading, the input control fluctuations and the glide slope. Some specific methods were also used to better determine the VRS entry points.

The insensitivity of the helicopter to the collective within the VRS area was observed.

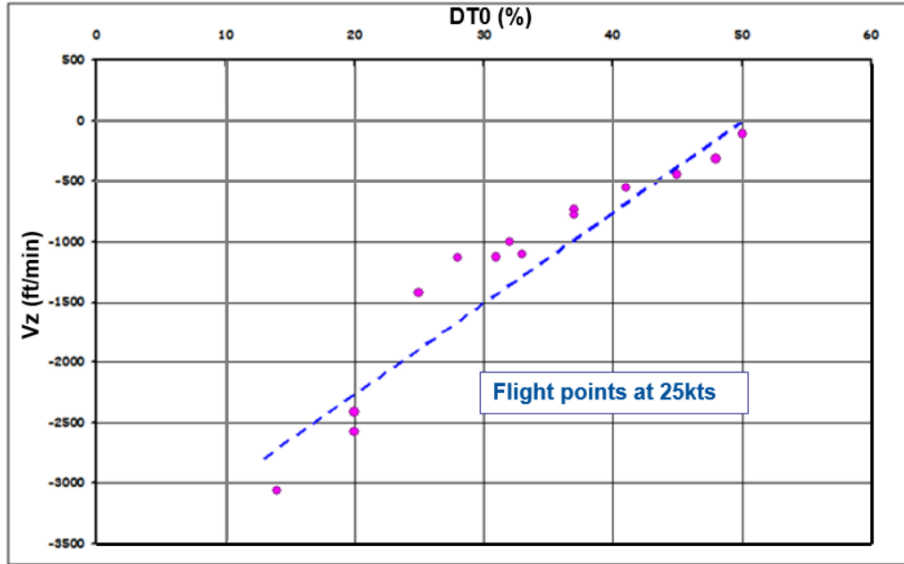
As the precise knowledge of the helicopter low airspeeds is required during these flights, helicopter longitudinal and lateral airspeeds were computed in real-time thanks to the determination of the wind magnitude and direction and the inertial unit. These components were then displayed in the cockpit, allowing the pilot to precisely reach and maintain speed targets during the flights.

7 flights were performed for a total of 8.6 flight hours. 2 flights dedicated to instrumentation and procedure validation, 5 dedicated VRS flight tests.

- Flight 1: Upper limit of the VRS domain was estimated, from V_x air = 25 kt to 0 kt by step of 5 kt. These points allow to determine the upper limit of the VRS domain. Two points were also made to find "the knee" of the VRS domain.
- Flight 2: The purpose of this flight was to find the lower part of the VRS domain. The air speed V_x was progressively reduced from 20 kt to 0 kt by steps of 5 kt. Initial vertical speed was around -2000 ft/mn. Increases of the collective were performed to reach VRS. The same type of point was carried out with $V_z = -2500$ ft/mn.
- Flight 3: Complementary test points were performed at given airspeed to complete upper and lower limits. An autorotation was performed.
- Flight 4: Autorotations were done at different airspeed. In addition, some additional flight cases were performed to complete the lower limit.
- Flight 5: Flight test cases were made in order to get the curve of the vertical speed according to the collective level. Successive decreases of the collective were done in order to reach a stabilized vertical speed in flight without power and for a rotor RPM of 400. These points can help to find the knee of the vortex domain (this procedure was applied at two different air speeds V_x : 20 kt and 25 kt). A low point of the domain and an autorotation were also carried out.

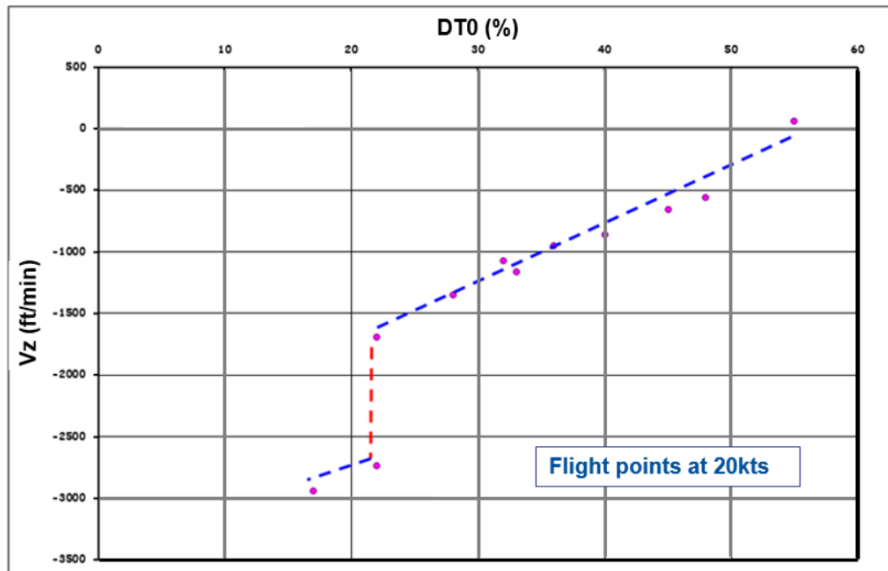
Performing decelerated manoeuvres to determine the "knee" of the VRS domain is one option, as previously mentioned in the Dauphin flight test campaign. Another one is to establish, for different stabilized airspeeds, the curve of the vertical speed according to the collective level. The following Figure 3-13 shows the level of collective (DT0 in % - 0% corresponding to full-down, 100% to full-up) as a function of the Vertical speed (V_z), at an airspeed of 25 kts. There's a slight dispersion of the points, but not a real discontinuity in the curve.

► **Figure 3-13** Collective as a function of vertical speed at 25 kts



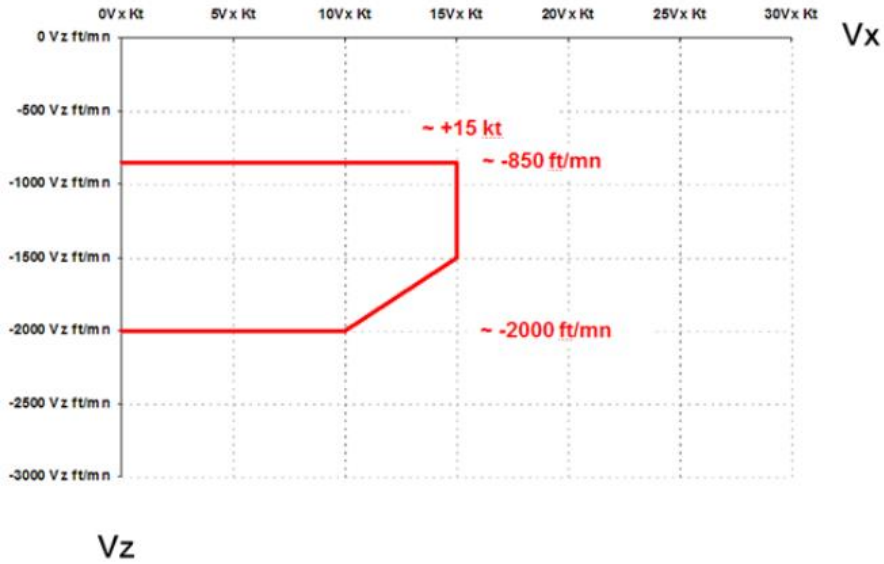
At 20 kts, as seen on Figure 3-14, a discontinuity can be observed on the curve, where the same collective level brings to two different vertical speeds. This discontinuity in terms of collective level with respect to vertical speed is also represented in Figure 3-17 and characterizes the VRS domain, providing upper and lower boundaries.

► **Figure 3-14** Collective as a function of vertical speed at 20 kts

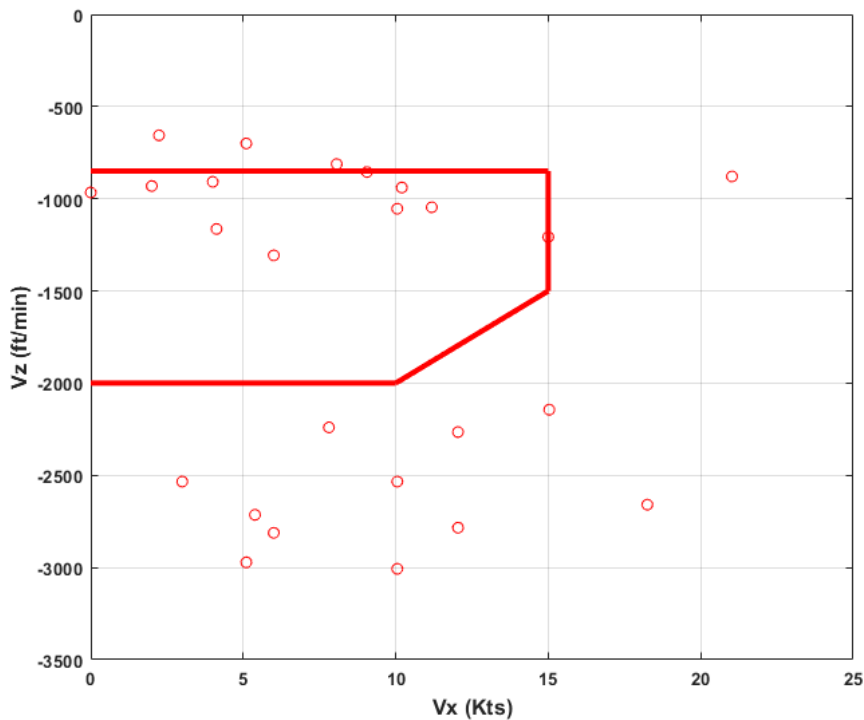


The analysis of the flights led to the evaluation of the following VRS domain for the Fenec helicopter. The average reduced mass (equal to Mass/σ where σ is the air density divided by 1.225) was 2430 Kg. Figure 3-15 shows the Fenec VRS domain given by Airbus Helicopters customer support. Figure 3-16 provides the comparison between flight tests data and estimated VRS domain from Airbus Helicopters.

► **Figure 3-15** AS350-U2 VRS boundaries from Airbus Helicopters customer support



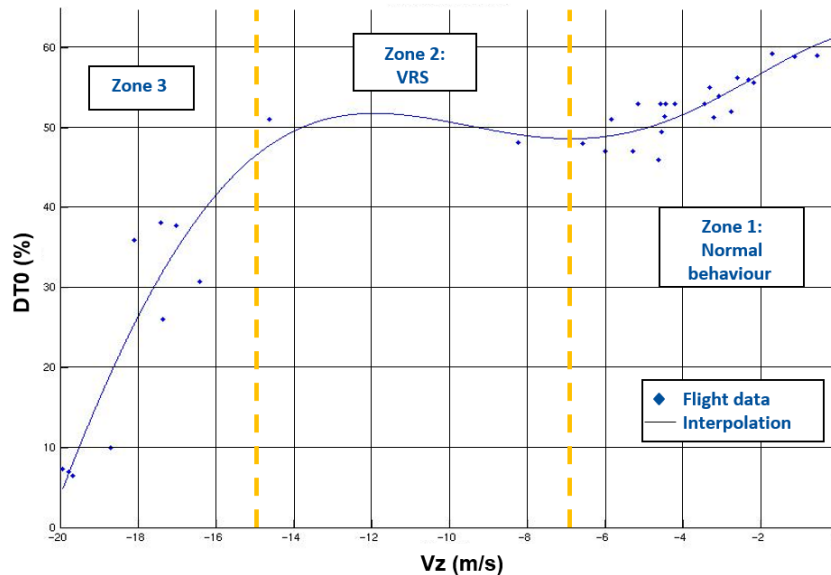
► **Figure 3-16** AS350-U2 VRS boundaries from flight test and compared to Airbus Helicopters customer support limits



As already seen in Figure 3-6 obtained thanks to the Dauphin flight tests, the recorded collective level (DT0 in %) can be plotted as a function of the vertical speed (Vz in m/s) (Figure 3-17).

The flight data corresponds to stabilized flight cases, at forward speeds between -2 m/s to 9.5 m/s (3.8 kts to 18.5 kts)

► **Figure 3-17** Collective as a function of the vertical speed – data from Fennec flights



Results are very similar to Dauphin test cases. Several conclusions can be drawn from these plots:

- In zone 1, the variation of the collective is monotonous (not considering the dispersion of the data), a decrease or increase of the collective corresponding to a lower or a higher vertical speed. This behavior can be observed up to descent speeds of around -5 m/s (-1000 ft/min ca)
- When the helicopter enters VRS "from above", a same value of DT0 corresponds to two flight points; one at Vz of around -5m/s (-1000ft/min ca) before VRS, the other around -15m/s (-3000ft/min ca) and therefore after VRS.
- There is no stabilized point in the zone 2, corresponding to the VRS. The helicopter is then subjected to a large variation of the vertical velocity at a constant collective pitch.
- We notice in zone 3 that the "slope" of the curve is much greater, which implies that a large variation of the collective corresponds to a small variation of the vertical speed. This difference in the efficiency of the collective between low and high speeds of descent could be observed during these tests.

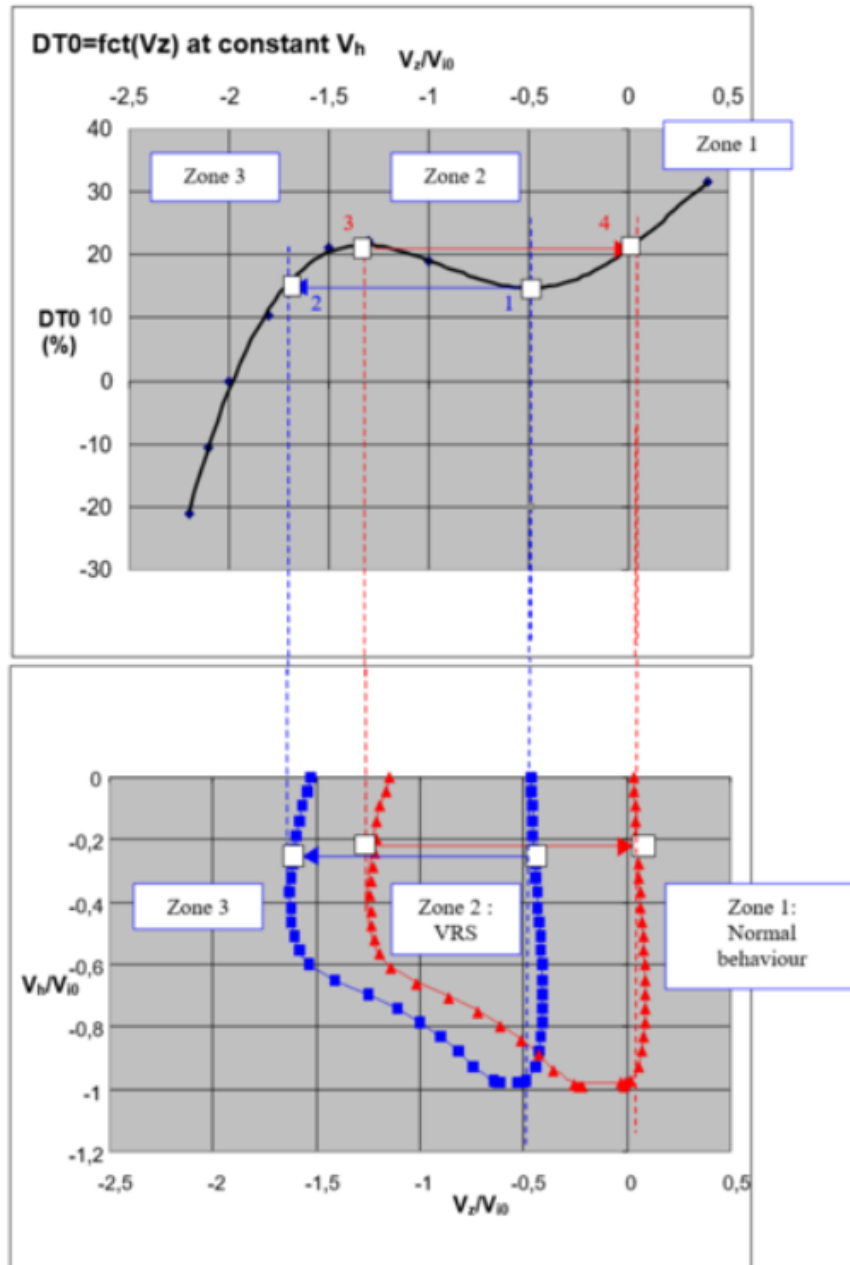
The following Figure 3-18 below is not plotted from flight tests. It has been generated for explanatory purposes, to show the link between the DT0/Vz curve and the Vh/Vz VRS domain. The 3 zones characterized in the previous paragraph are now shown with respect to the VRS domain.

If the VRS is entered from above (from point 1 in the figure), the "next" stabilized vertical speed will be at around $-1.7 V_z/V_{i0}$. With an entry from below (from point 3 in the figure), the "next" stabilized vertical speed is then around 0 (it has to be noted that the values given here are not representative. The figure has to be used as a graphical explanation). Thus, the real VRS domain would be "only" the zone between point 1 and 3.

These considerations are comparable to the bifurcation theory exposed previously (see Figure 2-37 from [35]). After the bifurcation from one stable branch (Helicopter branch for an entry "from above" the VRS domain, or "from below" for an entry from the Windmill branch), the helicopter stabilizes at vertical speeds which do not correspond to the VRS frontier but simply to the stabilization point on the other stable branch for the same condition (V_z , V_h , DT0). Therefore the VRS domain "stricto sensus" is narrower than the stable points corresponding to this hysteresis effect.

The evolution of the collective with respect to vertical speed is also indicated in [27], where it is mentioned that if the altitude margin is sufficient, it is possible to re-increase the collective to exit VRS from above. But the time needed is important and it is better to have a large power margin, so having a light mass.

► **Figure 3-18** Parallel between collective curve and VRS domain



During the analysis of the ONERA/DGA-EV flight tests, it can be assumed that the helicopter leaves the VRS when the rate of descent is stabilized, thus corresponding to point 2 in the figure.

3.1.3 Dauphin/Fennec flight tests “VibRS”

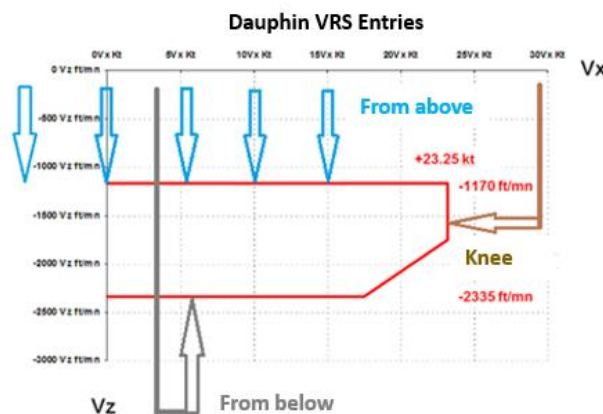
Following previous flight tests conducted in the years 2000-2004 and the common experience in the field, a contract called "VibRS" was signed in 2011 between ONERA and DGA-EV to carry out VRS test flights with two aircraft (Fennec and Dauphin) instrumented with accelerometers allowing the measurement of vibrations at different locations of the machines.

The main goal of these flights was the realisation of vibrations recording at various locations of the helicopters and their flight parameters, obtained in different types of VRS entries (by the upper limit, “the knee”, the lower limit). After these flights, ONERA performed the analysis of both flight parameters and vibration data to identify a characteristic signature of the VRS regime.

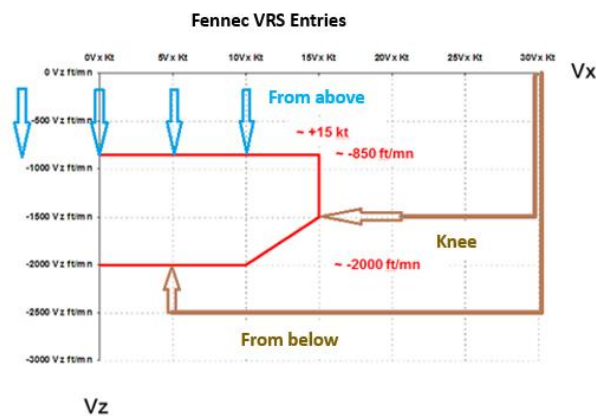
A total of 5 flights were performed, 2 on the Dauphin N°6111 and 3 on Fenec N°2851.

The manoeuvres performed to enter VRS domain are indicated in the following figures, and are very similar to the ones used in previous flights.

► **Figure 3-19** Dauphin VRS entry procedures



► **Figure 3-20** Fenec VRS entry procedures



The first flights on Dauphin and Fenec had a double objective. The first one was to validate the instrumentation and the second one being to provide a first series of vibratory recordings, but only in a restricted portion of the vortex entry domain (entry from HOGE at zero speed on the 3 axes).

73 entries in VRS were carried out, on the whole of the 5 flights, under various entry conditions (hover $V_x = 0$, $V_y = 0$, entry with positive and negative V_x and $V_y = 0$, by “the knee”, by the lower limit, from autorotation or by-passing the VRS domain).

- 26 VRS entries on DAUPHIN in 3.5h of flight
- 47 VRS entries on FENEC in 6.3h of flight

Each VRS entry was systematically doubled, in order to cross the opinions and comments of the pilots.

The phenomena announcing the approach of the entry domain in Vortex were the following:

- Low frequency vibrations (10 to 20 Hz) which can be perceived by the crew very clearly or weakly depending on the test case. These vibrations can be felt in the form of a "train of vibrations" (not continuous). Changes in frequency can also be perceived. They can be perceived for low RoD (from -300 ft/mn), their intensity generally increasing when the RoD increases (from -500 to -700 ft/mn).
- Acoustic noise was perceived, at low frequencies (10 hz to 20 hz), generally associated with the appearance of vibrations. These noises were sometimes audible, sometimes little (acoustic resonance phenomena of the cabin?).
- A reduction of effectiveness of the cyclic pitch controls was experienced, resulting in a decrease of the control power on longitudinal axis.
- A reduction of effectiveness of the pedals was also observed, leading to yaw motion.
- Each phenomenon being more or less felt according to the amplitude of the step in collective pitch decrease, the initial V_x , and the V_z .
- Pitch-up tendency: It was noted that for some upper VRS limit entries, the aircraft showed self pitch-up tendencies, after the appearance of the vibrations, which could be opposed according to the cases, to the departure in Vortex.

If the collective decrease step is too important, the announcing phenomena are erased, showing little or no flight control flutter, nor yaw departure.

3.1.3.1 VRS entries with negative speed

The vertical speeds obtained at the entry in VRS seemed to be more important for negative V_x speeds (-5 kt and -10 kt), around -1000 ft/mn. Only vibration changes. At the sudden rate of descent increase, the reduction of effectiveness of the pedals and the cyclic seem less important .

With the same weight, the aircraft entered more easily in VRS with negative speeds than with positive speeds. It has to be noted that trying to enter VRS from a V_x of -10 kt, the control margin (cyclic control stick) was reached laterally (center stick against pilot leg)

With a weight of - 150 kg compared to the reference weight, the entry in Vortex was more difficult to find.

3.1.3.2 VRS entries by the knee

The runs were carried out after having reached a vertical descent speed of -1500 ft/mn with a V_x of +20 kt. The entry in Vortex occurs towards +8kt by carrying out in reduction of speed V_x starting from +15 kt, always with an stabilized RoD of -1500 ft/mn.

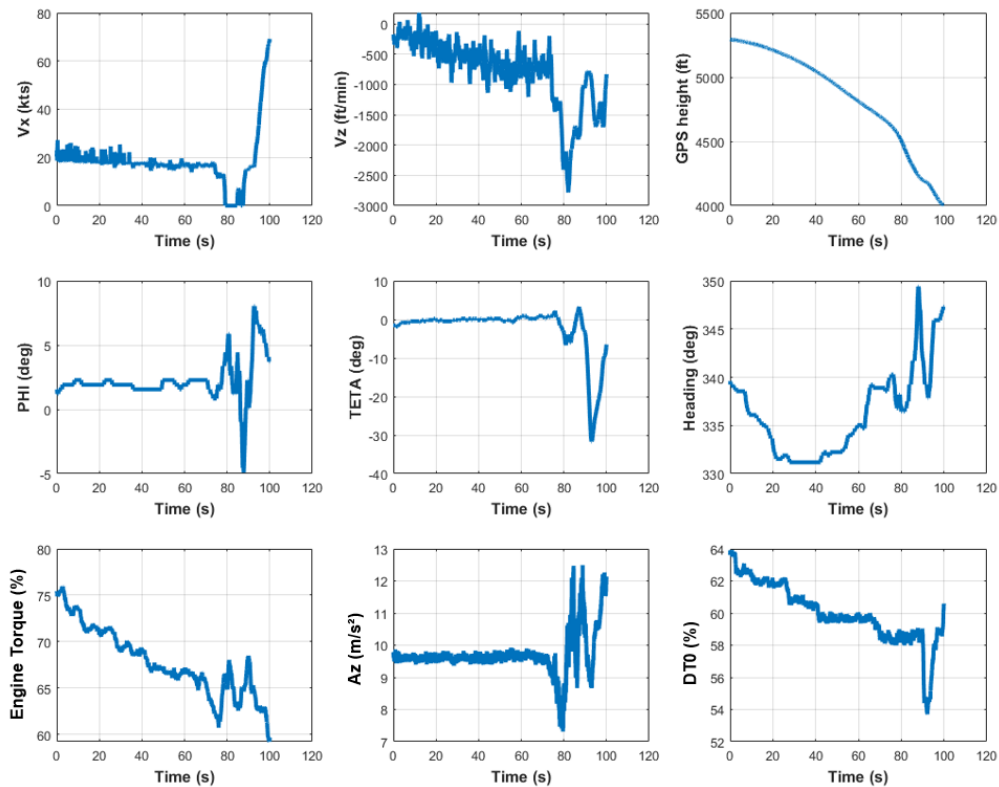
The warning signs were less perceptible, only a light yaw departure followed by a reduction of effectiveness of the pedals was observed.

The pilots found it was easier to detect the vortex on Fennec than on Dauphin. The increase of the vertical speed was generally more pronounced on Fennec than on the Dauphin.

3.1.3.3 Vibration analysis:

The following Figure 3-21 is showing a run of the 3rd Fennec flight, where a VRS entry was performed by a decrease of the collective (DT0). Helicopter mass was 2019Kg, the VRS entry occurred at 78s.

► **Figure 3-21 Fennec flight parameters – VRS Entry**



Pilot comments during flight:

- 1st collective decrease: the descent rate is setting up;
- 2nd collective decrease: $V_z = -400\text{ft/min}$;
- 3rd progressive collective decrease: $TQ = 67\%$, strange vibrations, at low frequencies, $V_z = -750\text{ft/min}$;
- 4th collective decrease: Increase of the descent rate, vibrations, controls are a bit floating, very smooth VRS entry at $TQ = 62\%$.

The following Figure 3-22 represents the spectrogram established on the data taken from the vertical axis of the accelerometer placed under the pilot seat.

A spectrogram is a visual representation of the spectrum of frequencies as it varies with time. As shown on the two graphs, a common format is a graph with two geometric dimensions: one axis represents time, and the other axis represents frequency; a third dimension indicating the amplitude (i.e. energy) of a particular frequency at a particular time is represented by the intensity or color of each point in the image.

In these cases, spectrograms are calculated from the time signal using the Fast Fourier transform.

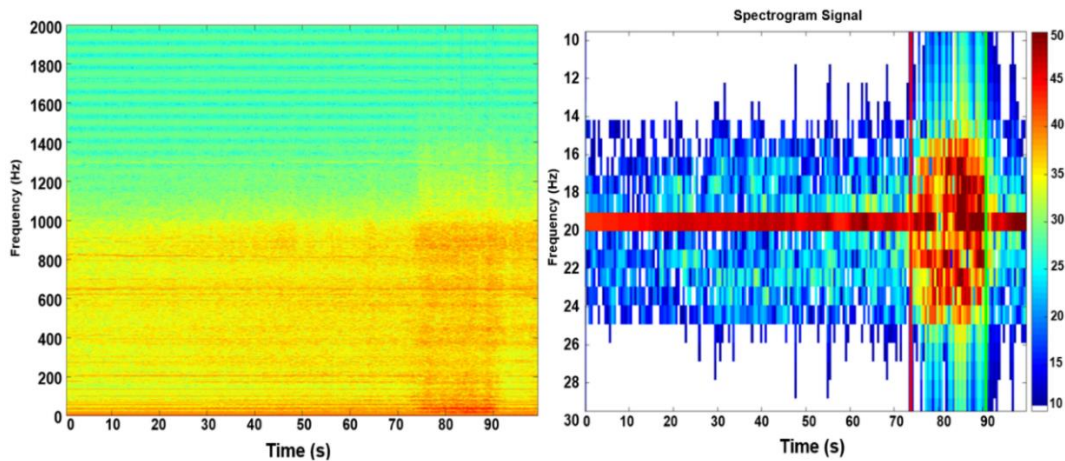
During the flight, the pilot indicated the VRS entry at 80s. From the post-treatment of the flight parameters, the entry could be estimated at 78.3s.

As the acquisition frequency of the accelerometers was 4000Hz, the left graph shows the frequencies contained in the signal up to 2000 Hz. The right graph focusses on the Fennec main rotor blade passing frequency equal to:

$$\text{Main rotor blade passing frequency} : \frac{\text{Rotor RPM} \times \text{Nb of blade}}{60}$$

$$\text{Here} : \frac{390 \times 3}{60} = 19.5\text{Hz}$$

► **Figure 3-22** Spectrogram applied on the signal of the accelerometer placed below pilot seat (vertical axis) – VRS entry



It can be seen that the vibration spectra is changed for low, but also for high frequencies. Rotor harmonics and energy are dissipated into a larger bandwidth signal.

Considering the changes in the frequency spectra, and the energy dissipation around the main rotor blade passing frequency, vibrations due to VRS set-up are visible at 73.8s. It can be seen that the vibration spectra returned to normal à 91s, corresponding to the VRS exit.

The following figures (Figure 3-23 and Figure 3-24) are showing a run of the 3rd Fenec flight, where the helicopter didn't enter VRS. Helicopter mass was 2071Kg.

► **Figure 3-23** Fenec flight parameters – No VRS

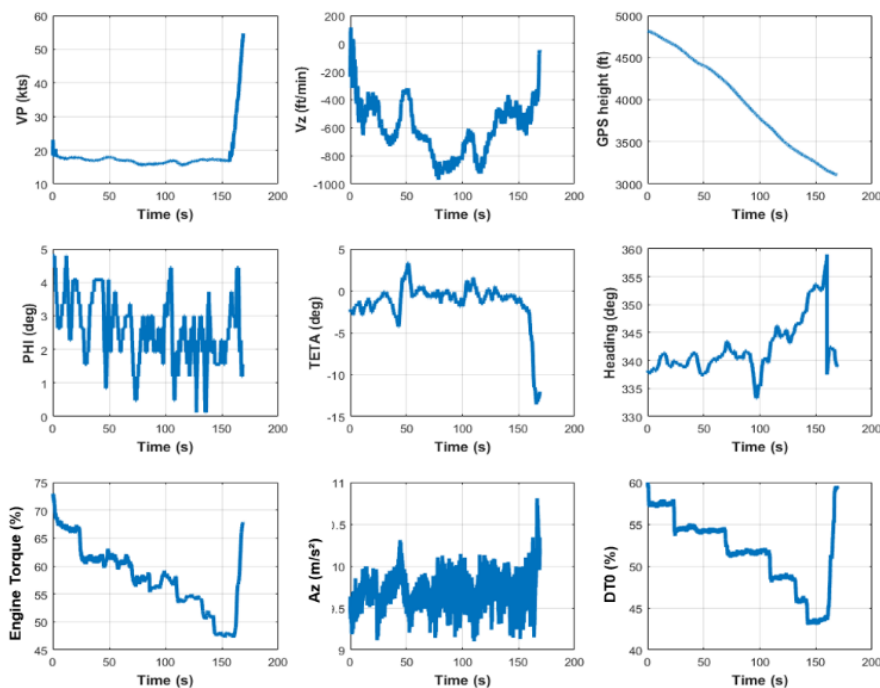
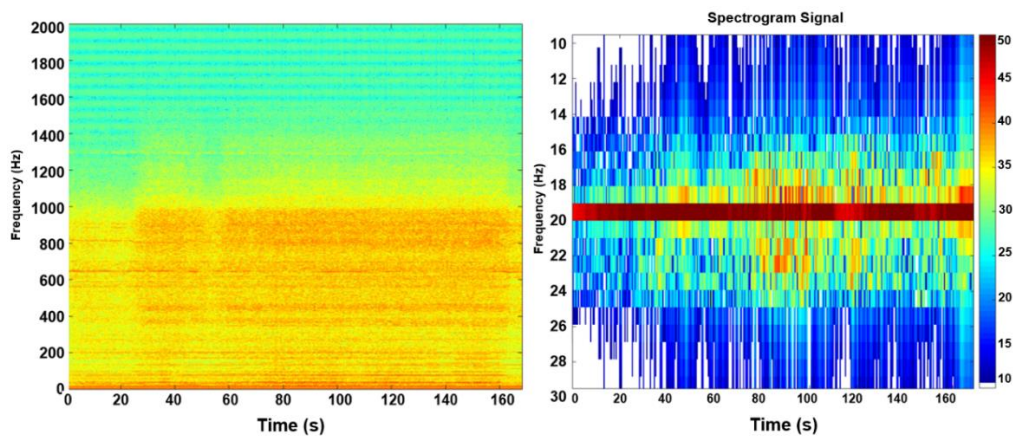


Figure 3-24 shows that, while not entering VRS, the vibration spectra is also changed for low and high frequencies. An energy dissipation around the main rotor blade passing frequency can be also observed. These changes start at 25s, corresponding to a vertical descent speed of -600 ft/min and an airspeed of around 14kt. From that moment, the helicopter was very close to the VRS domain, but never entered it. The spectrograms are quite similar to the previous ones, meaning that the vibration spectra changed as the helicopter get close to the VRS.

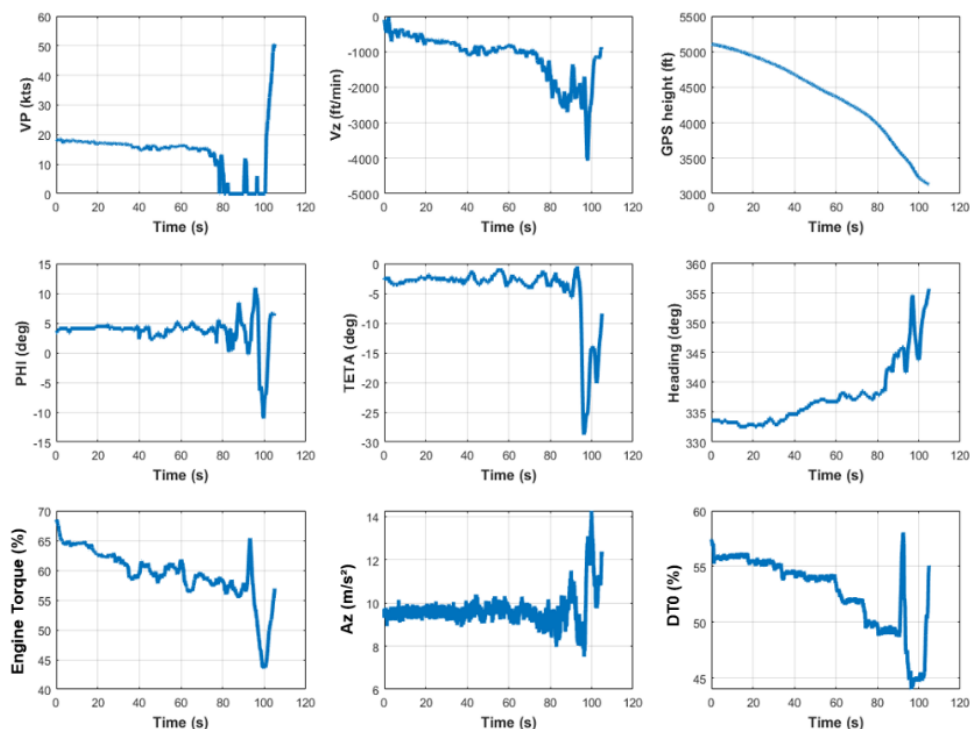
► **Figure 3-24** Spectrogram applied on the signal of the accelerometer placed below pilot seat (vertical axis) – No VRS



Pilot comments during flight:

- 1st collective decrease: the descent rate is setting up; vibrations can be felt, pitch-up, stable at Vz=-650 ft/min, Corrections on pitch angle, Vz=-700ft/min; vibrations are coming back; very close to the VRS;
- 2nd collective decrease: Vz around -850ft/min, vibration regime arrives, very very close but it doesn't want to enter into VRS...

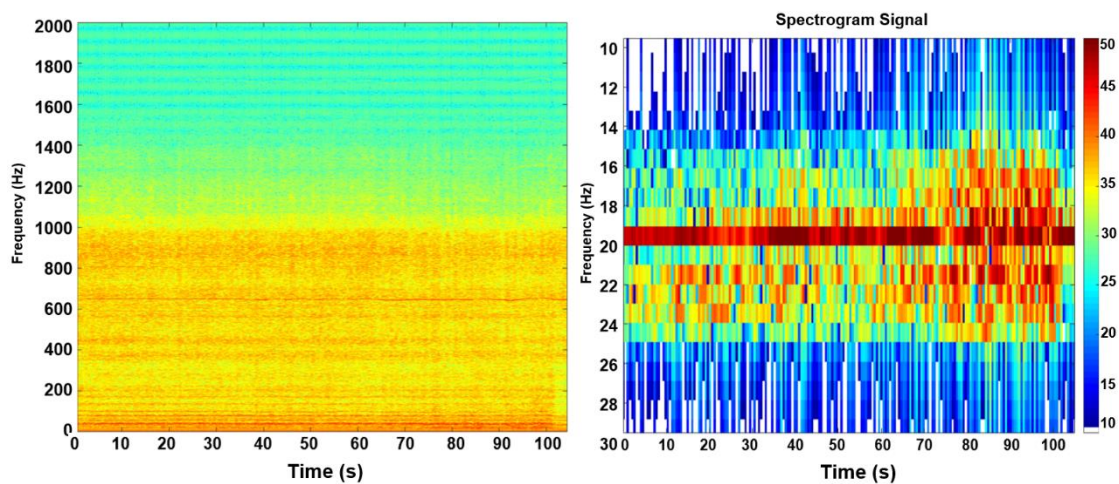
► **Figure 3-25** Fenec flight parameters – VRS entry



Finally, figures (Figure 3-25, Figure 3-26) are showing a run of the 3rd Fennec flight, where the helicopter entered the VRS at 71s. Helicopter mass was 2035Kg.

The spectrograms (Figure 3-26) shows a dissipation of the energy around the main rotor blade passing frequency during all the run, even “far” from the phenomenon at the beginning. Nevertheless, after 71s, it can be seen a slight increase of the energy on all frequencies between 15Hz to 23Hz, but the change in vibration spectra is less perceptible than on the first previous example.

► **Figure 3-26** Spectrogram applied on the signal of the accelerometer placed below pilot seat (vertical axis) – VRS entry



Pilot comments during flight:

- 1st collective decrease: TQ=62%
- 2nd collective decrease: vibrations felt
- 3rd progressive collective decrease: TQ=57%, It starts to enter but not frankly; It enters, V_z is decreasing to -2500ft/min Very few "warning signs", slight reduction of effectiveness of the pedals.

3.1.3.4 Conclusions about vibration flight tests:

- There’s no specific Vortex-Ring-State frequency “appearance” nor specific time/frequency pattern;
- The vibration spectra is changed for low, but also for high frequencies;
- Rotor harmonics and energy are dissipated into a larger bandwidth signal;
- The vibration spectra / vibration level are highly dependent on flight conditions, rotor loads and dynamics ;
- Levels of vibration felt, changes in the vibration spectra, are highly dependent of the helicopter type.

3.2 Review of published results from flight tests

3.2.1 V-22 flight test campaigns

After the V-22 crash in 2000 due to the entry into VRS conditions, an extensive flight test program has been conducted to evaluate the effects of VRS on this aircraft. The following overview of these test campaigns are taken from references [54], [55].

The manoeuvres have been performed at an altitude ranging from 3000 ft to 9000 ft to allow sufficient altitude to enter and recover. A boom-mounted ultrasonic anemometer was used to provide more accurate velocity readings in the low-speed/high rate of descent regime. Rotor thrust has been measured as a function of the combined yoke beam bending gauges for all blades and both rotors.

During testing, two main parameters have proved to be valid indicators of VRS. The first one was the behaviour of the Automatic Flight Control System (AFCS) on the lateral axis. The lateral stick in tiltrotors controls the differential collective pitch and hence the roll motion.

“When a lateral thrust asymmetry is encountered in VRS, AFCS will automatically apply a lateral control to compensate for the roll disturbance.”

As VRS builds up, more AFCS authority is required up to the saturation point where the system runs out of authority and the pilot is forced to apply lateral stick to keep the wings level. In further deep VRS, the full lateral stick is not enough to prevent the aircraft to roll-off.

The second useful parameter is the Roll Acceleration Error. The final input on the differential collective pitch produces differential thrust between the rotor and hence a rolling moment with a subsequent roll acceleration. The roll acceleration error is defined as the difference between the expected roll rate and the actual measured roll rate.

During normal operations, when lateral control is applied the expected roll acceleration is exactly the measured one. Since VRS interferes with thrust, roll acceleration error start to increase as the measured acceleration becomes more and more different then the desired one and an un-commanded roll arises.

Despite lateral axis of the AFCS response and roll acceleration error being very useful as VRS indicators, it has to be outlined that the lateral axis of the AFCS is good in detecting VRS but as soon as it approaches saturation it no longer gives useful information. The roll acceleration error, on the other hand, shows VRS symptoms early on but it is also capable of providing useful information in deep VRS, after the pilot applies full stick.

The main conclusions from these flight tests are and indicated in [54] are presented hereafter:

1. “The tiltrotor configuration is not more susceptible to VRS when compared to conventional rotorcraft. Non-dimensional VRS onset boundaries of the tiltrotor and conventional helicopter are remarkably similar.
2. The high disk loading of the V-22 makes the aircraft significantly less likely to encounter VRS in the operational environment because of the higher rates of descent required to initiate VRS onset. For the conditions tested, the lowest rate of descent where a loss of control was encountered was -1000 ft/min greater than the -800 ft/min operational flight limit.
3. Rotor blade stall does not play a significant roll in determination of the loss of control boundary. Parameters related to asymmetries across the rotor disk tend toward zero during rolloff events.
4. Tiltrotor handling characteristics at the VRS-onset boundary are unique in that the aircraft experiences control degradation in the roll axis, instead of the vertical axis, as with conventional helicopters, or the pitch or vertical axes, as with tandem rotor helicopters.
5. Dynamic maneuvers were shown to delay and reduce the effects of VRS.
6. Nacelle rotation provides the tiltrotor with a mechanically-actuated recovery technique that represents an improvement over conventional rotorcraft that depend on rotor aerodynamic flapping response to

cyclic commands. Recoveries with nacelle are intuitive and typically effective within 1 to 2 seconds of initiation.”

Main parameters that identify VRS are [55]:

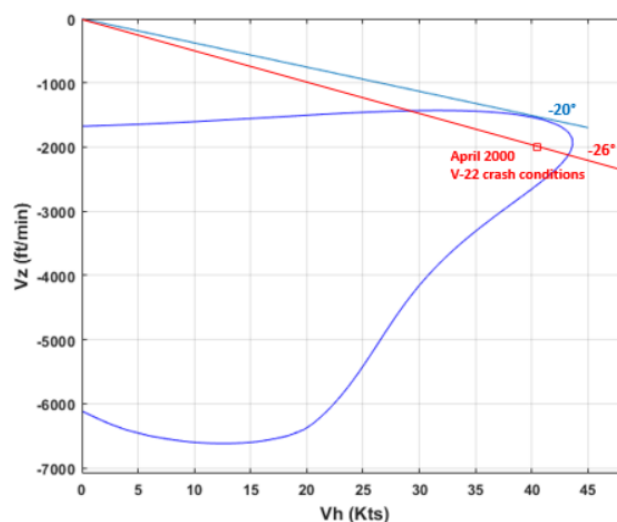
- Rotor Thrust Deficit
- Lateral AFCS Output Signal
- Roll Acceleration Error

As mentioned in [55], the V-22 testing also showed the followings:”

1. In fully developed VRS, the V-22 exhibits lateral control asymmetry, followed by uncommanded roll rate.
2. The initiation of forward nacelle tilt rapidly restores lateral control allowing flight out of the VRS boundary and releasing the rotors from VRS.
3. At low forward speed and increasing descent rate, VRS will be accompanied by increasingly higher output in the lateral control axis. This is because VRS interferes with rotor thrust, and produces a collective pitch asymmetry between the left and right hand rotors. Higher lateral AFCS port output is confined to airspeeds below approximately 45 kts, when the descent rate is higher than 1,500 ft/min (458 m/min).
4. The high lateral AFCS output region correlates with another lateral axis parameter, called the roll acceleration error. The roll acceleration error, identified by long record analysis, substantiates the independently derived VRS boundaries of Kisor et al. [54].
5. The VRS boundary defined in steady descent testing defines the most conservative boundary for encountering VRS symptoms. Control inputs, including yaw rate, roll rate, and rapid deceleration all tend to suppress/delay VRS symptoms. It was not possible to initiate VRS symptoms outside of the static VRS boundary during any dynamic maneuver.
6. Reasonable correlation to the measured V-22 VRS boundary is achieved by the simple engineering analysis of Newman et al. [34] by properly accounting for the V-22’s high rotor disk loading (thrust). The correlation achieved between measurements and the analysis demonstrates that the primary factor in determining the V-22 VRS boundary is disk loading, not blade twist, nor blade planform, nor side-by-side rotor interference.”

Considering a V-22 at the mass of 22 tones, the expected VRS domain given by ONERA’s criterion is shown on the following Figure 3-27. The V-22 crash conditions are also shown in the estimated VRS domain.

► **Figure 3-27 V-22 VRS estimated domain from ONERA criterion**



3.2.2 Royal Aircraft Establishment (RAE)

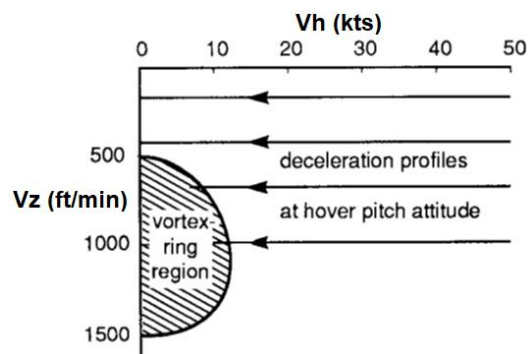
Specific characteristics of different aircraft types in vortex ring state are indicated in [20].

“Early tests at Royal Aircraft Establishment (RAE) produced results from loss of control to mild wallowing instability. The aircrew manual contains entries describing the particular features and best recovery procedures. One such manual notes that rates of descent can build up to -6000 ft/min if vortex ring becomes fully established and that the aircraft pitches sharply nose down if rearward flight is attained. Another refers to an uncontrollable yaw in either direction eventually occurring, and any increase in collective pitch during established vortex ring state creates a marked pitching moment.”

“Interest in the effectiveness of collective control during recovery prompted a series of trials being carried out by Gareth Padfield at RAE Bedford using Wessex 2 and Puma helicopters. The tests were qualitative in nature and aimed at exploring the behaviour of these two aircraft in the vortex-ring state and establishing the benefits to recovery profile of increasing collective pitch before the aircraft nose is lowered to gain air-speed. The test technique options for approaching the vortex-ring condition were somewhat constrained by the need to operate well above the ground (minimum height for initiating recovery action, 3000 ft above ground level) and the lack of reliable low airspeed measurement on both aircraft. The procedure adopted involved a deceleration from 50 knots to the hover, maintaining a constant pre-established (hover) attitude and rate of descent. The rate of descent was then increased incrementally until the vortex region was encountered (Figure 3-28). For both test aircraft the vortex region was quite difficult to find and apparently limited to a range of very low airspeed. With the Wessex, the region was first encountered with the entry profile at 800 ft/min rate of descent. To quote from the pilot’s report:

“... with the rate of descent at about 800 ft/min we settled into the vortex ring; the rate of descent increased through 2000 ft/min in spite of increasing power to 3000 ft lb (hover torque reading). The vibration level was marked and a considerable amount of control activity was required to hold the attitude, though the cyclic controls always responded normally. Applying full power produced a rapid reduction of the rate of descent as soon as the rotor moved into clear air.”

► **Figure 3-28** Decelerating profiles into VRS – taken from [20]



“A major result of the tests was that applying collective prior to lowering the nose resulted in a height loss of about 150 ft during recovery, whereas if the collective was lowered first and then increased when airspeed developed, the height loss was about 500 ft.

Similar results were found with the Puma, except that the pitching and rolling moments were of higher amplitude and frequency and became more intense as the collective lever was raised during recovery. It is emphasized here that the results discussed above are particular to type, and the beneficial use of collective during recovery may not read across to other aircraft. The difference in height loss during recovery for the two techniques is, however, quite marked and is operationally significant, particularly for low-level sorties.”

3.3 Summary of the knowledge gained through previous flight tests

VRS is very difficult to predict, because of its intrinsic turbulent and chaotic nature. Two VRS flights starting from close conditions could result in very different helicopter behaviours.

As confirmed by the dispersion of the experimental test points to determine VRS domain, how the phenomenon settles is very dependent of the airflow around the rotor, attitudes and dynamic of the helicopter, flight controls and thus, blade flapping, rotor/fuselage interferences, etc.

That's why determining the VRS boundaries of a helicopter type requires a lot of test runs, even considering a constant reduced weight (Mass/sigma).

This also explains why it is not surprising that VRS occurs and is felt by pilots very differently from one helicopter to another.

In addition, as explained in [30]:

“a complication in fully understanding the highly nonlinear flow physic of the VRS, and in predicting the VRS flight boundaries, is that the onset of the VRS appears to be flight path dependent. In other words, the flow conditions and transient airloads produced on the rotor in the VRS depend on both the initial rotor operating conditions and on the manner in which the VRS is approached.”

Moreover, while trying to perform smooth VRS entries (by decreasing the collective very progressively) in the same conditions, the helicopter may enter or not into VRS, even if vibrations and other VRS symptoms are present.

Nevertheless, among all the symptoms that can be found in the literature or can be experienced by crew, the rapid drop in vertical velocity is the main signature and dominant effect of the vortex on all types of helicopters.

4. Avoiding VRS – Recovery techniques

4.1 Avoiding VRS

As largely seen in previous chapters, keeping sufficient margins in terms of forward speed and rate of descent with respect to VRS domain is the best way to avoid it. Keeping these margins in stabilised maneuvers, good visual environment is one thing, this is much more difficult during dynamic manoeuvres and operation in degraded visual conditions.

To avoid vortex ring state, it is important to reduce rate of descent before reducing airspeed. For light helicopters, “a good rule to follow is to never allow the airspeed to be less than 30 kts until the rate-of-descent is less than 300 ft/min” as indicated in [56]; for medium or even heavy helicopters, a RoD in excess of -500ft/min should be avoided. To avoid “dynamic” VRS, avoid rapid decelerations below 30 KIAS, especially while in descent [12].

When in a degraded visual environment or at night, **it is essential to scan the instruments** (especially airspeed, RoD, power and pitch attitude).

As described in [57]:

“While in HOGE or flying at low airspeeds without immediate ground references (and not monitoring the instruments) it is possible to mishandle the helicopter and get in a situation which can lead to Vortex Ring State condition.

Therefore it is essential to be able to identify the conditions leading to it in order to avoid it and, if encountered, recognise the symptoms and carry out the correct recovery actions.

VRS should initially be recognized by a feeling of ‘lightness’ as in a low G and there will be no positive G-force feeling when the collective is raised. A further indication is a limp hanging yaw string or “woolometer”. A change in vibrations may be felt. And the rate of descent will continue to increase “

Thus, as already mentioned in sub-section 2.3.4 and in [58], the following operations should be conducted with great care:

- Confined areas reconnaissance and approaches
- Downwind approaches
- Downwind, turning quick stops and flares
- Steep approaches
- Transitions from approach to hover
- Hover Out of Ground Effect (HOGE) and (un)intentional vertical descent
- Low speed autorotation recovery
- Slow speed orbiting (Aerial photography)

4.2 Review of the recovery techniques and associated recommendations

It is possible to summarize the recovery techniques into four general procedures:

1. To recover by applying collective pitch and power;
2. To enter autorotation to break the vortex ring and, when cyclic authority is regained, increase forward airspeed;
3. To increase forward airspeed;
4. To increase lateral airspeed or at least, perform a lateral movement.

Procedure 3 is considered as the “classical” recovery technique while procedure 4 can be associated to the Vuichard Technique.

Procedure 1 can be applied in case of early warning detection, avoiding real VRS entry. It is found in literature that increasing collective in VRS may aggravate the situation while flight test performed by ONERA/DGA-EV demonstrated the insensitivity of the collective in fully developed vortex.

Entering into autorotation (procedure 2) is another to exit VRS, but leads to very high rates of descent and thus requires a large altitude margin.

Some recommendations are presented hereafter. Most of the time, the classical increase of the forward speed or the lateral exit are advised.

These recommendations were taken from existing safety notes or documents and are not the results of the present project.

It is possible to find in [17] the recommendations to exit VRS for different helicopters:

“H-60B: For retreat from the onset of the vortex ring state, reduce collective and increase airspeed. Power should be increased once the airspeed is above approximately 20 knots. The only solution for fully developed VRS is to enter autorotation to break the vortex ring and, when cyclic authority is regained, increase forward airspeed.

H-46D: Recovery requires forward cyclic and decreased collective.

MH-53E: Recovery is best made by increasing forward speed and decreasing collective pitch. Increased collective pitch may further worsen the condition.

According to the field manual, pilots tend to recover from a descent by applying collective pitch and power. If not enough power is available for recovery, applying collective pitch may aggravate power-settling. This results in more turbulence and a higher rate of descent. The pilot can recover by increasing airspeed and lowering collective pitch. Increasing airspeed is the preferred method of recovery, since usually less altitude is lost by this method than by the method of lowering collective pitch.

In tandem-rotor helicopters, recovery should be attempted using lateral cyclic and pedal inputs to make the transition to directional flight. Longitudinal cyclic inputs (differential collective) may aggravate the situation.”

In [56], Robinson helicopter company is recommending the Vuichard technique instead of the classical one.

From [57], the two main recovery techniques are described hereafter

“Recovery option 1: Standard recovery technique:

- Reduce collective
- Ease cyclic forward to adopt a nose down attitude
- Maintain heading by using the pedals
- When the airspeed is above translational lift, increase collective to maximum continuous power to climb

Recovery option 2: Vuichard recovery technique:

- Raise collective
- Maintain heading by using the pedals
- Apply lateral cyclic in the direction of the tail rotor thrust
- Once the descend is stopped, ease cyclic forward to regain airspeed”

In [27], the different ways to get out the VRS domain are explained:

“In the case of main rotors with two blades, the rotor control moment being weaker than for rotors with more blades, the method was to go out from the VRS through its down limit by lowering the collective. That means of course more lost of altitude. This kind of differences depending on the type of helicopter can also be impacted by other parameters (not the number of blades), for example the excentricity of the flapping hinge ...

It is of course quicker to get out the VRS through the front limit by pushing the longitudinal cyclic in order to increase the forward speed. In principle it could be even quicker to escape the VRS volume through its lateral envelop, simply because the roll inertia (I_{xx}) being lower than the pitch inertia (I_{yy}), a higher roll rate could be obtained more quickly than an equivalent pitch rate.

In spite of the apparent benefit, the conclusions found in [27] are the following:

- First reaction is to apply pitch-down attitude followed by an increase of power. Collective decrease is not necessary for, at least, rotor equipped with more than 2 blades.
- The lateral recovery technique is advised from a vertical descent if the lateral clearance is good, rather than in approach phases.
- The loss of height is all the more important as the collective decrease is achieved before the increase in speed. Thus, the loss of height is minimised if the forward speed increase is done before collective reduction.

In addition, for helicopters equipped with large horizontal stabilizers, at low forward speeds with such high descent rates in VRS, the horizontal stabilizer is strongly blown in the upward direction, therefore producing a natural pitch down tendency which helps anyway to get out through the front limit as recommended in the conventional way.

The efficiency of the cyclic controls may also be altered differently in VRS. Indeed, depending on the direction of the horizontal speed of the rotor relative to the air, the vortices agglomerated near the rotor can be distributed differently on the longitudinal and lateral direction of the rotor. The “vortex torus” is circular only in vertical descent. In descents with horizontal speed its shape is more elliptical. Thus the cyclic control effectiveness are impacted differently depending on the induced velocities by this not axisymmetric distribution of rotor wake vortices.”

In [20], as already mentioned in sub-section 3.2.3.:

“The standard recovery technique involves lowering the nose of the aircraft until sufficient speed is gained that the vortex is ‘washed’ away, and then applying collective pitch to cancel the rate of descent.”

It was observed that “applying collective prior to lowering the nose resulted in a height loss of about 150 ft during recovery, whereas if collective was lowered first and then increased when airspeed developed, height loss was about 500 ft.”

In Safety Information Notices [12] and [18], Airbus Helicopters communicated on how to escape VRS phenomenon:”

- The “classical technique” for escaping from VRS is :
 - If residual power is available, increase the collective pitch and decisively apply forward cyclic pitch to accelerate.
 - If no residual power is available, decisively apply forward cyclic pitch to accelerate and maintain the collective pitch control position.
 - Once airspeed is above 20-30 knots and the RoD is managed, adjust the cyclic and collective pitches to establish the desired attitude, airspeed, and altitude.
 - Inaction, or incorrect action, may allow VRS to progress to very high RoD.

- The “Vuichard recovery technique” differs in that the pilot is required to use the collective pitch, while applying lateral cyclic and maintaining heading control with the pedals. Thus, this technique is designed to escape the column of descending air by moving laterally.”

Hereafter, the “Vuichard recovery technique” was explained by Mr. Vuichard when he visited DGA-EV in May 2023:

Once VRS is detected by the pilot:

- A) Increase the collective up to the maximum available power (In order to reduce the rate of descent once the VRS is exited, otherwise it is possible to re-enter into VRS) + simultaneously apply crossed pedal input corresponding to anti-torque rotor thrust (for CCW rotor-system escape to the right and for CW rotor-system escape to the left) – The anti-torque thrust increase help to initiate the movement, then lateral cyclic action
- B) Pedal and lateral cyclic cross actions : actions of 1s – count “21” (to reach 15°/20° bank angle), “22” (0° bank angle), level flight. Keep in mind “Cross the controls” to avoid mistakes or wasting time thinking
- C) As soon as the rotor reaches the upwind part of the vortex, the recovery is completed

This technique uses the lateral force generated by the anti-torque rotor to escape laterally from the VRS, which mainly affects the main rotor.

In [18], Airbus Helicopters indicates that

“tests were performed to gather data for a more complete understanding of the aerodynamic loads on the helicopter. VRS is not considered as a normal part of the flight domain of any rotorcraft. Dynamic loads on some components of the rotor system increase significantly in full VRS and are not completely taken into account in the components service life. As an aircraft manufacturer, Airbus Helicopters do not recommend to place the helicopter in fully developed VRS.

As a conclusion of this safety notice:

- In flight, in case the pilot has not recognized the early warnings and is in a fully developed VRS, the “classical technique” is effective for the recovery.
- However, the “Vuichard recovery technique” may be applied in case of fully developed VRS in specific operational conditions like rear wind in final approach or helicopter in front of an obstacle.”

The project presented in [32] is funded by the Federal Aviation Administration through PEGASAS (Partnership to Enhance General Aviation Safety, Accessibility and Sustainability), FAA Center of Excellence on General Aviation. The project No. 2: Rotorcraft Aviation Safety Information Analysis and Sharing (ASIAS) is a partnership between PEGASAS researchers at the Georgia Institute of Technology, the FAA and the Helicopter Association International (HAI). This paper presents first works in the comparison between the classical and Vuichard recovery techniques. The results relies on piloted simulations done in a S-76 flight simulator “to determine pilots’ decision-making process during a VRS encounter and their ability to recover”. The scenarios were designed based on an analysis of VRS accident reports from the 13 biggest helicopter-operating countries.

As stated, “a preliminary comparison of the classical and Vuichard recovery showed that the former requires more aggressive control inputs and that the latter seemed overall more efficient (executed faster with less altitude loss)”.

The paper outlined “a common misconception regarding lateral displacement while performing the Vuichard recovery. Indeed some pilots believed that the space required to escape laterally made this technique unusable in a canyon. However, when flying the method in the simulator, pilots with some training were able to consistently recover with less than a rotor radius of lateral excursion, which concurs with the description of the technique.”

But, as indicated in this paper: “an obvious limitation is the use of an on-line simulation inflow model that does not provide the most accurate representation of the rate of descent build-up and is thus still an obstacle to a definitive comparison between the classical and the Vuichard recovery techniques. “

It is undeniable that evaluations performed in a simulator will depend on the realism of the rotor inflow model and its capability to well simulate the VRS phenomenon or at least, its effects, whatever the inflow model used. In addition, it has to be outlined that the classical recovery technique tested here consisted in lowering the collective and pitching down to establish forward flight speed to exit the vortex. While largely taught, demonstrated and even recommended in some flight manuals, this technique can also be done with an increase of the collective as indicated in Safety Information Notices from Airbus Helicopters [12] and [18]. It is also already known that decreasing the collective will lead to larger loss of altitude.

4.3 Summary of the review of the recovery techniques and associated recommendations

This chapter reviews and summarizes the different recommendations done by many stakeholders to exit VRS. The two main techniques generally implies to raise collective if power is available, and increase airspeed. Longitudinally for the classical method, laterally (in fact inducing a lateral motion rather than really increasing the lateral speed) for the Vuichard method. Nevertheless, it is interesting to see that the management of the collective during the classical recovery maneuver has evolved with time and can be different depending on the helicopter types. This remains a subject of questions and specific evaluations will be performed in the framework of this project.

Good arguments are given for both techniques, but it is almost impossible to find experimental and public data to corroborate the stated benefits.

It is hoped that the current project, while limited in terms of helicopter types and number of flights will provide objective tests data to have a clearer idea on the efficiency of these recovery techniques while both ONERA and EASA are fully aware that this research project could be further improved in terms of rotor types, helicopter mass and flight conditions, etc.

5. Review and analysis of alerting system patents

Most of the existing patents, and thus, systems, are based on the knowledge of a predefined VRS domain (evaluated in flight, or based on theoretical speeds). These VRS boundaries are considered in terms of forward and vertical speeds. So, the main approach consists in evaluating or estimating low forward and vertical speed to assess how far the helicopter is from the pre-defined VRS domain. Most of the VRS systems are in fact dedicated to the estimation of rotor airspeeds. In order to be more realistic, some systems take into account the “dynamic” vortex, by adjusting the VRS domain to the rotor airspeed and not only pure horizontal and vertical speed in earth frame. Accelerations can be also taken into account, to perform a numerical integration and estimate the speeds of the helicopter in a given “time window” in the future, this approach enabling to earlier alert the pilot.

Within this category of patents, one can cite:

- A. “Methods and systems for monitoring approach of rotatory wing aircraft” – Honeywell – 2008

A System and methods for generating an alert if a rotary wing is approaching a hazardous situation are detailed. Patent based on predefined airspeeds and estimation of tailwind.

- B. “Method and device for detecting and signalling the approach of a rotorcraft to a vortex domain” – Eurocopter – 2009

VRS domain is preliminarily determined for the helicopter. Estimation of the instantaneous airspeeds seen by the rotor and a predictive speed is computed. “Dynamic VRS domain” is also considered, by considering the airspeeds in the rotor frame.

- C. “Amélioration de la détection et de signalisation de l’approche du domaine de vortex par un giravion” – Airbus Helicopters – 2018

Improvement of the previous patent

- D. “Method for protection against vortex ring state and device” – Bell Textron – 2021

A method for protecting a rotorcraft from entering a vortex ring state is presented. The method includes the monitoring of the vertical speed of a rotorcraft, comparing the vertical speed to a vertical speed safety threshold, and performing vortex ring state (VRS) avoidance if necessary. The VRS avoidance includes determining a power margin available from one or more engines of the rotorcraft, limiting the vertical speed of the rotorcraft and increasing a forward airspeed of the rotorcraft.

- E. “System and method for protection against Vortex Ring State” – Textron Innovations Inc. – 2023

This application is a continuation of the previous patent.

Some patents are based on the possible generation of automatic controls on collective(s) (mainly tilt-rotor application) when operating close to the VRS domain, the generated blade-pitch fluctuations delaying the VRS phenomenon. The estimation of the approach of the VRS is here based on the measurement of thrust fluctuations:

- F. “Method and apparatus for preventing adverse effects of vortex ring state” – Bell Textron – 2004

- G. “Control system for rotorcraft for preventing the vortex ring state” – Bell Textron – 2006

Patents are focused on the way to alert the pilot, and the best way to indicate the approach of the phenomenon:

H. “Indicator for an aircraft capable of hovering and method for assisting performing a manoeuvre for the aforesaid aircraft” – Leonardo – 2022

A specific indicator is described, enabling to alert the pilot depending on where the aircraft is by comparison to a predefined VRS “static” domain in terms of horizontal/vertical speeds.

Finally, the two following patents are a bit different, and deal with the detection of the VRS phenomenon by itself, or one of its symptoms. The pre-determination of the VRS domain is then not required.

I. “A method and system for anticipating the entry of a rotorcraft into a vortex domain” – Airbus Helicopters – 2018

Airbus Helicopters developed a system and a method analysing the rotor flow by the measurement of the unsteady pressure variations on the fuselage. This signal processing can then detect a specific low frequency (lower than 1Hz), which is supposed to characterised the VRS regime. Once detected, an alert can be generated.

J. “Device for detecting the approach of a vortex ring state, rotary-wing aerodyne comprising said device, and associated method” – ONERA/DGA – 2021

ONERA and DGA developed algorithms to analyse vibration measurements at various location in the helicopter. Several algorithms are performing parallel computations to detect a variation of the energy in the overall signal.

These two approaches can be added to a predefined logic taking into account horizontal and vertical airspeeds, in order to prevent the systems to generate false VRS detections (when the helicopter is climbing for example) or just to avoid to run the system when performing a level flight at 80kts.

5.1 Summary of the alerting system patents

Measuring precisely low forward speed and vertical speed is still a great challenge and developing a system capable of that could be important and usefull for VRS avoidance and for many other aspects.

The knowledge of the VRS domain of a helicopter requires specific and dedicated flight tests, which is costly and time consuming. This will be still necessary as long as VRS avoidance systems are based on the capability to position the helicopter airspeeds (and preferably the rotor airspeeds) with regards to a predefined and predetermined VRS domain.

That’s why it seems very important to develop systems capable of measuring and/or analysing the VRS phenomenon by itself or one of the associated symptoms. Various options would be possible: Vibrations, thrust fluctuations, sound, pressure and/or rotor loads. The main problem is the instrumentation required, its cost, weight and maintenance for such a very specific problem. Another issue remains the development of robust signal processing methods, because the signals are very noisy, highly dependent of the flight conditions and manoeuvres and because VRS is a higly turbulent and chaotic regime with no specific signature.

6. Gap analysis of the current knowledge for the complete description and prediction of the phenomena

6.1 VRS domain knowledge

For an isolated rotor, as being isotropic, the VRS domain in terms of horizontal and vertical speeds is certainly symmetrical. But due to the closeness of the fuselage and the potential aerodynamical interferences, this symmetry is not ensured. There's no experimental data on the subject. ONERA flight tests seem to show that the VRS entry with negative horizontal speed occurred at different vertical speeds than with "same" positive horizontal speed.

The behaviour of the helicopter is different on longitudinal and lateral axes. This may have an impact on how VRS develops and interacts with the helicopter.

Most recent hybrid computational methods could be useful to investigate the impact the fuselage shape, rotor/fuselage interaction on the development and the occurrence of the vortex-ring-state phenomenon.

6.2 Dynamic VRS

Taking into account the vertical speed seen by the rotor is essential in order to remain "far" from the VRS domain. But this is certainly not sufficient, and only considering this vertical speed is less important than the ratio between rotor vertical speed and induced velocity.

During stabilised manoeuvres, the vertical speed monitored by the pilot and the one seen by the rotor are very similar. In addition, the induced velocity will remain relatively constant. In these conditions, the traditional domains provided in terms of V_h/V_z are representative of the VRS.

However, during dynamic manoeuvres, the vertical speed seen by the rotor may be quite different from that which the pilot will track. Moreover, pilot actions in these phases (on collective and/or cyclics) will modify the induced velocity and thus, the ratio V_z/V_i . The so-called "dynamic vortex" is insidious and can catch even very experienced pilots. Performing dedicated flight tests to deeply analyse these flight cases is a challenge, and carrying out numerical studies is just as difficult, if not more.

Dedicated flight test campaigns would be necessary to well determine and understand all the aspects of these flight cases. The main problem is the capability to reproduce comparable and similar the flight conditions leading to dynamic VRS. The analysis of this kind of test cases is also much more difficult. A precise estimation of the speeds seen by the rotor disk would also imply a specific instrumentation (low airspeed measurement associated with blade flapping measures).

Using numerical methods to perform almost identical and repeatable dynamic manoeuvres would be useful for such analysis but require a strong coupling between flight mechanics, rotor wake model, and control technics to realise the manoeuvre in offline simulations, which remain an arduous task. Nevertheless, the development of free wake models enables to realistically reproduce the rotor wake dynamics and their potential coupling to flight mechanics codes allows to carry out more complex manoeuvres than in the past. While being a complex work, this is the only way to better understand the establishment and the occurrence of VRS during dynamic manoeuvres.

To our understanding, questions remain:

- VRS is generally considered to occur when the rotor disc is completely surrounded by a vortex ring torus, which is certainly the case when the VRS is gradually establishing. But what happens if only a part of the rotor surface is caught in the vortex, which can be the case when the aircraft's attitude changes? Does this

lead to the same consequences?, i.e.: does the degraded lift over a more or less large area of the rotor surface lead to a general VRS?

- While the mean induced velocity at the rotor disk is generally considered as the basis for calculating the vertical speed/induced velocity ratio, the induced velocity is far from being uniformly distributed over the rotor disc and a mean induced velocity is an extreme simplification. The induced velocity being not uniformly distributed over the rotor disc during stabilised manoeuvres, this is even less the case during dynamic manoeuvres. Does this have an impact on the establishment of the vortex?
- During dynamic manoeuvres, the interactions between the rotor and the highly disturbed wake are extremely complex and the establishment of the VRS is particularly difficult to predict. However, is it possible to define criteria for estimating, with good probabilities, the occurrence of VRS during such manoeuvres (e.g.: pitch angles/angular rates versus V_z)?

6.3 Predicting methods/simulations

Most of the time, computations are performed on isolated rotor. Computational methods are mainly used to better understand/estimate the airflow around the rotor in VRS conditions. It is still very difficult (costly and long) to perform full CFD helicopter simulations.

Fully coupled helicopter/rotor wake simulations are rare and generally the helicopter trajectory is imposed, enabling the generation of a realistic rotor wake but not representing the effect of this wake on rotor loads and thus on helicopter trajectory.

Simulation of dynamic VRS are rare, as well as the simulation of recovery techniques.

Realisation of realistic maneuvers require a strong coupling between flight mechanics, rotor wake model, and control technics to stabilise and "pilot" the helicopter model in offline simulations.

Real-time simulations still require fast and simple models to simulate the VRS phenomenon, or at least its principal symptoms. But it is almost certain that the use of more accurate free-wake models will be possible within the next years in piloted simulations.

6.4 Recovery techniques

The different techniques have been evaluated by helicopter manufacturers but there's a lack of public data/feedback. Moreover, recovery techniques are generally not a subject of "scientific" researches.

Considering the Vuichard technique, while theoretically more efficient due to the capability of helicopters to faster accelerate on their lateral axis (lateral inertia being lower), it is most of the time recommended on specific types of approaches (very low speed or tailwind).

In chapter 4.2, as it can be read in [56] (Robinson Safety Note): "When flown properly, the Vuichard recovery produces minimal altitude loss". The terms "when properly" have to be outlined. Does it mean that if not properly flown, this technique leads to identical or even large loss of altitude than the classical recovery maneuver? And it tends to show (but this can be guessed from the maneuver description) that the Vuichard technique is (much?) more complex to perform than "just" applying forward cyclic stick.

Nevertheless, and in order to be fair, it has to be noted (as highlighted in chapter 4.2), that the management of the collective during the classical recovery maneuver seems to remain an open question. So, if this technique is relatively simpler, how to handle collective pitch seems to be helicopter dependent and has evolved with time.

In a general manner, the complexity of the recovery maneuver and the skills required by pilots to properly perform both techniques will have to be taken into account in our evaluations.

6.5 Rotor technologies

All helicopter main rotor types and architectures (Single Rotor, Tandem, Coaxial, Intermeshing) are exposed to VRS. However, each combination may feature different characteristics and symptoms during the development of the phenomenon, when the helicopter is in a fully developed VRS, and during recovery maneuvers.

We can certainly assume that rotor technology has little influence on the establishment of the phenomenon, but a larger one on the perceived symptoms, helicopter behaviour once in VRS, cross-coupling magnitudes (see chapter 6.6) and efficiency of the recovery maneuvers.

It has been reported that rigid rotors are more susceptible to be damaged during VRS while it is almost impossible to find public information about that.

Are the rotor load fluctuations more severe on rigid rotors in VRS, generating more vibrations and/or constraints on rotor head? No study was either found on the subject.

6.6 Pitch-roll cross-coupling considerations

Helicopters are well known to present cross-couplings in every axis. Nevertheless, cross-coupling considerations are certainly not sufficiently taken into account during studies on VRS and more particularly evaluation of recovery techniques that all require large and rapid attitude variations.

Thus, it can be found in [59] that:

“Pitch-roll and roll-pitch cross-couplings can be powerful and insidious. The natural sources of both are the gyroscopic and aerodynamic moments developed by the main rotor and, in dynamic manoeuvres with large attitude excursions, the uncommanded and sometimes unpredictable off-axis motion can require continuous attention by the pilot. Generally, the magnitude of the pitch-to-roll couplings are more severe than roll to pitch, due to the large ratio of pitch to roll moment of inertia, but are, arguably, more easily contained by the pilot, at least at low to moderate frequencies. Roll-to-pitch coupling effects can have a much stronger impact on flight path and speed control and hence handling qualities in moderate to large manoeuvres.”

An overview of the primary and secondary responses of each control input is given in Table 6.1, taken from [60].

► Table 6-1 Cross-coupling responses

Input / Response	Pitch	Roll	Heave	Yaw
Longitudinal cyclic	Primary response	Due to lateral flapping	Desired in forward flight	Negligible
Lateral cyclic	Due to longitudinal flapping	Primary response	Descent with roll angle	Undesired
Collective input	Due to longitudinal flapping	Due to lateral flapping and side-slip	Primary response	Due to change in torque requires tail rotor thrust
Tail rotor collective	Negligible	Due to tail rotor thrust and side-slip	Undesired	Primary response

Thus, cross couplings experienced during flight in fully VRS and/or during the recovery, needs further investigations.

This project might be an opportunity to do it, but helicopters operated by DGA-EV have semi-rigid rotors and cross-coupling effects will be probably minored compared to rigid rotors.

6.7 New architectures (eVTOL / UAM)

Although VRS is known and has been studied for a long time in the helicopter community, there are still many aspects that raise questions. This is all the more true when considering the many specific features that can be found on the new and potential future eVTOL architectures and aerodynamic challenges they involve.

Thus, reference [48] exposes the basic physics of the Vortex Ring State in order to assess the likely impact of this phenomenon on the safety and operational characteristics of this new class of vehicles. This paper reviews and analyses many aspects and characteristics of these new vehicles and shows how the vortex phenomenon should not be overlooked.

Thus, their high disk loadings, their distributed lift over numerous rotors on either side of the fuselage and their specific blade shapes are just a few of the characteristics that could expose them to the vortex phenomenon. In addition, since their purpose is to transport people in urban environments, trajectories will be more or less imposed and the external air conditions (tailwinds, shear or vertical) could prove to be an additional risk factor, even though the possibility of entering a vortex should be avoided at all costs.

First and foremost, we need to acquire some basic knowledge of the main characteristics and features of this type of machine and their influence on the appearance and development of the vortex phenomenon, such as:

- Effects of rotor/blade shape (small rotor size, twist, propeller-like blade, tip shape, etc.)
- Ducted/shrouded rotor
- Close counter-rotating rotors
- Rotor wake interferences due to multi-rotor configuration, in close proximity to each other
- Effect of aerodynamic interaction (wing and/or aerodynamic elements close to rotors)
- Rotor RPM variation on induced velocity establishment and VRS generation
- Induced velocity response due to RPM variation

Studying the impact of a VRS entry due to specific configurations and control strategies of eVTOL would be also necessary. As an example, the use of differential thrust strategy may lead to the occurrence of VRS on one or different rotors, causing pitch or roll motions or due to manoeuvres within a complex aerology.

The impact of the urban environment in which these machines will operate should also be taken into account and studied, by considering wind gusts, wind shear, tailwind or updrafts combined with some manoeuvres which together (aircraft and air mass motion) may trigger a VRS entry on some of the rotary wings.

Finally, the implementation and analysis of vortex recovery techniques and strategies should be studied in the event of a vortex entry. Ideally, automatic systems would be developed to always ensure VRS avoidance or to automatically manage the recovery manoeuvre.

7. Conclusions

This document presents our current knowledge and understanding of the complex Vortex-Ring-State phenomenon. This state of the art has been established thanks to a large bibliographical review but it is also based on the common experience of ONERA and DGA-EV on the subject, experience gained since more than 20 years through the realisation of numerous VRS researches and flight test campaigns.

The following aspects are addressed in this report:

- Theory of the VRS;
- Analysis of the available analytical and numerical methods for prediction and simulation of the VRS.
- Analysis of the previous research studies on the VRS with particular regard to the experimental flight test programmes.
- Gap analysis of the current knowledge for the complete description and prediction of the phenomena

As far as possible, a critical analysis and synthesis of the relevant information have been done for these different topics.

Aerodynamic processes involved in the development of the VRS can be well captured and analysed through numerical methods. Significant advances have been done while progresses are still needed for being able to simulate complete helicopter configuration in more complex flight phases, with realistic rotor dynamics (involving Computational Structural Dynamics methods), realistic rotor wake (CFD and/or hybrid methods), flight dynamics and helicopter control strategies.

Besides, the impact of the VRS on the rotor, depending on its technology, would certainly merit further investigation.

While these numerical methods are essential to better understand all the mechanisms involved in VRS generation, experimentations remain a key element. But VRS flight tests are (and will continue to be) very demanding in terms of instrumentation, competences and costs.

Necessary to validate numerical approaches, necessary from an operational perspective, results of VRS flights remain, however, highly dependent on the tested helicopter.

Unfortunately, the scope of the work cannot be infinite in the framework of a project, as well as the number of flights and helicopter types. ONERA, DGA-EV and EASA are fully aware that the current research project will not answer all the remaining questions about VRS, but it is nevertheless expected that the flight tests performed will contribute to provide further information in the characterisation of the VRS as well as recovery techniques.

Bibliography

1. Leishman, J. G., Bhagwat, M. J. & Ananthan, S., "The vortex ring state as a spatially and temporally developing wake instability". American Helicopter Society International Specialists Meeting on aerodynamics, Acoustics and Test & Evaluation, San Francisco, CA, Jan. 23–25, 2002.
2. BOLNOT, H., "Instabilités des tourbillons hélicoïdaux : application au sillage des rotors », « Instabilities of the helicoidal vortices – application to the rotor wake”, Ph. Dissertation, Aix-Marseille University, 20 Dec. 2012.
3. Meijer Drees, J. & Hendaal, W. P., "Airflow patterns in the neighbourhood of helicopter rotors : A description of some smoke tests carried out in a wind-tunnel at Amsterdam". *Aircr. Eng. Aerosp. Tec.* 23, 107–111, 1951.
4. Johnson, W., "Helicopter Theory", Princeton University Press, Princeton, New Jersey, 1980.
5. Johnson, W., "Model for vortex ring state influence on rotorcraft flight dynamics". Technical Report TP 213477, NASA Ames Research Center, 2005.
6. Jimenez, J., "Etude expérimentale et numérique du comportement d'un hélicoptère en descente à forte pente: modélisation de l'état d'anneaux tourbillonnaires". Ecole doctorale de mécanique, physique et modélisation – Option : Mécanique des fluides. 6 Décembre 2002.
7. Brotherhood, P., "Flow through a helicopter rotor in vertical descent", Reports and Memoranda N°2474, NACA, 1951.
8. Castles W. G. R. "Empirical relation between induced velocity, thrust, and rate of descent of a helicopter rotor as determined by wind tunnel test on four model rotors". Technical Note n° 2474, NACA, 1951.
9. Brotherhood, P., "Flight measurements of the stability and control of a westland whirlwind helicopter in vertical descent", Technical Report N°68021, Royal Aircraft Establishment, January 1968.
10. Washizu, K., Azuma, A., Koo, J., Oka, T., "Experiments on a model helicopter rotor operating in the vortex ring state", *Journal of Aircraft*, vol.3 (n°3), May-June 1966.
11. Taamallah, S., "A Qualitative Introduction to the Vortex-Ring-State, Autorotation, and Optimal Autorotation", National Aerospace Laboratory NLR, NLR-TP-2010-282, May 2011
12. Airbus Helicopters Safety Information Notice N° 3123-S-00 - 2022-04-12
13. Chen., C., "Development of a Simplified Inflow Model for a Helicopter Rotor in Descent Flight". PhD thesis, Georgia Institute of Technology, 2006.
14. Van Vyve, H., "Simulation of a helicopter in Vortex Ring State through a coupled simulation of multi-body dynamics and aerodynamics". Ecole polytechnique de Louvain, Université catholique de Louvain, 2019.
15. Leishman, J.G, Bhagwat, M.J., Ananthan, S., "Free-vortex wake predictions of the vortex ring state for single rotor and multi-rotor configurations". In 58th Annual Forum of the American Helicopter Society, 2002.
16. Taghizad, A., Jimenez, J., Binet, L., Heuzé, D., "Experimental and theoretical investigations to develop a model of rotor aerodynamics adapted to steep descents". In 58th Annual Forum of the American Helicopter Society, 2002.
17. Johnson, W., "Model for vortex ring state influence on rotorcraft flight dynamics". Technical Report TP 213477, NASA Ames Research Center, 2005.
18. Airbus Helicopters Safety Information Notice N° 3463-S-00 - 2021-09-28
19. AP3456. The Central Flying School (CFS) – Manual of Flying
20. Padfiel, G., "HELICOPTER FLIGHT DYNAMICS - The Theory and Application of Flying Qualities and Simulation Modelling"
21. Fundamentals of Flight - FM 3-04.203 – Headquarters, Department of the Army, Washington, D.C. 7 May 2007

22. <https://www.heli-archive.ch/en/helicopters/in-depth-articles/kaman-k-1200-k-max>
23. Taghizad, A., Binet, L., "Assessment of VRS risk during steep approaches". American Helicopter Society 62nd Annual Forum, Phoenix, Arizona, USA, May 9-11, 2006.7
24. Taghizad, A., Haverdings, H., Riviello, L., "Vortex-Ring State entry conditions. GREEN ROTORCRAFT Grant Agreement", n°: CSJU-GAM-GRC-2 008-001, October 2009.
25. Newman, S., Brown, R., Perry, J., Lewis, S., Orchard, M., Modha, A. "Comparative numerical and experimental investigations of the vortex ring phenomenon in rotorcraft". In 57th Annual Forum of the American Helicopter Society, 2001.
26. G.A. Ahlin and R.E. Brown. "Predicting the onset of the vortex ring state under accelerated flight conditions". In 61st Annual Forum of the American Helicopter Society, 2005.
27. B. Certain, VORTEX – Customer Support-Technical Department, EUROCOPTER, May 2009
28. Jimenez, J., Desopper, A., Taghizad, A., Binet, L., "Induced velocity model in steep descent and vortex ring state prediction". In 27th European Rotorcraft Forum, 2001.
29. Jimenez, J., Taghizad, A., Arnaud, A., "Helicopter flight tests in steep descent: Vortex-Ring-State analysis and induced velocity models improvement", CEAS Aerospace Aerodynamics Research Conference, 2002.
30. Brown, R.E., Leishman, J.G., Newman, S.J., Perry, F.J., "Blade twist effects on rotor behaviour in the vortex ring state". In 28th European Rotorcraft Forum, 2002.
31. Brown, R.E., Line, A.J., Ahlin, G.A., "Fuselage and tail-rotor interference effects on helicopter wake development in descending flight". In 60th Annual Forum of the American Helicopter Society, 2004.
32. Sotiropoulos-Georgiopoulos, E., Payan, A., Johnson, C., Mavris, D., "A Comparison of Traditional And Vuichard Vortex Ring State Recovery Techniques Using On-Line Simulation", Vertical Flight Society's 79th Annual Forum & Technology Display, West Palm Beach, FL, USA, May 16–18, 2023.
33. Basset, P-M., Chen, C., Prasad, J.V.R, Kolb, S., "Prediction of Vortex Ring State Boundary of a Helicopter in Descending Flight by Simulation", Journal of the American Helicopter Society, 2008, vol. 53 (2), p. 139-151, ISSN 0002-8711
34. Newman, S., Brown, R., Perry, J., Lewis, S., Orchard, M., Modha, A., "Predicting the Onset of Wake Breakdown for Rotors in Descending Flight", Journal of the American Helicopter Society, Vol. 48 (1), Jan. 2003.
35. Kolb, S., "Théorie des bifurcations appliquée à l'analyse de la dynamique du vol des hélicoptères". École Doctorale Mathématiques, Sciences et Technologies de l'Information, Informatique. Institut National Polytechnique de Grenoble. 27/06/2007
36. Prasad, J.V.R, Chen, C., Basset, P-M., Kolb, S., "Simplified modeling and non-linear analysis of a Helicopter rotor in vortex ring state". In 30th European Rotorcraft Forum, 2004.
37. Van Hoydonck, W.R.M., H. Haverdings, H., Pavel, M.D., "A REVIEW OF ROTORCRAFT WAKE MODELING METHODS FOR FLIGHT DYNAMICS APPLICATIONS", 35th European Rotorcraft Forum 2009
38. Lee, H., Sengupta, B., Araghizadeh, M.S., Myong, R.S., "Review of vortex methods for rotor aerodynamics and wake dynamics". 2022, Advances in Aerodynamics, <https://doi.org/10.1186/s42774-022-00111-3>
39. Komerath, N., Smith, M.J., "Rotorcraft wake modelling: Past, Present, Future", 35th European Rotorcraft Forum 2009
40. Rodriguez B., "Numerical Simulation of Blade Vortex Interaction and Vortex Ring State Aerodynamics using a Fully Time Marching Unsteady Wake Model", 33rd European Rotorcraft Forum, Kazan, Russia, September 2007
41. Bailly, J., "A Qualitative Analysis of Vortex Ring State Using a Fully Time Marching unsteady Wake Model", 36th European Rotorcraft Forum, Paris, France 7-9 septembre 2010
42. He, C., Syal, M., Tischler, M.B., Juhasz, O., "State-Space Inflow Model Identification from Viscous Vortex Particle Method for Advanced Rotorcraft Configurations", Advanced Rotorcraft Technology, Inc. US

Army Aviation Development Directorate, 73rd American Society Forum, Forth Worth, Texas, May 9-11, 2017.

43. He, C., Zhao, J., "Modeling rotor wake dynamics with viscous vortex particle method". 2009, AIAA J 47(4):902–915. <https://doi.org/10.2514/1.36466>
44. Tan, J.F., Hao-wen Wang, H-W., "Simulating unsteady aerodynamics of helicopter rotor with panel/viscous vortex particle method", Aerospace Science and Technology 30 (2013) 255–268
45. Opoku, D.G., Triantos, D.G., Nitzsche, F., Voutsinas, S.G., "ROTORCRAFT AERODYNAMIC AND AEROACOUSTIC MODELLING USING VORTEX PARTICLE METHODS" , Carleton University, Ottawa, Canada, National Technical University of Athens, Greece
46. Ahlin, G.A., Brown, R.E., "Investigating the Physics of Rotor Vortex Ring State using the Vorticity Transport Model", 31st European Rotorcraft Forumn Florencen Italy, Sept. 13-15, 2005.
47. Ahlin, G. and Brown, R., "The Vortex Dynamics of the Rotor Vortex Ring Phenomenon," Proceedings of the American Helicopter Society 63rd Annual Forum, 2007.
48. Brown, R.E., "ARE eVTOL AIRCRAFT INHERENTLY MORE SUSCEPTIBLE TO THE VORTEX RING STATE THAN CONVENTIONAL HELICOPTERS?", 48th European Rotorcraft Forum, Winterthur, Switzerland, 6-8 Sept. 2022.
49. Kim, H.W., Kenyon, A.R., Duraisamy, K., Brown, R.E. "Interactional aerodynamics and acoustics of a propeller-augmented compound coaxial helicopter", 9th American Helicopter Society Aeromechanics Specialists' Meeting, 23-25 January 2008, San Francisco, California
50. Hoinville, E., "Etude du sillage de rotors d'hélicoptère en configuration de Vortex Ring State. Modeling and Simulation". Université d'Orléans, 2007. France.
51. Hoinville, E., Renaud, T., "CFD simulation of helicopter rotor in the Vortex Ring State regime". 63rd AHS Forum, Virginia Beach, USA 1-3 mai 2007
52. Wang, L., XU, G., SHI, Y., "High-resolution simulation for rotorcraft aerodynamics in hovering and vertical descending flight using a hybrid method", National Key Laboratory of Science and Technology
53. Stalewski, W., Surmacz, K., "Investigations of the vortex ring state on a helicopter main rotor based on computational methodology using URANS solver". Lukaszewicz Research Network - Institute of Aviation Al. Krakowska 110/114, 02-256 Warszawa, Poland
54. Kisor, R., Blyth, R., Brand, A., MacDonald, T., "V-22 LOW-SPEED/HIGH RATE OF DESCENT (HROD) TEST RESULTS", American Helicopter Society 60th Annual Forum, Baltimore, MD, June 7–10, 2004.
55. Brand, A., Kisor, R., Blyth, R., Mason, D., Host, C., "V-22 HIGH RATE OF DESCENT (HROD) TEST PROCEDURES AND LONG RECORD ANALYSIS", American Helicopter Society 60th Annual Forum, Baltimore, MD, June 7–10, 2004.
56. Robinson helicopter Compagny. Safety Note SN-22. October 2016
57. For Helicopter Flight Instructors – Training Guide, together4safety - EASA, 2022.
58. Safety considerations - Methods to improve helicopter pilots' capabilities - Training leaflet - European Helicopter Safety Team (HEST)
59. <http://heli-air.net/2016/04/21/pitch-to-roll-and-roll-to-pitch-couplings/> - Posted on April 21, 2016
60. Wellens, L., "Model Predictive Control for Helicopter Flight Control Evaluating Linear and Nonlinear Model Predictive Control for Reducing Cross-coupling Effects in Helicopter Flight". Master of Science in Aerospace Engineering at the Delft University of Technology, 2021.



European Union Aviation Safety Agency

Konrad-Adenauer-Ufer 3
50668 Cologne
Germany

Mail EASA.research@easa.europa.eu
Web www.easa.europa.eu

An Agency of the European Union

